SLU

Soil structure and water functions in agricultural soils of the temperate-boreal zone in a changing climate

TOBIAS KLÖFFEL

Soil structure and water functions in agricultural soils of the temperate-boreal zone in a changing climate

Tobias Klöffel

Faculty of Natural Resources and Agricultural Sciences
Department of Soil and Environment
Uppsala

SLU

SWEDISH UNIVERSITY
OF AGRICULTURAL
SCIENCES

DOCTORAL THESIS

Uppsala 2024

Cover: Compilation of (some) typical soils of the temperate-boreal zone. From left to right: photo 1-4 by Tobias Klöffel, photo 5 © Peter Schad.

Swedish University of Agricultural Sciences, Department of Soil and Environment, Uppsala, Sweden

Print: SLU Grafisk service, Uppsala 2023

Soil structure and water functions in agricultural soils of the temperate-boreal zone in a changing climate

Abstract

Climate change may affect the productivity of cropping systems in the temperate-boreal zone by increasing the frequency of periods with water excess and shortage. Soils have the capacity to buffer such extreme weather events by regulating water storage and fluxes, which are mainly a function of soil structure. However, climate itself is linked to the evolution of soil structure through a multitude of processes (e.g., freezing and thawing, soil management). The main objective of this thesis was to improve our understanding of the effects of climate-driven processes on the pore-space structure of agricultural soils in order to identify potential implications for soil water functions in the context of climate change. This was done using a wide range of approaches including a meta-analysis, a laboratory experiment, and the application of machine learning to a newly developed index of soil structure based on relative entropy. It was revealed that climate is an important driver of the structural pore space of arable soils in Sweden and Norway. Warmer and wetter regions showed a less developed structure compared to cooler and drier regions, in particular in the subsoil, although it remains unclear whether this was the result of direct or indirect climate-driven processes. With climate change, the number and intensity of freeze-thaw cycles is expected to increase in some parts of the temperate-boreal zone. Results from this thesis show that this may lead to increased drainage rates in compacted soil layers under near-saturated conditions as well as improved pore connectivity, especially in fine-textured soils. Furthermore, most changes in pore-space structure induced by freezing and thawing were found for pores of diameters <200 µm. The findings are discussed in the context of wetter soil conditions, early summer droughts, and an intensification of agricultural practices expected for different parts of the temperate-boreal zone in the future.

Keywords: freezing and thawing, soil compaction, soil hydraulic properties, soil management, soil organic matter

Markstruktur och vattenfunktioner i jordbruksmark i den tempererade-boreala zonen i ett föränderligt klimat

Sammanfattning

Klimatförändringar förväntas utmana jordbrukets produktivitet i den tempererade boreala zonen genom en ökad frekvens av perioder med vattenöverskott och vattenbrist. Jordar har kapacitet att dämpa sådana avvikelser i vattentillgång genom att reglera vattenflöden, som huvudsakligen är en funktion av deras porstruktur. Klimatet i sig påverkar dock både direkt och indirekt utvecklingen av porstrukturen genom en mängd olika processer (till exempel frysning, upptining och markskötsel). Huvudsyftet med denna avhandling var att undersöka effekterna av klimatdrivna processer på markens porstruktur för att bedöma potentiella konsekvenser för markvattenfunktioner i samband med klimatförändringar. Detta gjordes med hjälp av olika metoder, inklusive en metaanalys, ett laboratorieexperiment, matematiska samband och statistisk modellering. Med hjälp av ett nyutvecklat index för markstruktur fann man att klimatet är en viktig drivkraft för utvecklingen av porstruktur i jordbruksjordar inom Sverige och Norge. Varmare och fuktigare regioner uppvisade en mindre välutvecklad struktur jämfört med kallare och torrare regioner, särskilt i alven, även om det fortfarande är oklart om detta är en konsekvens av direkta eller indirekta klimatdrivna processer. Utöver detta har klimatdrivna förändringar i frysning- och tinings-mönster potential att öka dräneringshastigheten för kompakterade jordlager vid nära mättade förhållanden. Detta kräver dock ett ökat antal och intensivare frysning- och tiningscykler. Förändringar i porstrukturen på grund av frysning och upptining observerades särskilt för porer med <200 μm diameter. Dessutom tyder resultaten på att fördelarna för markstrukturen kan vara störst för jordar med fin textur. Konsekvenserna av dessa resultat sätts i sammanhang med fuktigare markförhållanden, försommartorka och ett intensifierat av jordbruk i den tempererade boreala zonen.

Sökord: frysning och upptining, jordbearbetning, markens hydrauliska egenskaper, markpackning, organiskt material

Bodengefüge und Bodenwasserhaushalt in Ackerböden der gemäßigt-borealen Zone in einem sich verändernden Klima

Zusammenfassung

Klimaveränderungen stellen eine Herausforderung für die landwirtschaftliche Produktivität in der gemäßigt-borealen Zone dar, nicht zuletzt wegen der zunehmenden Häufigkeit von Zeiträumen mit Wasserüberschuss und -knappheit. Böden sind in der Lage, Schwankungen in der Wasserverfügbarkeit abzumildern, indem sie Wasserflüsse regulieren, welche hauptsächlich von deren Porengefüge abhängen. Das Klima selbst jedoch beeinflusst sowohl auf direkte wie auch auf indirekte Weise die Entwicklung des Porengefüges durch eine Vielzahl von Prozessen (z.B. durch Frost-Tau-Zyklen oder durch Bodenbearbeitung). Das Hauptziel dieser Doktorarbeit war es, die Auswirkungen klimabedingter Prozesse auf das Porengefüge von Ackerböden zu untersuchen. Daraus können Folgen für den Bodenwasserhaushalt mit Hinblick auf den Klimawandel abgeschätzt werden. Mithilfe eines neu entwickelten Bodengefügeindexes wurde festgestellt, dass das Klima einen wichtigen Faktor für das Porengefüge von Ackerböden in Schweden und Norwegen darstellt. Wärmere und feuchtere Regionen wiesen im Vergleich zu kälteren und trockeneren Regionen ein weniger gut entwickeltes Gefüge auf. Weiterhin wurde mithilfe eines Laborexperimentes festgestellt, dass eine erhöhte Anzahl und Intensivierung von Frost-Tau-Zyklen durch den Klimawandel zu einer erhöhten Entwässerungsrate und Durchwurzelbarkeit verdichteter Bodenschichten führen kann. Diese Vorteile sind vor allem für tonreiche Böden zu erwarten. Des Weiteren wurden Veränderungen des Porengefüges durch Frost-Tau-Zyklen insbesondere in Poren mit einem Durchmesser von <200 µm beobachtet. Die Ergebnisse werden im Zusammenhang mit feuchteren Bodenbedingungen, frühsommerlicher Trockenheit und einer Intensivierung der Landwirtschaft in der gemäßigt- borealen Zone diskutiert.

Suchwörter: Bodenbearbeitung, bodenhydraulische Eigenschaften, Bodenverdichtung, Frost-Tau-Wechsel, organische Bodensubstanz

Dedication

To my grandma Margot Hofmann.

Contents

List of publications

This thesis is based on the work contained in the following papers, referred to by Roman numerals in the text:

I. Klöffel, T., Larsbo, M., Jarvis, N., Barron, J. (2023). Freeze-thaw effects on pore space and hydraulic properties of compacted soil layers and potential implications in the context of climate change. (submitted)

II. Klöffel, T., Jarvis, N., Yoon, S. W., Barron, J., Giménez, D. (2022). Relative entropy as an index of soil structure. European Journal of Soil Science, 73, e13254. DOI: 10.1111/ejss.13254

III. Klöffel, T., Jarvis, N., Yoon, S. W., Barron, J., Giménez, D. (2023). Erratum to "Relative entropy as an index of soil structure". European Journal of Soil Science, 74, e13407. DOI: 10.1111/ejss.13407

IV. Klöffel, T., Barron, J., Nemes, A., Giménez, D., Jarvis, N. (2023). Soil, climate, time and site factors as drivers of soil structure evolution in agricultural soils from a temperate-boreal region. (submitted)

Papers II and III are reproduced with the permission of the publisher.

The contribution of Tobias Klöffel to the papers included in this thesis was as follows:

I. Planning of experiment, sampling, performance of laboratory analyses (expect for soil water retention curve measurements), data analysis, manuscript writing

II. Model development, code writing, data collection, data analysis, manuscript writing

III. Manuscript writing

IV. Data collection, code writing, formal analysis, data analysis, manuscript writing

Abbreviations

h	Pressure head [L]
K	Hydraulic conductivity [L T^{-1}]
PWP	Permanent wilting point
r	(Equivalent) pore radius [L]
SWRC	Soil water retention curve
θ	Soil water content [L^3 L^{-3}]
ϕ	Total soil porosity [L^3 L^{-3}]
ϕ_{tex}	Total porosity of the reference soil without structural pores [L^3 L^{-3}]
ϕ_{vis}	X-ray visible porosity [L^3 L^{-3}]
χ	Euler-Poincaré number [-]
ψ_m	Soil matric potential [M L^{-1} T^{-2}]

1. Introduction

The climate in the temperate-boreal zone is changing fast. The early summer drought of 2018, which had a profound impact on the agricultural sector in northern Europe (Rousi et al., 2023), was a reminder that climate change is already happening. The temperate-boreal zone, here defined as the geo-climatic area where the temperate midlatitudes transition into the boreal zone (Schultz, 2005), is expected to experience such weather phenomena more often in the future (Grusson et al., 2021; Spinoni et al., 2018). On the other hand, periods of water excess will be observed more frequently in late summer, autumn and winter (Donnelly et al., 2017; Roudier et al., 2016; Strandberg et al., 2014). And while higher temperatures may lead to more favourable conditions for crop production in this part of the world (Klöffel et al., 2022), more frequent periods of "too much" and "too little" water pose a threat to the productivity of cropping systems and, ultimately, food production (Boyer, 1982).

Soils are key for maintaining the productivity of cropping systems. Their ability to retain and transport water ensures water supply during times of demand and the removal of excess water from the root zone to prevent hypoxia or anoxia (Fang and Su, 2019; Gupta et al., 2022a; Kukal et al., 2023). The water storage and transport functions of soils are determined by their hydraulic properties. These, in turn, depend on the characteristics of the soil pore space or, in other words, soil structure (Rabot et al., 2018; Scarlett et al., 1998). A "good" soil structure may therefore help alleviate water anomalies by regulating soil water functions (Wolf et al., 2023).

The structure of agricultural soils is not static but changes in response to various anthropogenic and natural factors (Bodner et al., 2013b; Ghezzehei and Or, 2003; Hirmas et al., 2018; Leuther et al., 2023). These factors are interlinked and, by altering soil structure, affect key soil hydrological
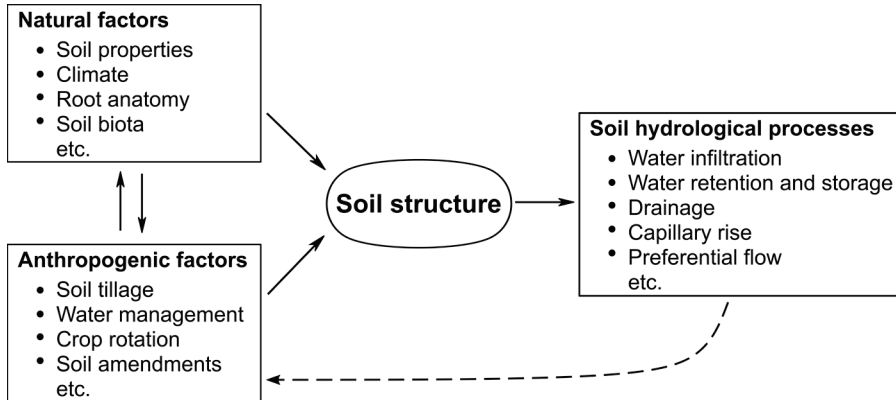
Figure 1. The structure of agricultural soils is affected by natural and anthropogenic factors, which have direct consequences for various soil hydrological processes (solid arrows). In turn, quantification of soil hydrological processes can inform soil and water management strategies (dashed arrow). Partly based on Rabot et al. (2018), Skaalsveen et al. (2019) and Vereecken et al. (2022).

processes such as water infiltration, retention and drainage (Figure 1, solid arrows). Thus, these factors may play a decisive role in determining whether soil structure develops in favour or against the water regulating functions desired for agricultural soils. On the other hand, the quantification of soil hydrological processes can provide insights for soil and water management strategies that aim to support such water regulating functions by influencing soil structure (Figure 1, dashed arrow).

Climate constitutes one of the factors driving the development of soil structure. Belonging to the five factors of soil formation (the other four being parent material, biota, time and relief), climate drives pedogenic processes and creates identifiable, structural patterns in soils (Jenny, 1941; Zech et al., 2022). By controlling long-term soil temperature and moisture regimes, climate exerts an important influence on the rate and magnitude of physical, chemical and biological soil processes (Dominati et al., 2010; Robinson et al., 2019). Besides this, climate determines the way agricultural soils are managed. It is therefore timely to ask whether climate change, by altering temperature and precipitation patterns, may lead to biophysical and chemical feedbacks in soils that might alter soil hydrological processes and soil

moisture states at both short and long time scales (Hirmas et al., 2018; Robinson et al., 2019). This is also relevant in the context of physical soil degradation processes such as soil erosion and compaction, which depend on the soil moisture state and may accelerate with climate change (Amundson et al., 2015; Gregory et al., 2015). It is therefore crucial to understand the causal relationships between climate-driven processes and soil structure as well as their implications for soil hydrological processes, both to inform soil management strategies and to foresee potential adverse effects with climate change.

2. Background

2.1 The concept of soil structure

Soil structure, increasingly also referred to as soil architecture (Vogel et al., 2022; Young et al., 2001), has been defined as "the spatial heterogeneity of the different components of soil" (Dexter, 1988) or, explicitly acknowledging its non-solid component, as "the spatial arrangement of solids and voids across different scales without considering the chemical heterogeneity of the solid phase" (Rabot et al., 2018). In line with these definitions, soil structure may be regarded as a broad concept that helps to describe and convey information about the physical status of soils.

Two contrasting perspectives have been suggested from which soil structure can be approached: (i) the solid perspective, and (ii) the pore perspective (Rabot et al., 2018; Vogel et al., 2022). While the former uses the size distribution and various stability indices for aggregates as indicators of soil structure, the latter focuses on different pore-space characteristics. In agricultural soils, the concept of aggregates has contributed to our understanding of, for example, seedbed quality, soil surface crusting and sealing, and soil erosion (Dexter, 1988; Håkansson et al., 2002; Young et al., 2001). However, for the study of water-related soil processes and functions, it has been advocated to focus on the soil domain in which water is actually stored and transported, that is, the pore space (Rabot et al., 2018; Young et al., 2001). This is why, in this thesis, the concept of soil structure is used with a focus on the characteristics of the soil pore space.

Soil structure shows three important characteristics. First, as entailed in the definition by Rabot et al. (2018), soils are structured at multiple scales (Figure 2), with each scale showing different mechanisms and driving factors
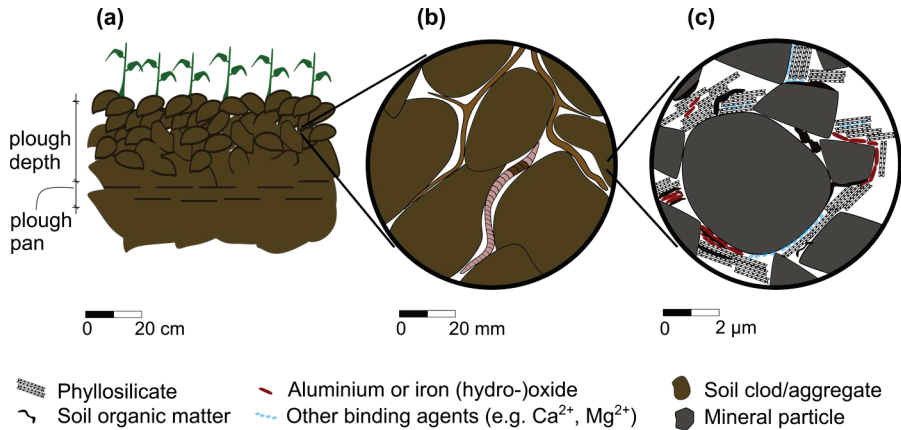
Figure 2. Soils are structured at multiple scales. **(a)** At field scale, soil management is an important driver of soil structure, leading to the creation of large pores and a fragmented, dynamic topsoil layer (plough layer). This topsoil layer is commonly underlain by a compacted soil layer (the "plough pan") lacking large structural pores and showing a platy macrostructure. **(b)** At medium scale, soil structure is strongly modified by biotic factors such as root growth and the activity of soil biota. **(c)** At smaller scales, soil structure is mainly determined by the packing and properties of mineral soil particles as well as their aggregation by soil organic matter turnover, aluminium and iron (hydro-) oxides, and other binding agents. Illustration inspired by Totsche et al. (2018), Lucas et al. (2020) and Or et al. (2021).

of soil structure formation. Larger soil pores are mainly affected by soil management interventions (e.g., soil tillage), the activity of soil biota and plant roots, while the characteristics of smaller pores are largely determined by the packing and properties of the mineral soil phase, their aggregation by different binding agents, and the turnover of soil organic matter (Bodner et al., 2023; Fiès and Bruand, 1998; Lu et al., 2020; Meurer et al., 2020; Or et al., 2021; Totsche et al., 2018). The second characteristic of soil structure is that it cannot be described by a single soil property. Instead, a holistic characterisation of soil structure requires information about a set of different soil properties, which are also referred to as soil structure metrics. For example, Vogel et al. (2010) proposed the four Minkowski functionals (interpretable as porosity, surface density, mean curvature and pore connectivity, all as a function of pore diameter), extended by a pore-size

distribution function, as measures for a concise description of the pore space structure. Lastly, soil structure (and with it also its metrics) is not static but highly dynamic and constantly evolving (Sullivan et al., 2022). In agricultural soils, these dynamics result from the various natural and anthropogenic factors, which act in concert and at a wide range of spatial and temporal scales (Figure 1).

2.2 Soil hydraulic properties and their link to the soil pore space

Hydrological processes in soils are strongly affected by their hydraulic properties, of which the two most important ones are soil water retention and soil hydraulic conductivity (K). Naturally, these properties depend to a large extent on the characteristics of the soil pore space. For example, the importance of soil structure for water flow under (near-)saturated conditions has been recognised at plot (e.g., Eck et al., 2016; Jarvis and Messing, 1995), and increasingly also at continental scale (e.g., Bonetti et al., 2021; Fatichi et al., 2020; Hirmas et al., 2018; Jarvis et al., 2013).

An important pore-space characteristic with respect to soil hydraulic properties is the total soil porosity, ϕ, which defines the upper limit of water volume that can be taken up by a soil. The total soil porosity can be divided into sub-volumes of the same pore size, resulting in the pore-size distribution. This characteristic gives crucial information about the water retention and transport capacity of soils, because pores of different sizes can be associated with different soil hydrological processes (Greenland, 1977; Luxmoore, 1981). For example, Sekera (1951) and DeBoot (1957) introduced four pore-size classes, namely, wide coarse pores (>50 µm pore diameter), narrow coarse pores (50-10 µm pore diameter), medium pores (10-0.2 µm pore diameter), and fine pores (<0.2 µm pore diameter). In their classification, pores larger than around 10 µm are expected to drain under the influence of gravity (Luxmoore, 1981), while water present in pores <0.2 µm is bound too strongly to the soil matrix for plants to take it up. The water stored between these two thresholds is considered plant available, where the upper and lower thresholds are also known as "field capacity" and "permanent wilting point" (PWP), respectively (Veihmeyer and Hendrickson, 1931, 1928). However, the still common habit of strictly relating both field capacity and PWP to specific pore sizes (or matric

potentials) has been criticised on several grounds. The original purpose of introducing the concept of field capacity was to describe the situation where the water flux out of the rooting zone becomes negligible, or where the redistribution of soil water due to water potential gradients is considered "minor" (Cassel and Nielsen, 1986; Gardner, 1965; Nasta et al., 2023). However, for a given water potential gradient, this water flux is not only controlled by a single pore size alone, but depends on the distribution of pore sizes in general as well as on their connectivity. Consequently, establishing a fixed pore-size limit across soil types not possible (Assouline and Or, 2014; Luxmoore, 1981). The PWP, on the one hand, is also controlled by the soil water flux and thus its pore-size limit can be criticised for the same reason (Carminati and Javaux, 2020; Czyż and Dexter, 2013; Dexter et al., 2012). On the other hand, the PWP is dependent on plant physiological traits and is therefore not solely a soil property (Czyż and Dexter, 2013; Torres et al., 2021; Wiecheteck et al., 2020). Another example of relating pore sizes to soil hydrological processes is the functional threshold for macropores "with respect to water flow and solute transport" as suggested by Jarvis (2007) between pore diameters of 300 and 500 µm.

Pores have also been subdivided conceptually based on their formation pathway and in this way linked to soil hydrological processes. In particular, pores created through the packing and properties of soil particles have been referred to as "primary", "matrix" or "textural pores", whereas pores formed by structural development from abiotic factors (e.g., swelling-shrinking, freezing-thawing) or biotic factors (e.g., animal burrows, root channels, tillage), have been referred to as "secondary" or "structural pores" (Nimmo, 2013, 1997). The structural pore domain encompasses macropores, which, by virtue of their large size, significantly impact soil water flow under saturated and near-saturated conditions, even though they usually constitute a small fraction of the total pore space (Jarvis, 2007; Luo et al., 2010). Structural pores can therefore have significant effects on infiltration and drainage rates of soils. However, as indicated in Section 2.1, structural pores are found across a wide range of pore sizes, suggesting that they are not only relevant for water transport under saturated and near-saturated conditions, but also affect pore sizes in the range that is relevant for water storage (Bodner et al., 2023; Fukumasu et al., 2022). Similarly, large textural pores of sandy soils exhibit flow rates under saturated and near-saturated conditions that are comparable with the ones of structured soils with finer

textures (Bonetti et al., 2021). It is this overlap in pore sizes that prevents a clear cut-off value between textural and structural pores.

Information about soil porosity and the pore-size distribution alone cannot convey whether water is able to flow, nor how fast it can flow between two locations in the soil for a given water potential gradient (Scarlett et al., 1998). Additional information about the geometrical and topological configuration of the soil pore space is needed (Lucas et al., 2020; Luo et al., 2010; Vogel et al., 2010). As water flow is mainly determined by the largest water-filled pores, their connectivity is an important indicator for the flow rate. In this context, the largest bottleneck of the water-filled pore space (also referred to as "critical pore diameter") has been shown to be a relevant factor for water flow (Koestel et al., 2018).

2.3 Methods and tools to characterise the soil pore space and soil hydraulic properties

2.3.1 The soil water retention curve

The soil water retention curve (SWRC) is one of the most important soil hydraulic characteristics as it conveys information about several soil hydrological and agricultural functions including the hydraulic conductivity function, infiltration capacity and plant-available water (Assouline, 2021). The soil water retention curve describes the relationship between the soil water content, θ, and the soil matric potential, ψ_m, under equilibrium conditions (Figure 3). The soil water content is expressed volumetrically or gravimetrically, whereas ψ_m is commonly expressed in units of negative pressure (De Swaef et al., 2022). The soil matric potential is also referred to as (matric) suction, capillary height, or pressure head, h, and can thus be expressed in units of length (De Swaef et al., 2022).

The soil matric potential results from the interaction between soil solids and water molecules and lumps together two different mechanisms (Luo et al., 2022; Tuller et al., 1999): (i) capillarity and (ii) adsorption. Although these two mechanisms usually overlap, they dominate ψ_m in different matric potential ranges. In particular, capillarity is the dominant mechanism in the wet range, while adsorption prevails in the dry range of the SWRC (Lu, 2016).
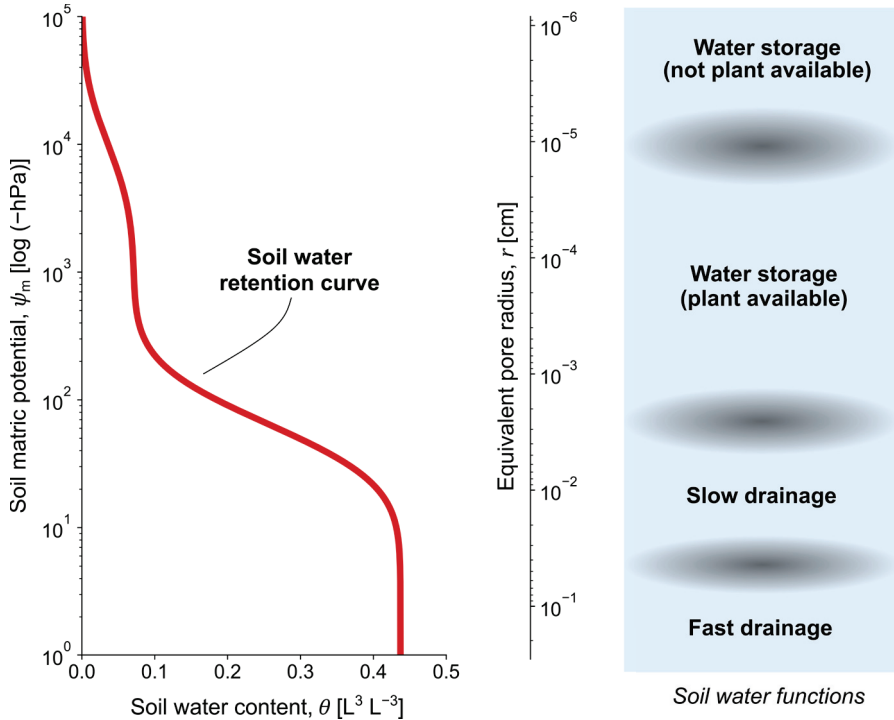
Figure 3. The soil water retention curve describes the relationship between the soil water content (θ) and the soil matric potential (ψ_m) under equilibrium conditions (left side). By converting ψ_m to the equivalent pore radius (r) via the Young-Laplace relationship, different ranges of the soil water retention curve can be linked to different soil water functions (right side; *cf*. Section 2.2).

The SWRC is often used to estimate the pore-size distribution of a soil using the capillary equation, also known as the Young-Laplace relationship. With this, different ranges of the SWRC can be linked to different soil water functions (Figure 3; *cf*. Section 2.2). The estimation of the pore-size distribution from the SWRC requires the simplified assumption that the soil pore space can be represented as a bundle of cylindrical capillary tubes with different radii. Consequently, the assumption can only be justified in the matric potential range, where capillarity is the dominant mechanism (Lu, 2020). The Young-Laplace relationship, representing the physical linkage between ψ_m and pore radius, r, is given as (e.g., Brutsaert, 1966)

$$r = -\frac{4\,\gamma_l \cos\alpha}{\psi_m\,\rho_w\,g}, \tag{1}$$

where γ_l is the surface tension between water and air, α the contact angle between liquid and solid phase, ρ_w the density of water and g the gravitational acceleration. Equation (1) is often simplified by making several assumptions, which may represent potential sources of error: α is usually set to zero signifying full contact between liquid and solid phase and thereby neglecting water repellency. For γ_l and ρ_w, values at 20°C are assumed, being $7.28\ 10^{-2}$ N m^{-1} and 1000 g cm^{-3} respectively. With these simplifications, Equation (1) can be reduced to

$$r = -\frac{0.149}{\psi_m}. \tag{2}$$

The SWRC is obtained by fitting a mathematical function or model to a set of (ψ_m/r, θ) measurement pairs. In the case of drying curves, these pairs are commonly obtained by controlling ψ_m of a soil sample through the application of suction or pressure, followed by weighing of the sample at equilibrium. The evaporation method (Peters and Durner, 2008; Schindler et al., 2010) constitutes another approach, which allows for relatively quick and quasi-continuous measurements of (ψ_m, θ) pairs in the matric potential range $0 > \psi_m > 1000$ hPa. It has been noted that a quick and reliable method between $-1000 >$ and -15000 hPa is still missing (Lu, 2020). Thus, measuring (ψ_m, θ) pairs in this particular matric potential range is time consuming.

Many models have been proposed to describe the SWRC (Assouline, 2021; Du, 2020; Sillers et al., 2001). One well-established (semi-)empirical model is the one by Kosugi (1996), which was consistently used throughout this thesis. The Kosugi (1996) model is based on the assumption that the pore sizes of a soil are log-normally distributed. In contrast to its predecessor (Kosugi, 1994), the model lacks an air-entry point, which reduces the number of parameters from five to four without notably compromising goodness-of-fit (Kosugi, 1996). The model can be classified as a "single-segment model" (unimodal) and should therefore only be used to describe the range of the SWRC in which soil water is dominated by capillary water (Du, 2020).

The expression of the Kosugi (1996) model, where θ is a function of r, is given as

$$\theta(r) = \theta_r + \frac{1}{2}(\theta_s - \theta_r) \, \text{erfc}\left[-\frac{(\ln r - \ln r_m)}{\sqrt{2}\sigma}\right] \tag{3}$$

and its derivative form describing the pore-size distribution is given as

$$\frac{\delta\theta}{\delta r} = \frac{(\theta_s - \theta_r)}{\sqrt{2\pi}\sigma r} \, \exp\left\{-\frac{(\ln r - \ln r_m)^2}{2\sigma^2}\right\}, \tag{4}$$

where θ_r and θ_s are the residual and saturated water content [L^3 L^{-3}], respectively, "erfc" denotes the complementary error function, r_m is the median (or geometric mean) pore radius [L], and σ the standard deviation of $\ln(r)$ [-]. A major advantage of the Kosugi (1996) model is that its parameters have clear physical meaning, which implies that they can be physically constrained (Fernández-Gálvez et al., 2021).

The large time investments commonly associated with the measurement of SWRCs led to the development of models that derive (ψ_m/r, θ) pairs from easier-to-measure soil physical properties such as the particle-size distribution and bulk density (e.g., Arya and Heitman, 2015; Arya and Paris, 1981; Chang et al., 2019; Mohammadi and Vanclooster, 2011; Pollacco et al., 2020). A well-known empirical model is the one by Arya and Paris (1981). In this model, the particle-size distribution of a soil is split up into several classes (or "domains"), which represent assemblages of particles of the same size packed with the same density as the bulk soil. From this, the pore-size distribution can be calculated given the following assumptions: (i) the particle shapes of each size class can be approximated by uniform-sized spheres with a respective mean particle radius, and (ii) the resulting pores can be approximated by uniform-sized cylindrical capillary tubes. It is important to note that the Arya and Paris (1981) model, similar to the other models, supposes that soil particles and the density to which they are packed are the main determinants of the resulting pore sizes. This implies that these models do not account for structural development (e.g., through aggregation, shrinkage cracks, earthworm borrows) and thus should not be used once soils show a strong structural development (Nimmo et al., 2007).

2.3.2   Soil structure and the soil water retention curve

Several attempts have been made to derive quantitative information about soil structure from the SWRC. For example, structured soils usually show a

multi-, often bimodal trajectory in their SWRCs, which has been associated with the presence of "textural" and "structural" pore domains (*cf.* Section 2.2; Nimmo, 1997; Reynolds, 2017). Thus, one approach has been to subdivide the SWRC by fitting two superimposed unimodal water retention models (e.g., Dexter et al., 2008; Durner, 1994; Jensen et al., 2019; Romano et al., 2011; Ross and Smettem, 1993; Zhang et al., 2022), where one of these models is associated with the structural pore domain and is therefore assumed to provide information about the size and distribution of the structural pores. However, due to the overlap of pore sizes of textural and structural pores, a multimodal SWRC does not necessarily imply a well-developed soil structure, but can also result from the grading of soil particles (Fredlund et al., 2000). Similarly, the presence of structural pores at smaller scales does not necessarily cause deviations from a unimodal SWRC.

Another attempt to derive quantitative information about soil structure from the SWRC is the so-called "S-index" proposed by Dexter (2004a, 2004b, 2004c). This index uses the magnitude of the slope at the inflection point of the SWRC, where θ is a function of $\ln(h)$, as a measure of soil structure (Dexter, 2004b). In essence, a steep slope at the inflection point was thought to suggest a larger degree of soil structure or soil structural quality. However, Dexter (2004a) himself showed that the S-index is strongly dependent on soil texture. For example, applying the index to structureless homogeneous sandy soils would lead to false conclusions about the degree of soil structure since they will show a steep slope at the inflection point (Reynolds et al., 2009).

Finally, Yoon and Giménez (2012) applied the concept of Shannon entropy to the SWRC and proposed this as a potential measure of soil structure. This approach was motivated by the observation that the development of soil structure increases ϕ as well as the heterogeneity (or variance) of the pore-size distribution (e.g., Crawford et al., 1995; Hwang and Choi, 2006), consequently leading to an increase in Shannon entropy. However, this approach is similarly sensitive to soil texture as, for example, the variance of pore sizes usually increases with increasing clay content (Hwang and Choi, 2006).

It is evident that the problem inherent in these approaches is the difficulty in separating the textural from the structural pore space when using the SWRC to derive information about soil structure. This is the consequence of the previously noted multi-scale nature of soil structure and the overlap in

pore sizes between textural and structural pores (*cf.* Section 2.1). Deriving quantitative information about the degree of structural development that is comparable across textural classes therefore requires a method that can account for the effects of soil texture on the SWRC.

2.3.3 X-ray computed tomography

The SWRC can only provide estimates of the pore-size distribution of a soil, while other soil structure metrics that are important for soil hydrological processes are difficult to derive. X-ray computed tomography (X-ray CT) is a non-invasive and non-destructive imaging technique, which enables the direct study of the soil pore space down to micrometer resolutions (e.g., Jarvis et al., 2017b; Luo et al., 2010; Young et al., 2001). In recent years, X-ray CT has become a key technology for improving our understanding of soil structure (Young et al., 2001). Figure 4 shows an exemplary pore space derived from X-ray CT measurements for a soil with silt loam texture.

Various pore-space characteristics relevant in the context of soil hydrological processes can be derived from X-ray CT measurements. These include direct measurements of the X-ray visible porosity, ϕ_{vis}, and the pore-size distribution within the visible range of the X-ray. Furthermore, different metrics of pore connectivity can be derived from X-ray CT measurements. Two commonly used metrics are the Euler-Poincaré number, χ, and the connection probability of two randomly chosen pore voxels, Γ. A low χ indicates a high connectivity of pores, which is however not necessarily equivalent with a long-range connectivity of pore clusters (Renard and Allard, 2013). The connection probability Γ better reflects this long-range connectivity due to its relation to the percolating fraction of the pore space (see below; Jarvis et al., 2017b; Lucas et al., 2020). The value of this metric lies between 0 (many small unconnected pore clusters) and 1 (one large connected pore cluster) and is given as (Renard and Allard, 2013)

$$\Gamma = \frac{1}{N_p^2} \sum_{k=1}^{N_i} n_k^2 \, , \tag{5}$$

where N_{p} is the number of all pore voxels, n_{k} the number of pore voxels in cluster k and N_{i} the number of clusters.
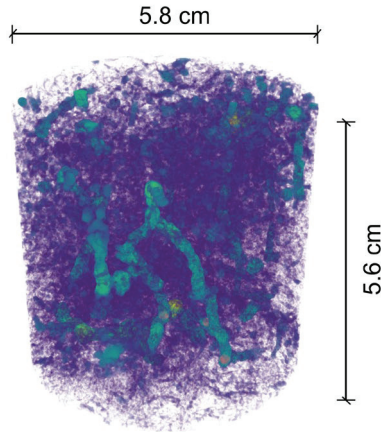
Figure 4. Example of a pore space derived from X-ray CT measurements. The different colours represent different pore sizes. The soil column was scanned at 55 μm X-ray resolution and the soil has a silt loam texture.

Due to the large spatial heterogeneity of soil structure, the situation may arise where a relatively high Γ does not result in a percolating pore space (i.e., a pore space that is connected from top to bottom) for a soil volume of interest. Thus, a third useful metric for pore-space connectivity in the context of soil water flow is the percolating fraction of the X-ray visible pore space across a given soil volume, F_P (Jarvis et al., 2017b; Koestel et al., 2020). This fraction can be considered as an indicator of the pore network contributing to soil water flow. It is important to note that pore-space connectivity is positively related to ϕ_{vis} (Jarvis et al., 2017b; Lucas et al., 2020). In particular, as ϕ_{vis} increases from 0 to larger values, the two connectivity metrics Γ and F_P commonly show a strong increase, which gradually levels off close to a value of 1, thus exhibiting a logistic ("S-shaped") relationship with ϕ_{vis} (Lucas et al., 2020). The exact relationship, however, is dependent on the interplay between X-ray resolution and soil volume as pore connectivity metrics are sensitive to both of these aspects (Koestel et al., 2020; Lucas et al., 2020). Lastly, X-ray CT can be used to identify the critical pore diameter, that is, the smallest pore neck encountered along the path of least resistance through a given soil volume. The critical pore diameter has

been found to be a useful metric for predicting saturated K (Koestel et al., 2018).

The use of X-ray CT as a means to quantify soil structure involves some limitations. For example, the resolution of X-ray images stands in direct conflict with the sample size in that higher resolutions require smaller samples. This lowers the chances to cover the full spatial heterogeneity of the structural pore space. Koestel et al. (2020) recommended soil samples larger than the commonly used volume of 100 cm^3 to appropriately describe soil hydraulic processes that depend on macropore network connectivity. Furthermore, Lucas et al. (2020) pointed out that pores smaller than four voxels in diameter may not be captured properly and are thus sensitive to image processing routines. Another important aspect is the amount of data produced by X-ray CT (Young et al., 2001) and the high computational demands when processing this data. Finally, data processing is time-consuming, which can become an important factor given that many samples are needed to adequately represent the spatial heterogeneity of soil structure.

2.3.4 Saturated and near-saturated hydraulic conductivity

Saturated and near-saturated hydraulic conductivity, K, are controlled by the largest pores in soil. Thus, measurements of saturated and near-saturated K can be used as surrogates for the characteristics of these pores (e.g., Luo et al., 2010; Sandin et al., 2017). Under laboratory conditions, measurements of saturated K are commonly carried out with the constant head method. However, determining saturated K from undisturbed soil samples of limited size in the laboratory often produces highly variable data due to the large spatial heterogeneity of soil structure in the field, even at small spatial scales (Luo et al., 2010; Schwen et al., 2011). A large number of replicates is necessary to account for this heterogeneity, which similarly applies to measurements in the field. This issue is less pronounced for measurements of K in the near-saturated range using tension infiltrometers (e.g., Alletto and Coquet, 2009; Messing and Jarvis, 1993; Sandin et al., 2017). Saturated K can also be determined indirectly through, for example, extrapolation of near-saturated K measurements using regression models (Messing and Jarvis, 1993), estimations from the SWRC (Pollacco et al., 2017), or the derivation from pore-space characteristics (Eck et al., 2016).

2.4 Climate and its link to the dynamics of soil structure and soil hydraulic properties

The structure of agricultural soils is constantly remodelled through both *direct*, *abiotic* and *indirect*, *biotic* climate-driven processes. Examples of such processes are listed in Table 1. As a result, climate variables constitute important predictors for soil structure metrics and soil hydraulic properties at different time scales (e.g., Gupta et al., 2021; Wu et al., 2023).

Table 1. Examples of direct, abiotic and indirect, biotic climate-driven processes affecting soil structure and soil hydraulic properties.

Direct, abiotic processes	Indirect, biotic processes
Rainfall	Root growth
Freezing and thawing	Soil biota activity
Wetting and drying (including shrink-swell processes)	Soil management (e.g., soil tillage, irrigation)
	Soil organic matter input

2.4.1 Short-term seasonal dynamics

Short-term seasonal dynamics of topsoil structure and hydraulic properties in response to climate-driven processes have been extensively studied. Rainfall, wet-dry cycles (associated with swell-shrink dynamics), and freeze-thaw cycles all have shown to contribute to the seasonal dynamics of the pore space. For example, Bodner et al. (2013b) demonstrated that intra-seasonal variability of the pore-size distribution of an arable soil in a temperate climate was strongly related to different climatic parameters, while inter-seasonal dynamics were mainly influenced by soil mechanical disturbance. Similarly, Strudley et al. (2008) stressed that temporal differences in infiltration and K due to seasonal climate-driven processes were greater than differences in response to soil management practices.

Rainfall has been shown to decrease saturated and near-saturated K, infiltration capacity, macropores and ϕ in the topsoil, which is the result of the mechanical impact of raindrops, and is often accompanied with soil surface sealing (Alletto and Coquet, 2009; Bodner et al., 2008; Messing and Jarvis, 1993; Sandin et al., 2017; Schwen et al., 2011). In the event of a preceding tillage activity, the drying period after rainfall commonly leads to

a phenomenon known as "hydraulic compaction" (Ghezzehei and Or, 2000). Hydraulic compaction refers to the coalescence of loosely-packed soil aggregates induced by increasing capillary tensile stresses upon soil drying and often leads to a decrease in ϕ, macroporosity and saturated K (Mapa et al., 1986; Mubarak et al., 2009; Or and Ghezzehei, 2002; Zhang et al., 2017). The opposite effect on these soil properties as well as an increase in pore connectivity has been attributed to the impact of repeated wet-dry cycles in soils containing a sufficient amount of clay and/or organic matter (Alletto and Coquet, 2009; Arthur et al., 2013; Bodner et al., 2013b; Carter, 1988; Hu et al., 2012; Kreiselmeier et al., 2019). These wet-dry cycles lead to swelling and shrinking of the soil matrix and thereby induce changes in soil structure, especially in the macropore region, which are mostly reversible (Bodner et al., 2013a; Diel et al., 2019; Leuther et al., 2023). However, it has been observed that these changes can also be irreversible, for example after periods of intense soil drying (Peng et al., 2007; Robinson et al., 2016). There is evidence that this phenomenon occurs as soon as the maximum degree of drying a soil has experienced is exceeded, shifting the soil into an "alternative stable state" with permanent implications for soil water functions (Bruand and Prost, 1987; Peng et al., 2007; Robinson et al., 2016).

While reported effects of rainfall and wet-dry cycles on soil structure are mostly consistent between studies, the effects of freezing and thawing seem conflicting. In particular, studies report both increases and decreases in ϕ (Asare et al., 1999; Ma et al., 2019; Starkloff et al., 2017; Unger, 1991), macroporosity or ϕ_{vis} (Arthur et al., 2013; Carter, 1988; Fu et al., 2019; Starkloff et al., 2017), pore connectivity (Leuther and Schlüter, 2021; Starkloff et al., 2017) and saturated K (Asare et al., 1999; Benoit and Bornstein, 1970; Bodner et al., 2013b). The reasons for these contrasting results, however, remain unclear.

Several factors may control how large the effects of climate-driven processes on soil structure and soil hydraulic properties are. For example, some studies point towards the role of soil management, where no-tillage systems often show a higher stability (or resilience) of the soil pore space and soil hydraulic properties compared to conventional or reduced-tillage systems (Alletto and Coquet, 2009; Kreiselmeier et al., 2019; Miranda-Vélez et al., 2023; Schwen et al., 2011). Furthermore, the impact of wetting and drying on soil structure strongly depend on clay mineralogy and soil organic matter content, both of which determine the shrink-swell behaviour of soils

(Arthur et al., 2013; Cornelis et al., 2006; Peng et al., 2007). However, uncertainty still remains with respect to the role of soil organic matter on the effects of freezing and thawing (Taina et al., 2013).

2.4.1.1 Long-term dynamics

The effects of climate-driven processes described above on soil structure and soil hydraulic properties seem mostly ephemeral (Leuther et al., 2023), although compelling evidence for this is still missing. Despite the comparatively small number of studies, there are indications that climate has the potential to profoundly shape soil structure over longer time scales. For example, Jarvis et al. (2013) compiled a database from studies measuring near-saturated K in arable soils within Europe, North America and the Middle East. From these studies, saturated K, K measured at -10 hPa (K_{10}) and the contribution of macropores (defined as the difference between saturated K and K_{10}) were derived and their main controlling factors investigated. The authors revealed a positive correlation between K_{10} and annual average temperature. Although the reason for this relationship was not clear, it was suggested that it could be the result of farm vehicle trafficking on wetter soils in cooler climates, which would cause compaction, thereby decreasing K_{10}. This finding was supported by a follow-up study, which used the same database but a model with higher predictive power (Jorda et al., 2015). It turned out that annual precipitation and annual average temperature were the most important predictors for K_{10}. Along similar lines, Hirmas et al. (2018) found that macroporosity is driven by climate at the continental scale and that macroporosity is more pronounced under drier and warmer climates compared to cooler, more humid climates. This pattern was visible in both surface and subsurface horizons, and it was even apparent in ploughed horizons. Finally, a precipitation manipulation experiment on prairie soils showed that a 35% increase in water input in the form of irrigation water for 25 years caused a decline in mean infiltration rates by up to 30% for pores with equivalent diameters from 545 to 2000 µm (Caplan et al., 2019).

A common feature of the studies presented above is the challenge to separate the effects of the individual climate-driven processes and to determine their relative importance (Chandrasekhar et al., 2018; Strudley et al., 2008). In other words, it is unclear whether changes in pore-space characteristics and soil hydraulic properties were induced by direct or indirect climate-driven processes (*cf.* Table 1). Nevertheless, the studies

suggest that changes in temperature and precipitation patterns have the potential to profoundly modify the soil pore space. This can occur at relatively short time scales and may result in changes in soil hydraulic properties, particularly in the (near-)saturated range.

3. Objectives and Scope

The main objective of this thesis was to improve our understanding of the effects of climate-driven processes on the pore space structure and hydraulic properties of agricultural soils. This is important to assess potential implications for water functions in these soils in the context of climate change. The geographical focus of the thesis is the temperate-boreal zone, particularly Scandinavia. As outlined in Chapter 2, the evolution of soil structure and soil hydraulic properties is related to climate through a plethora of direct and indirect processes, and not all of these processes could be considered. Thus, the scope was limited to two main research questions that were addressed in this thesis:

1. What are the effects of freezing and thawing on the soil pore space and soil hydraulic properties, and how will a change in freeze-thaw patterns in the context of climate change affect soil water functions?

2. How important is climate relative to other factors for the evolution of the soil pore space and what are its interactive effects at larger spatial scales?

The two research questions were investigated using a variety of approaches including a meta-analysis, a laboratory experiment (**Paper I**), the application of mathematical concepts (**Paper II** and **III**), and machine learning (**Paper IV**). In the following, research question 1 and 2 will be addressed in Chapter 4 and 5 respectively. Based on the findings and discussions presented therein, the main conclusions of this thesis and future perspectives are presented in Chapter 6.

4. Freezing and Thawing

This chapter addresses research question 1 and summarizes the work on how freezing and thawing affects the soil pore space and soil hydraulic properties. The work is subdivided into two parts: (i) a meta-analysis of previous studies that investigated the effects of freezing and thawing on the soil pore space (Section 4.1), and (ii) a laboratory experiment investigating freeze-thaw effects on pore space and hydraulic properties of compacted soil layers while considering potential consequences in the context of climate change (Section 4.2). The latter is based on **Paper I**.

4.1 Freeze-thaw effects on the soil pore space: a meta-analysis

The effects of freezing and thawing on soil structure have been studied for decades. However, early studies mainly focussed on soil properties related to the soil solid phase such as aggregate-size distribution, aggregate stability, mean aggregate diameter and soil erodibility (e.g., Bryan, 1971; Dagesse, 2013; Edwards, 2013). These studies show that freezing and thawing generally leads to the breakdown of larger into smaller soil aggregates, where this effect is more pronounced with a higher number of freeze-thaw cycles, higher freezing intensity, higher soil moisture contents at the time of freezing, and lower clay contents. Furthermore, the breakdown of larger aggregates and the destruction of cohesive forces in response to freezing and thawing lead to an increased susceptibility of soils to erosion. While the effects of freezing and thawing on these soil properties seem relatively well understood, their effect on the soil pore space remain largely unclear. One reason is probably that research attention has shifted towards the soil pore space only relatively recently, enabled by the increased availability of

advanced imaging technologies such as X-ray CT (Taina et al., 2013). Furthermore, seemingly contradictory findings have been reported with respect to different pore-space characteristics (*cf.* Subsection 2.4.1). Thus, notwithstanding the still comparatively small number of studies, a meta-analysis was conducted with the aim to explain some of these contradictory findings reported in previous freeze-thaw studies focussing on the soil pore space.

Ten studies that systematically investigated the effects of freezing and thawing on different pore-space characteristics were included in the meta-analysis. It should be noted that these studies only investigated soils with properties resembling agricultural soils. The data used for analysis were extracted directly from tables or from figures using a graph data extractor. Table 2 gives an overview of the included studies as well as the pore-space characteristics they investigated. In the following, only those pore-space characteristics are discussed, which were reported in at least three of the ten studies.

Table 2. Studies included in the meta-analysis of the effects of freezing and thawing on different soil pore-space characteristics.

Study	Investigated soil pore-space characteristics
Benoit and Bornstein (1970)	ϕ
Asare et al. (1999)	ϕ
Starkloff et al. (2017)	X-ray visible porosity (ϕ_{vis}), χ, pore-size distribution (X-ray), connected porosity, specific surface area, mean pore diameter, fractal dimension
Fu et al. (2019)	ϕ, pore-size distribution (estimated from SWRC)
Ma et al. (2019)	ϕ
Leuther and Schlüter (2021)	ϕ, ϕ_{vis}, χ, Γ, mean pore diameter, mean pore distance, pore-size distribution (X-ray)
Liu et al. (2021a)	ϕ_{vis}, χ, fractal dimension, pore-size distribution (X-ray)
Liu et al. (2021b)	Number of pores
Ma et al. (2021)	ϕ_{vis}, χ, number of pores, pore-size distribution (X-ray)
Miranda-Vélez et al. (2023)	ϕ_{vis}, pore-size distribution (X-ray), mean pore diameter, mean pore distance

All studies reported changes in either ϕ, ϕ_{vis}, or both (Table 2). The analysis revealed that the effects of freezing and thawing on ϕ and ϕ_{vis} depend on the initial bulk density of the soil. As shown in Figure 5a, freezing and thawing generally leads to a decrease in ϕ at relatively low initial bulk densities, while ϕ increases at relatively high initial bulk densities. This demonstrates that freezing and thawing can have both a consolidating and a loosening effect on soils, depending on the state of compaction. Besides this, freeze-thaw effects on ϕ_{vis} seem to be dependent on the resolution of the X-ray CT. Specifically, Figure 5b shows that freezing and thawing tended to have larger positive effects on ϕ_{vis} at higher X-ray resolution (i.e., at a lower X-ray resolution limit), while negative or no effects were observed at lower resolution (i.e., at a higher X-ray resolution limit), depending on the initial bulk density. A high resolution with relatively smaller pores being covered by the X-ray CT implies a smaller sample size (*cf.* Subsection 2.3.3). This suggests that freeze-thaw effects may be more pronounced in relatively smaller pores. Indeed, studies that reported changes in pore volume for different pore-size ranges showed that most changes occur in pores with diameters <200 µm. This is illustrated in Figure 6, where absolute and relative changes are shown for different pore-size ranges, normalized by the largest mean absolute or mean relative change respectively. The variability within the individual pore-size ranges, which is largest in pores with diameters <200 µm, can partly be explained by the number of freeze-thaw cycles. Specifically, the relationship shown in the inset of Figure 6 suggests that the pore space is continuously modified with each freeze-thaw cycle, especially in relatively smaller pores. Although freezing and thawing can lead to either an increase or a decrease in the abundance of relatively smaller pores (Figure 6), mean pore diameters have shown to decrease in response to freezing and thawing (Leuther and Schlüter, 2021; Miranda-Vélez et al., 2023; Starkloff et al., 2017), suggesting that smaller pores tend to become more abundant relative to larger ones.

Four of the ten studies investigated changes in pore connectivity in response to freezing and thawing (Table 2). All of them used the Euler-Poincaré number, χ, as a measure of pore connectivity, albeit normalized to different dimensions (e.g., volume, pixels) or without reporting units (Ma et al., 2021). Besides χ, one study used the connection probability, Γ (Leuther and Schlüter, 2021), and another the connected porosity (Starkloff et al., 2017) as additional measures of pore connectivity. In general, the studies
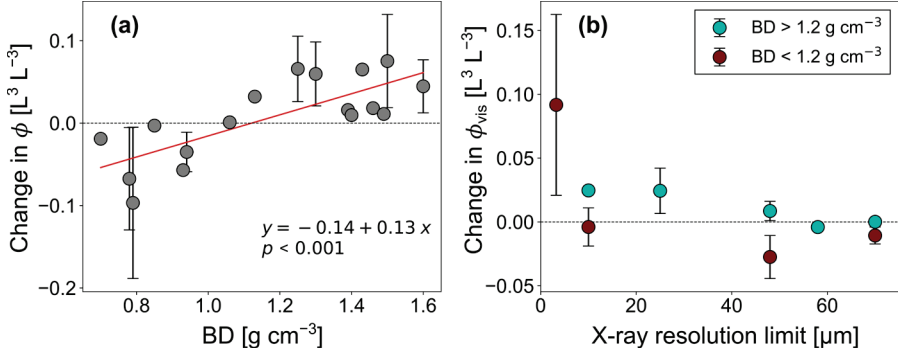
Figure 5. Effects of freezing and thawing on total porosity (ϕ) and X-ray visible porosity (ϕ_{vis}) depend on initial bulk density (BD; **a**) and X-ray resolution limit (**b**) respectively. Error bars indicate standard errors of the mean.

reported increases in pore connectivity (expressed by a decrease in χ or an increase in Γ and connected porosity) for concomitant increases in ϕ_{vis} (Leuther and Schlüter, 2021; Liu et al., 2021; Ma et al., 2021), while the opposite was the case for a decrease in ϕ_{vis} (Leuther and Schlüter, 2021; Starkloff et al., 2017). Thus, the observed variability in effects of freezing and thawing on pore connectivity can at least partly be explained by its variable effects on ϕ_{vis}. As previously noted, the positive relationship between pore connectivity and ϕ_{vis} is well-known and has been demonstrated in several studies (e.g., Jarvis et al., 2017b; Koestel et al., 2020; Lucas et al., 2020). One exception, however, was reported by Leuther and Schlüter (2021), where pore connectivity increased despite a decrease in ϕ_{vis} for a disturbed and undisturbed silty clay measured at 10 µm X-ray resolution. This suggests that a positive relationship between pore connectivity and ϕ_{vis} may not always hold. Whether this observation is a particular characteristic of the effects of freezing and thawing on the soil pore space remains to be investigated.

Other factors may also have contributed to the contrasting results reported in the different studies. For example, soil samples with both undisturbed (Fu et al., 2019; Leuther and Schlüter, 2021; Ma et al., 2019, 2021; Miranda-Vélez et al., 2023; Starkloff et al., 2017) and disturbed (Asare et al., 1999; Benoit and Bornstein, 1970; Leuther and Schlüter, 2021; Liu et al., 2021) soil structure have been investigated. In addition, these samples varied with
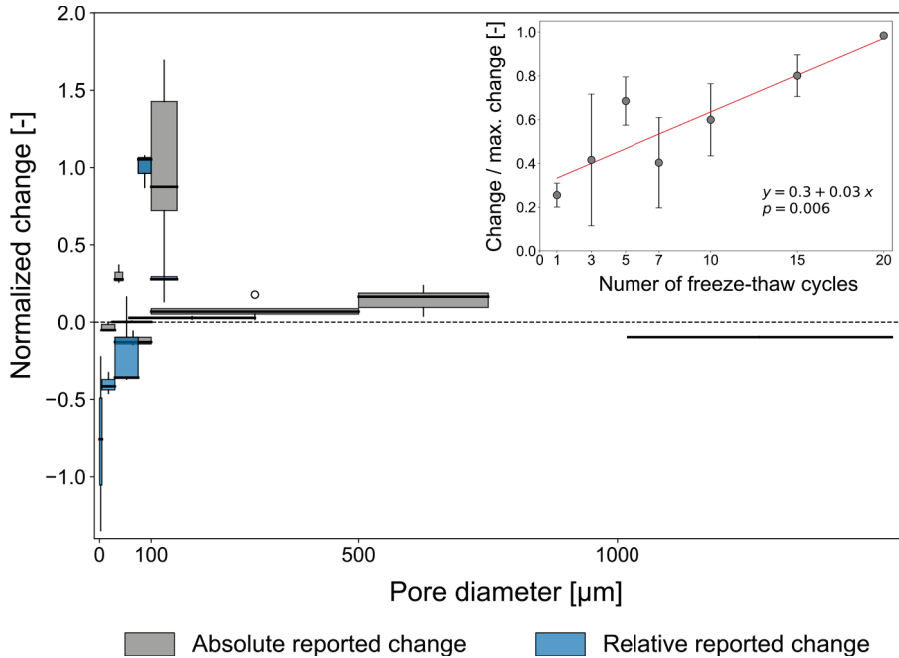
Figure 6. Freezing and thawing affects the pore space mostly in relatively smaller pores. The boxplots show absolute (gray) and relative (blue) changes in pore volume reported for different pore-size ranges, which are indicated by the width of the boxplots. The reported changes were normalized by the largest reported mean absolute and mean relative change respectively. The inlet shows changes across all pore-size ranges normalized by the maximum changes reported in the different studies (both absolute and relative) as a function of the number of freeze-thaw cycles. Errorbars indicate standard errors of the mean.

respect to soil texture, soil water content at the time of freezing, and temperature amplitudes. In this analysis, no clear relationship between these factors and the effects on the investigated pore-space characteristics could be identified, which may be related to the fact that some of the factors were only sparsely reported in the studies (e.g., soil water content at the time of freezing) and that the number of studies was relatively small. However, it has been demonstrated that these factors partly control the effects of freezing and thawing on different soil aggregate parameters (e.g., Bryan, 1971; Bullock et al., 1988). Finally, it should be noted that simulated temperature

amplitudes, and also rates of shifts between freezing and thawing, were sometimes far from what would occur under natural conditions (Asare et al., 1999; Starkloff et al., 2017). This may have led to unrealistic effects on the soil pore space (Henry, 2007; Dagesse, 2010). Considering natural boundary conditions when designing future freeze-thaw experiments should thus be a priority.

4.2 Freeze-thaw effects on the structure and hydraulic properties of compacted arable soils and implications in the context of climate change

The studies discussed in the previous section focussed exclusively on the uppermost topsoil layer. However, in the temperate-boreal zone, the freezing front can penetrate to greater depths, thereby also affecting the structure of the subsoil (Jabro et al., 2014). This is particularly relevant for agricultural soils, which often exhibit a deterioration of soil structure below tillage depth and, as a result, a decrease in hydraulic conductivity and drainage rates (Coquet et al., 2005; Richard et al., 2001; Schlüter et al., 2020).

Freeze-thaw patterns are expected to change in response to winter warming in the temperate-boreal zone (Donnelly et al., 2017; Jungqvist et al., 2014; Shiklomanov, 2012; Strandberg et al., 2014). This is mainly the result of a decrease in the thickness and extent of snow cover, which acts as an insulation layer between the soil and the atmosphere (Luomaranta et al., 2019; Pulliainen et al., 2020). The gradual shrinkage of this insulation layer is expected to increase soil temperature fluctuations and thereby the number of freeze-thaw cycles, while it may also lead to increased freezing intensities, that is, lower minimum soil temperatures (Decker et al., 2003; Demand et al., 2019; Halim and Thomas, 2018). Potential consequences of these changing freeze-thaw patterns for the soil pore structure and soil water functions have not been explored. This knowledge, however, is relevant because the increase in rainfall during winter (Donnelly et al., 2017; Roudier et al., 2016) and the increased likelihood of droughts during early summer (Grusson et al., 2021), which are projected for parts of the temperate-boreal zone, may challenge the capacity of agricultural soils to buffer such water anomalies.

For these reasons, a laboratory experiment was performed in **Paper I** with the aim to investigate the effects of freezing and thawing on different pore-

space characteristics and soil hydraulic properties of untilled, compacted soil layers. Furthermore, potential consequences of changes in these soil properties in the context of climate change were considered.

4.2.1 Outline of laboratory experiment

Intact soil cores (diameter: 6.5 cm, height: 7.5 cm) were taken from two soils in central Sweden, which were under the same reduced tillage management since 1997. One soil was classified as Stagnic Phaeozem having a silt loam texture (hereafter referred to as "silt loam"), while the other soil was classified as Eutric Cambisol having a silty clay loam texture (hereafter referred to as "silty clay loam"). The sampling depth was 12-20 cm, which corresponds to the compacted and untilled soil layer directly below the plough layer. Three freeze-thaw treatments were simulated in this laboratory experiment: "Present I", "Present II" and "Future". Present I and Present II scenario were derived from soil temperature observations close to the two sampling sites, while the Future scenario was derived from climate change projections for central Sweden. Relative to Present I and Present II scenario, the Future scenario is characterised by an increase in the number of freeze-thaw cycles and freezing intensity. A summary of the freeze-thaw characteristics of the three different scenarios is provided in Table 3.

Table 3. Definition of freeze-thaw scenarios simulated in this laboratory experiment. Reproduced from **Paper I**.

Freeze-thaw scenario	Number of simulated freeze-thaw scenarios	T_{min} [°C]
Present I	0	-
Present II	1	−3
Future	5	−5

The workflow of the laboratory experiment was made up of five components: (i) sample preparation, (ii) measurements of pore-space characteristics by X-ray CT, (iii) simulation of freeze-thaw scenarios, (iv) measurement of soil water retention curves, and (v) measurements of infiltration rates in the near-saturated range. Sample preparation comprised water saturation of the cores and subsequent equilibration at a pressure head

of −40 cm. Furthermore, the cores were insulated from the sides and bottom to ensure top-down freezing and thawing. To study changes in different pore-space characteristics, X-ray CT was applied at a resolution of 55 µm before, during (i.e., after the first freeze-thaw cycle in the Future scenario) and after simulation of the freeze-thaw scenarios. Five pore-space characteristics, which were considered relevant for water flow and retention, were calculated from the X-ray CT images: X-ray visible porosity (ϕ_{vis}), pore-size distribution, the percolating fraction of ϕ_{vis} (F_P), connection probability (Γ), and the critical pore diameter (d_c). The freeze-thaw scenarios were simulated in a programmable cooling incubator, where soil temperature was monitored in four independent samples using soil temperature probes. After the last X-ray CT scan, water retention was measured at eight pressure heads (−10, −30, −50, −100, −300, −600, −1000, and −15000 cm) using sandboxes, ceramic plates and pressure plate extractors. From these measurements, the pore-size distribution was derived using Equation (2). Lastly, infiltration rates were measured at −6 and −1 cm pressure head using mini-disk infiltrometers to estimate changes in near-saturated K (Zhang, 1997).

4.2.2 Changes in pore-space characteristics and soil hydraulic properties

X-ray visible porosity increased in both soils in response to freezing and thawing. The increase was on average larger in the silt loam (Present II scenario: $p = 0.003$; Future scenario: $p = 0.012$) compared to the silty clay loam (Present II scenario: $p = 0.094$; Future scenario: $p = 0.05$). The analysis of X-ray-derived pore-size distributions revealed that the increase in ϕ_{vis} was mainly due to increases in pore volume fractions between the X-ray resolution limit up to around ca. 0.2 mm pore radius (Figure 7). In contrast, pore radii greater than 0.2 mm showed seemingly random changes in both soils. These observations match well with the identified trends shown in Figure 5 and 6.

Based on changes in the two pore connectivity metrics (F_P and Γ), freezing and thawing increased the X-ray visible pore-space connectivity in the silt loam ($p < 0.05$), while there was only weak evidence for an increase in the silty clay loam after the Future scenario ($p < 0.1$). The reason for this is probably the larger variability of effects observed in the silty clay loam, where some of the samples showed quite substantial increases in pore
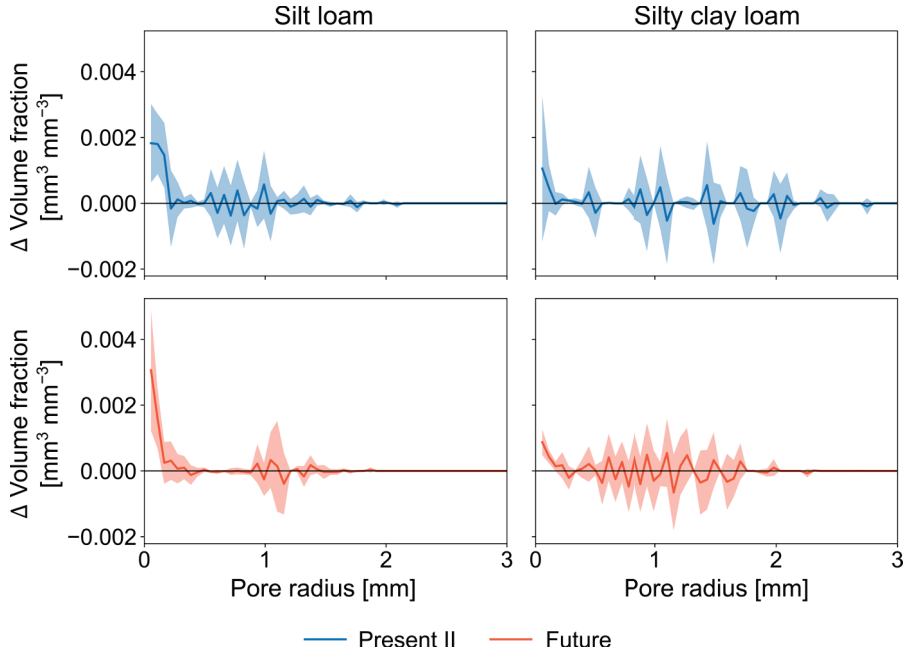
Figure 7. Absolute changes (Δ) in pore volume across pore radii measured by X-ray CT at the end of Present II (blue) and Future (red) scenario. Lines and shaded areas indicate arithmetic means and 95% confidence intervals respectively. Adapted from **Paper I**.

connectivity (e.g., up to 250% increase in Γ), while others showed only minor, no, or even slightly negative changes. Nevertheless, the increase in both pore connectivity metrics was on average larger in the silty clay loam compared to the silt loam, although the silt loam showed larger increases in ϕ_{vis}. This was because ϕ_{vis} in the silt loam was relatively large in the beginning and therefore the pore system was already highly connected so that freezing and thawing only showed minor positive effects on average. In contrast, the smaller changes in ϕ_{vis} in the silty clay loam had on average a relatively large effect on pore connectivity. Lastly, there was no evidence that d_c increased in response to freezing and thawing in the silt loam ($p >$ 0.5), whereas there was little (Present II scenario: $p = 0.109$) to moderate (Future scenario: $p = 0.031$) evidence for an increase in the silty clay loam. These findings make sense as the increase in pore-space connectivity was on average larger in the silty clay loam and, with this, the likelihood of finding

a continuous pathway through a sample with a larger minimum diameter should also be higher.

The soil water retention measurements revealed that freezing and thawing changed the distribution of pore sizes below the X-ray resolution limit in both soils. These changes seemed mostly random and without much pattern, which is in line with the findings by Liu et al. (2021a). The reasons for these seemingly random shifts in pore-size distribution are not clear, but may be related to the continuous re-distribution of water within the soil column during freezing and thawing (Koopmans and Miller, 1966; Mohammed et al., 2018; Stähli et al., 1999). More studies at smaller scales are required to reveal the underlying mechanisms.

Freezing and thawing led to an increase in near-saturated K in both soils (Figure 8). On average, near-saturated K was always smallest after Present I scenario and largest after the Future scenario, except in the silt loam at -1 cm tension. There, near-saturated K after Present II scenario tended to be larger than after the Future scenario (Figure 8). The p-values from pairwise comparisons suggest that the differences between the scenarios were in general clearer in the silt loam (smaller p-values) than the silty clay loam (larger p-values). The overall trend in near-saturated K observed for the different freeze-thaw scenarios is in line with two other studies, which investigated changes in saturated K after different numbers of freeze-thaw cycles (Asare et al., 1999; Ma et al., 2019). However, these studies indicate that the extent of changes in saturated K with an increasing number of freeze-thaw cycles may be soil-type dependent. In particular, they have demonstrated that soils with larger clay contents are more likely to show changes beyond on freeze-thaw cycle. Similar observations were made in this laboratory experiment, where modifications in the X-ray visible pore-space characteristics after the first freeze-thaw cycle were restricted to the silty clay loam (e.g., Γ and d_c), which also corresponded to the observed trends in near-saturated K at -1 cm tension. This may be related to the larger cohesive strength of soils with higher clay contents, which requires more frequent cycles of freezing and thawing to be overcome (Bullock et al., 1988). Furthermore, finer-textured soils can become more compacted as compared to coarser-texture soils in response to repeated trafficking and tillage (Gebhardt et al., 2009; Smith et al., 1997). This was also visible in this study, where the silt loam and silty clay loam had an initial bulk density of 1.30 g cm^{-3} and 1.63 g cm^{-3} respectively. Besides this, freezing and
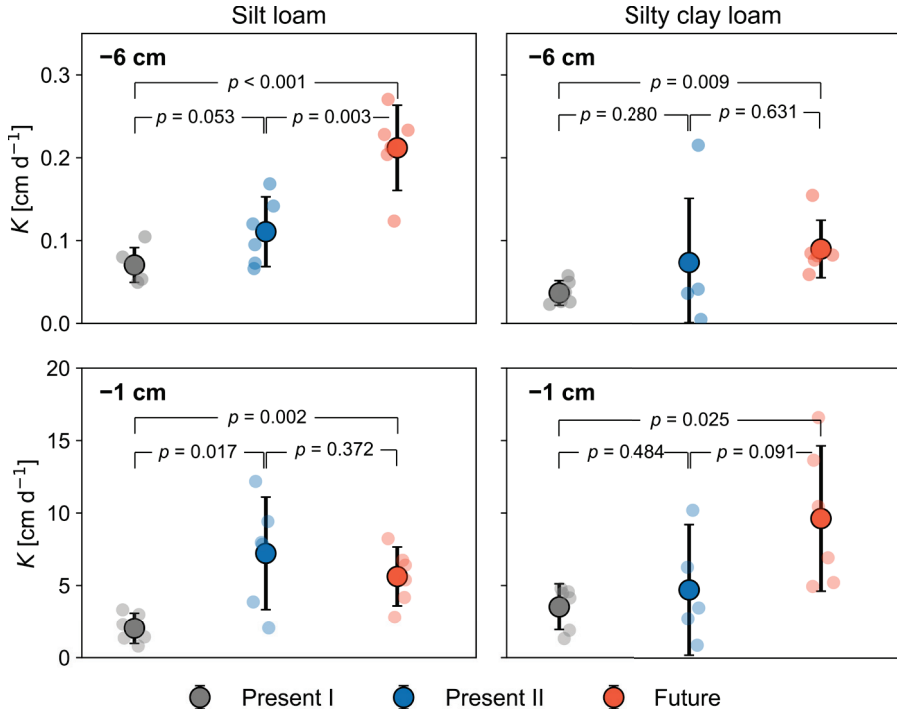
Figure 8. Hydraulic conductivity (K) in the near saturated range derived from infiltration measurements at two pressure heads: −6 cm (upper row) and −1 cm (lower row). Errorbars indicate 95% confidence intervals. Reproduced from **Paper I**.

thawing increased the variation in near-saturated K between individual samples of the same scenario in either soil (Figure 8). This suggests that it had relatively large effects on some samples, while it had only small or no effects on others. As the largest pores that were water filled during the measurements of near-saturated K were covered by the X-ray analysis, the increases in near-saturated K are expected to be the combined result of an increased fraction of pores with <200 µm radius, increases in pore-space connectivity and larger d_c. The latter two, however, mostly apply to the silty clay loam.

5. Climate and Other Drivers of Soil Structure at the Regional Scale

This chapter addresses research question 2 and summarizes the work that was conducted to investigate the main drivers of soil structure evolution in agricultural soils of the temperate-boreal zone. Of particular interest was the importance of climate. The work includes the development of a new index of soil structure (Section 5.1; **Paper II** and **III**), as well as its application to a large dataset including agricultural soils from Sweden and Norway (Section 5.2; **Paper IV**).

5.1 A new index of soil structure

Studying the role of different factors for the evolution of soil structure requires first its quantification. At regional scales, methods to quantify soil structure should ideally only require data from routine soil physical analyses, because these are available for a wide range of geo-climatic areas (e.g., European Commission, 2013; Hohenbrink et al., 2023; Nemes et al., 2001). Furthermore, such methods should be able to account for the multi-scale nature of soil structure.

A new quantitative index of soil structure was developed in **Paper II** and **III**, which only requires data on water retention, soil texture and ϕ. The index is based on the idea by Yoon (2009), who regarded soil structure as the difference in pore-size distribution between a structured soil and a hypothetical reference soil without structure, quantified using the concept of relative entropy. The initial approach presented by Yoon (2009) was refined and further developed here to account for changes in pore-size distribution and ϕ, both of which characterize soil structure formation (Bodner et al., 2023; Hayashi et al., 2006). Furthermore, the applicability of the index was

greatly extended, for example by taking into account the multi-modality in SWRCs.

5.1.1 Relative entropy as an index of soil structure

The concept of relative entropy, also known as the Kullback-Leibler divergence (KL divergence; Kullback and Leibler, 1951), originates from information theory and is a measure of the difference between two probability distributions of the same random variable, where one of the probability distributions acts as reference distribution (Kullback and Leibler, 1951). The KL divergence is always non-negative and increases as the difference between the two probability distributions becomes larger, while a value of zero indicates two identical distributions (Bishop, 2006, p. 55). Applied as an index of soil structure, the probability distributions are represented by two pore-size distributions, where one pore-size distribution is that of a structured soil and the other that of the same soil without structural pores, the (hypothetical) so-called reference soil (Yoon, 2009).

The pore-size distribution of the structured soil is estimated from the SWRC using Equation (1), while the SWRC is obtained by fitting a suitable model to measured (ψ_m, θ) pairs. The description of the SWRC should be as detailed as possible, which requires a flexible model that can account for the bi- or even multi-modal pore-size distributions found in structured soils (Jensen et al., 2019; Ross and Smettem, 1993). Prominent examples of such models are the bimodal versions of the Kosugi (1996) model (Romano et al., 2011) and the van Genuchten (1980) model (Durner, 1994), or the bimodal exponential model proposed by Dexter et al. (2008).

The pore space of the reference soil is assumed to be solely determined by the particle-size distribution and the packing density, which makes it conceptually equivalent to the textural pore space of a natural soil (Meurer et al., 2020; Nimmo, 1997). Thus, the pore-size distribution of the reference soil is estimated from the particle-size distribution, using one of the models that have been proposed for this purpose (e.g., Arya and Paris, 1981; Chang et al., 2019; Mohammadi and Vanclooster, 2011; Pollacco et al., 2020; You et al., 2022). These models use a scaling factor that maps the particle- to the pore-size distribution, often in a linear fashion. Finally, the porosity of the reference soil, ϕ_{tex}, requires a realistic estimate (e.g., Nimmo, 2013).

If $p(r)$ and $q(r)$ represent the pore-size distributions of the structured and reference soil respectively, the KL divergence (D_{KL}) can be calculated as

$$D_{KL} = \int_0^{r_{max}} p(r) \ln\left(\frac{p(r)}{q(r)}\right) dr \,, \tag{6}$$

where r_{max} is the maximum pore radius. Examples of a poorly-structured loamy sand and a well-structured clay are shown in Figure 9. It is evident that the difference in pore-size distribution between the structured and the reference soil is larger for the clay, which also results in a larger KL divergence compared to the loamy sand.

An analytical expression of Equation (6) was derived for the case where both pore-size distributions are described with the Kosugi (1996) model. This expression reads as

$$D_{KL} = (\theta_s - \theta_r)\left(\ln \frac{(\theta_s - \theta_r)\sigma_R}{(\phi_{tex} - \theta_r)\sigma_S} - \frac{1}{2} + \left[\frac{\sigma_S^2 + (\ln r_{m,S} - \ln r_{m,R})^2}{2\sigma_R^2} \right] \right), \tag{7}$$

where the additional subscripts "S" and "R" refer to the parameters of the Kosugi (1996) model of the structured and reference soil respectively. Equation 7 illustrates that the KL divergence increases with an increase in total porosity (expressed by θ_s), width of the pore-size distribution (expressed by σ_S) and median pore radius (expressed by $r_{m,S}$). Furthermore, Equation 7 shows that the KL divergence is most sensitive to model parameters related to the width (or heterogeneity) of the pore-size distributions as they appear as squared terms. This implies that the KL divergence is most sensitive to the effects of soil structure on the pore-size distribution, while it is relatively less sensitive to total porosity. The parameters ϕ_{tex} and $r_{m,S/R}$ have shown to be the least important (see **Paper II**).

5.1.2   Testing the new index of soil structure

The new index of soil structure was tested on soil data from two Swedish field experiments to see whether it follows expected trends in soil structure due to changes in soil management and land use. The first dataset included
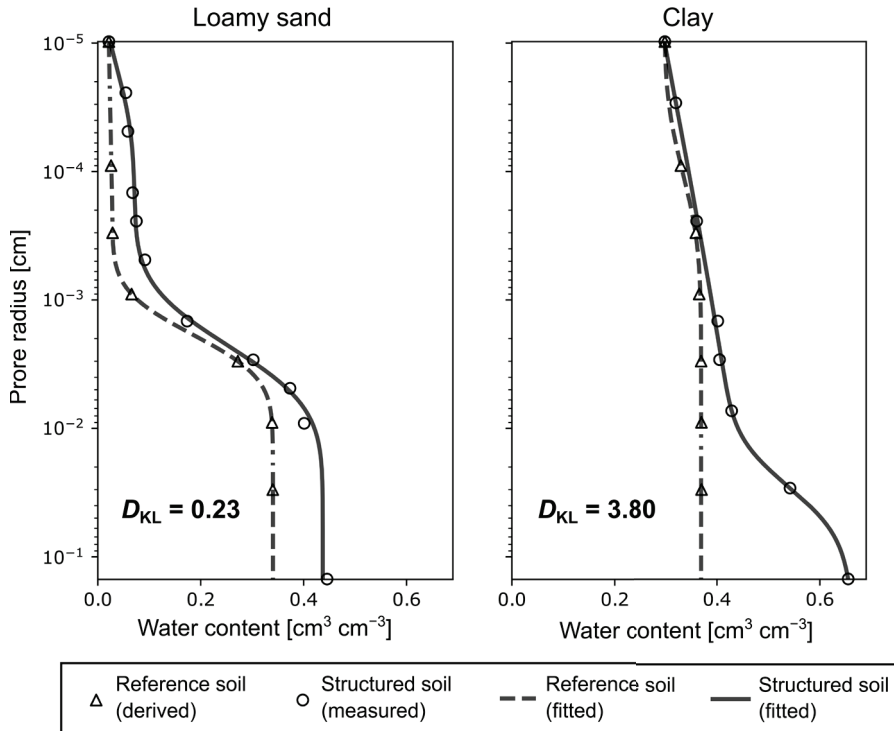
Figure 9. The KL divergence (D_{KL}) increases with an increased difference between pore-size distributions of the reference (dashed lines) and structured soil (solid lines). The data points of the reference soil (triangles) were derived from the particle-size distribution using the method by Chang et al. (2019), while the data points for the structured soil (circles) originate from measured water retention data. Both derived and measured points were fitted with the bimodal Kosugi (1996) model. Adapted from **Paper IV**.

topsoil samples (0-5 cm) from a long-term field experiment on how fertilizer management (fallow vs. inorganic fertilizer vs. manure) affects soil organic carbon contents, crop yields and soil physical properties (Kirchmann et al., 1994; Svensson, 2020). The soil at this site was relatively fine-textured with a clay content of around 37%. The second dataset was taken from Messing et al. (1997), who investigated soil hydraulic properties of nearby sites at different depths in the topsoil (0-30 cm), which differed in land use (afforested land vs. agricultural land dominated by grass/clover ley). This dataset included three locations characterised by relatively coarse-textured

soils with clay contents ranging from 8 to 11%. It was hypothesised that soils treated with manure and soils below forest would show a better developed soil structure and thus have larger KL divergences.

The test showed encouraging results with the KL divergence following the expected trends as a result of changes in soil management and land use. For the first dataset, the KL divergence increased on average in the order fallow < inorganic fertilizer < manure treatment. The difference was smallest between fallow and inorganic fertilizer treatment ($p = 0.99$) and largest between fallow and manure treatment ($p = 0.076$). The larger KL divergences in the manure treatment resulted from an increase in the heterogeneity of the pore-size distribution and an increase in ϕ, which is characteristic for long-term additions of manure (e.g., Anderson et al., 1990; Naveed et al., 2014; Zhang et al., 2021). In contrast, the addition of inorganic fertilizer in the form of $Ca(NO_3)_2$ only lead to an increase in ϕ, without noticeable changes in the pore-size distribution. Although the addition of calcium can affect the structure of fine-textured soils (e.g., Bölscher et al., 2021), the amount added in the form of $Ca(NO_3)_2$ was probably not enough to have caused marked changes in the pore-size distribution (Frank et al., 2020; Haynes and Naidu, 1998). The second dataset revealed a decrease in KL divergence with soil depth on afforested land in all three of the included sites ($p < 0.05$), which was not apparent for the sites on agricultural land. Furthermore, the KL divergence was consistently larger at the sites under forest in the upper soil layers and smaller in the lower soil layers compared to the sites on agricultural land, where regular tillage has probably led to a homogenization of the topsoil structure. The variation in KL divergence was found to be closely linked to the variation in soil organic carbon contents, exhibiting a strong positive correlation across all sites, land uses and treatments (Pearson's $r = 0.374$, $p < 0.001$), which is shown in Figure 10. This makes sense because soil organic matter is known to be an important driver for soil aggregation and structural development, affecting the pore space over a wide range of pore sizes and having a positive effect on ϕ (e.g., Bodner et al., 2023; Dignac et al., 2017; Fukumasu et al., 2022; Vidal et al., 2021).

5.1.3 Uncertainties

Some uncertainties in applying the KL divergence as an index of soil structure can be noted, in particular with respect to the definition of the
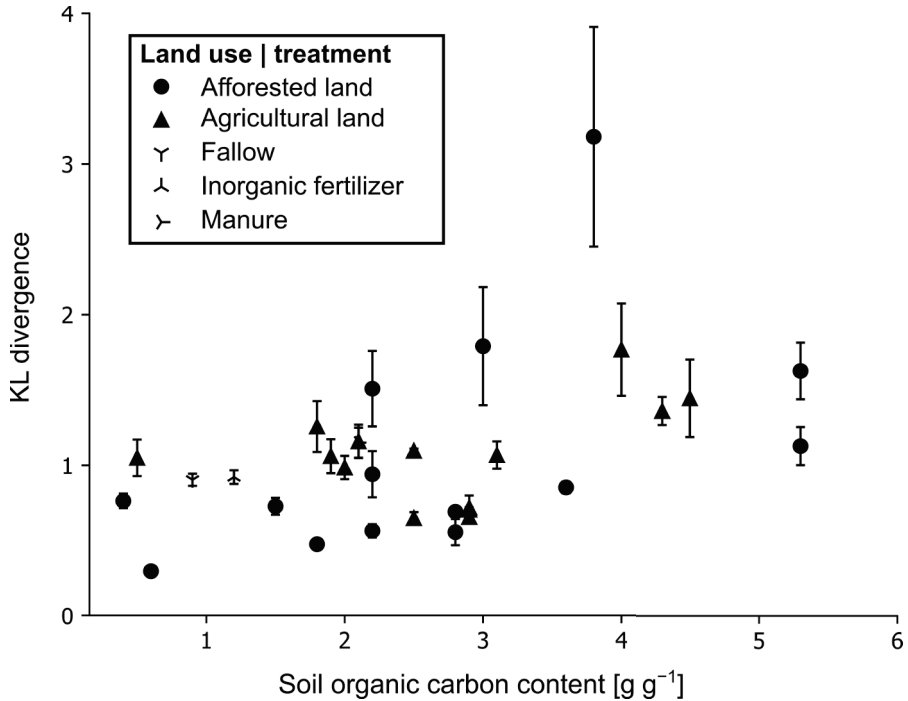
Figure 10. The KL divergence shows a strong positive correlation with soil organic carbon content (Pearson's $r = 0.374$, $p < 0.001$). Error bars indicate standard errors. Adapted from **Paper II**.

reference soil without structure. One critical point is the assumption of linearity between particle- and pore-size distributions as well as the selection of the scaling factor, which differs between models (Assouline and Or, 2013; Assouline and Rouault, 1997). For example, while Chang et al. (2019) suggest a scaling factor of 0.3 for soils with mixed particle sizes, Arya and Heitman (2015) derived a factor of 0.523 for closed-packed spheres. It was also suggested that a linear relationship between particle and pore size might not hold true for both multicomponent sphere packs and natural soils, and that a more complex, non-linear relationship (e.g., given through a power function) would be more appropriate (Hwang and Powers, 2003; Hwang and Choi, 2006; Rouault and Assouline, 1998). Furthermore, there are indications that the scaling factor varies with soil texture, pore size and, not surprisingly, with soil structural development (Hwang and Powers, 2003;

Pollacco et al., 2020; Vaz et al., 2005). Nevertheless, experimental and theoretical evidence suggests that a close relationship between particle-and pore-size distribution is a valid assumption for soils with little or no structural development (Fiès et al., 1981; Fiès and Bruand, 1998, 1990; Nimmo et al., 2007; Rouault and Assouline, 1998). Finally, additional uncertainties remain with respect to the estimation of ϕ_{tex}, and it is unlikely that one value of ϕ_{tex} is appropriate for all soils. However, as mentioned above, the KL divergence is relatively insensitive to ϕ_{tex}, so that its exact determination is not of critical importance.

5.2 Factors of soil structure evolution in agricultural soils of Sweden and Norway

A major advantage of the new index of soil structure is its applicability to a growing number of databases that contain data on water retention, soil texture and ϕ (e.g., Gupta et al., 2022b; Hohenbrink et al., 2023; Nemes et al., 2001). These databases usually cover a wide range of geo-climatic areas, soil management regimes, parent materials, soil depths and sampling times. Thus, the index was considered suitable for identifying the relative importance of different factors (or covariates), one of them being climate, and their interactive effects on soil structure.

In **Paper IV**, the KL divergence was applied to a dataset comprising 431 soil samples from 89 sites across Sweden and Norway (Figure 11). These sites cover gradients in annual precipitation increasing from east to west, and in mean annual air temperature increasing from north to south. The variation in KL divergence was explained with a random forest approach using a set of soil, climate, time and site factors as covariates, which were selected based on their availability for each site and their expected relevance for the evolution of soil structure. These covariates are listed in Table 4. The relative importance of each covariate for explaining the variation in KL divergence was determined from the random forest analysis, and their non-linear/non-monotonic effects were derived using partial dependencies (e.g., Gupta et al., 2022a; Jorda et al., 2015). The analysis was applied to three separate scenarios including (i) all samples, (ii) only topsoil samples (soil depth ≤30 cm; $n = 174$), and (iii) only subsoil samples (soil depth >30 cm; $n = 257$). Furthermore, the analysis was repeated 100 times on each scenario, every time including 90% of randomly selected samples. This was done to test
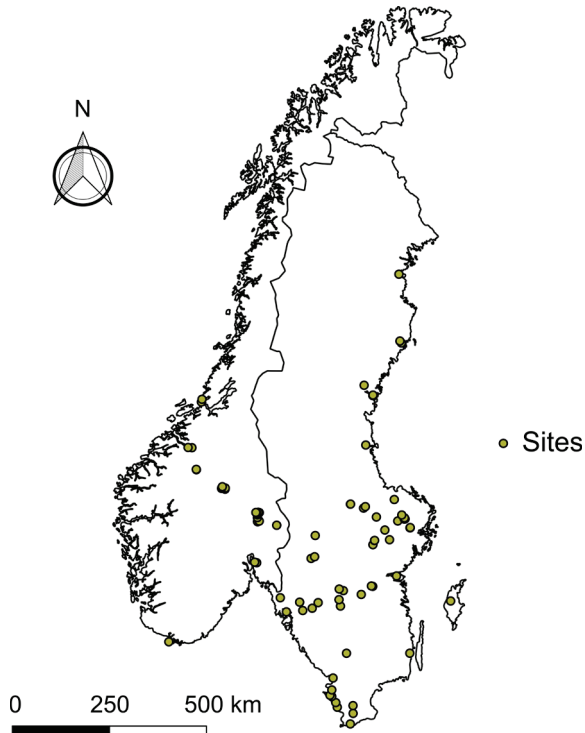
Figure 11. Distribution of sites investigated in **Paper IV**.

whether the performance of the random forest models was robust or whether it depended on the inclusion of a specific subgroup of samples.

The nine covariates were able to explain on average more than 50% of the variation in KL divergence for the scenarios where all samples and only subsoil samples were included. In contrast, none of the random forest models was able to explain 50% or more of the variation in the topsoil samples. This is probably due to the multitude of processes that affect the evolution of structure in agricultural topsoils, many of which could not be accounted for. These include soil tillage and subsequent consolidation, the high activity of soil biota and plant roots, and the effects of short-term weather events (Assouline, 2004; Ghezzehei and Or, 2003; Lucas et al., 2022; Meurer et al., 2020). Thus, in the following, the relative importance of the different covariates and their interactive effects on the KL divergence will only be discussed for the scenarios including all samples and subsoil samples.

Table 4. Covariates used to explain the variation in KL divergence. Reproduced from **Paper IV**.

Category	Covariate	Range / categories	Unit
Soil property	Clay content	[0, 81.3]	weight-%
	Silt content	[0, 93.3]	weight-%
	Soil depth [a]	[0, 93]	cm
	Soil organic carbon content	[0, 8.7]	weight-%
Climate	Mean annual air temperature	[2.3, 8.8]	°C
	Annual precipitation	[430, 1215]	mm
Time	Sampling year	[1954, 2017]	year
	Sampling season	spring, summer, autumn, winter	-
Geology	Parent material	aeolian sediments, fluvial sediments, glacial sediments, gyttja, lacustrine sediments, marine sediments, organic material, postglacial sediments, shore, till	-

[a] Soil depth was not considered for topsoil and subsoil analysis.

[b] Spring: April-May, summer: June-August, autumn: September-October, winter: December-March

5.2.1   Soil properties and parent material

Parent material was the most important factor for explaining the variation in KL divergence in both scenarios (all samples and only subsoil samples). The partial dependence analysis suggested that soils developed on "gyttja" sediments showed relatively large KL divergences, while the difference between the other parent materials was smaller (Figure 12). Gyttja sediments are characterised by high clay and soil organic carbon contents and, upon drainage, show a strong structural development (Berglund, 1996; Berglund and Berglund, 2010). This explains the relatively large KL divergences of these soils. Clay content was the most important soil property in both
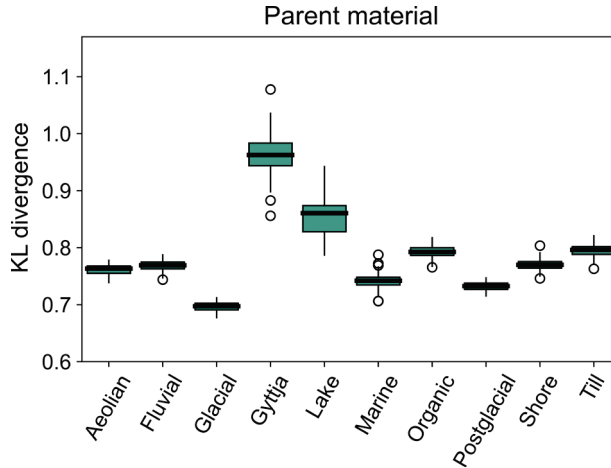
Figure 12. Partial dependence plot of parent material for the scenario including all samples. Reproduced from **Paper IV**.

scenarios, ranking second for all samples and fifth for only subsoil samples. The KL divergence increased markedly for soil samples with clay contents ≥60%, which was evident in both scenarios (Figure 13a). This increase can be explained by the gyttja soil samples, which had the highest clay contents in the dataset. Relative to clay content, silt content was less important in both scenarios and did not show any notable trends with the KL divergence. Soil depth was the fifth most important covariate for the scenario including all samples and, as expected, the KL divergence strongly decreased with increasing soil depth, reaching a minimum at around 30 cm and remaining relatively constant for soil layers below this depth (Figure 13b). While agricultural topsoils are subject to regular soil loosening through tillage, intensive root growth and the activity of soil biota (Meurer et al., 2020; Or et al., 2021), the minimum is probably the result of soil compaction, which is a common feature in agricultural soils just below plough depth (Batey, 2009; Håkansson and Medvedev, 1995; see also Figure 2).

Soil organic carbon content was the least important soil property for explaining the variation in KL divergence, which seems contradictory to many studies that stress the importance of soil organic matter for soil structure formation (e.g., Anderson et al., 1990; Bronick and Lal, 2005; Naveed et al., 2014). There are several explanation for this finding: first, soil
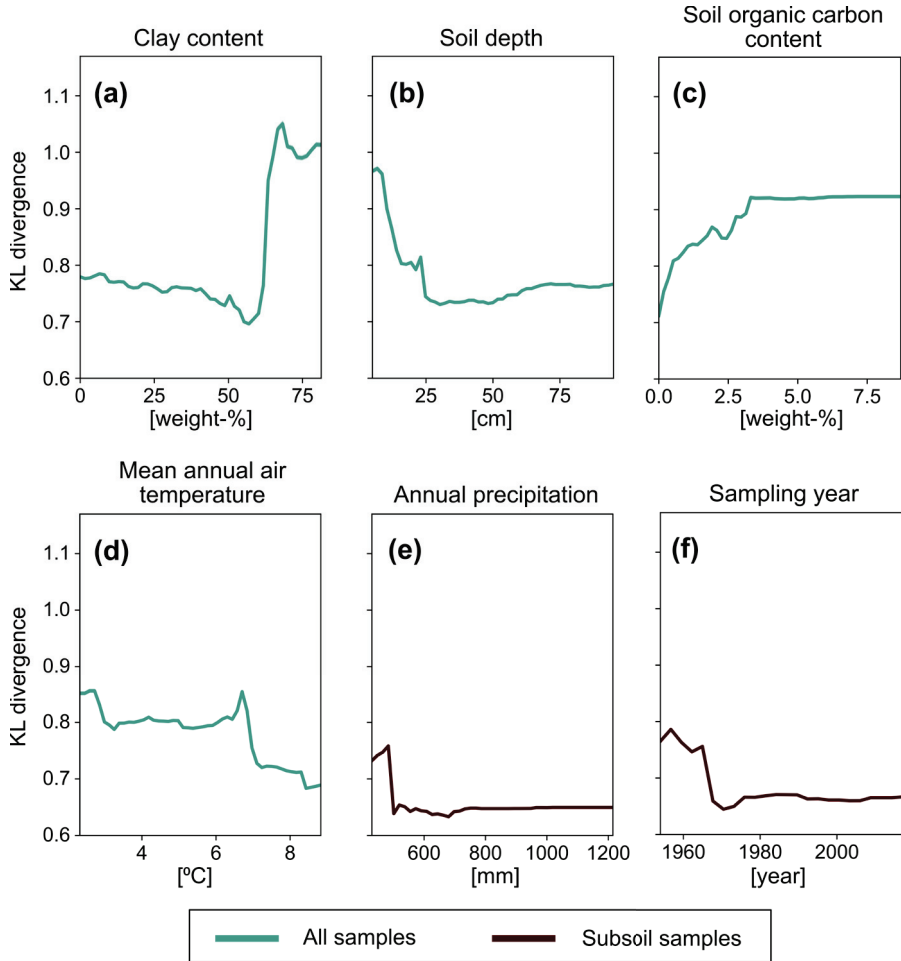
Figure 13. Partial dependence plots of a selection of continuous covariates for the scenarios including all samples **(a-d)** and only subsoil samples **(e-f)**. Adapted from **Paper IV**.

organic carbon contents were estimated from loss on ignition measurements for most samples in this dataset (71%), which themselves are subject to various uncertainties (Chatterjee et al., 2009; Hoogsteen et al., 2015). This might have distorted the relationship with the KL divergence. Second, soil organic matter in agricultural soils is mostly found in the mineral-associated fraction, driving soil structure formation mostly at smaller scales and with

little direct effects on larger structural pores (Fukumasu et al., 2022; Jarvis et al., 2017a; Poeplau et al., 2018). Third, the dataset is dominated by subsoil samples, which might hide the positive relationship between soil organic carbon and the KL divergence. Lastly, regular mechanical disturbance through tillage and vehicle trafficking may destroy larger structural pores and thereby override the effects of soil organic carbon on soil structure. The partial dependence analysis revealed an interesting relationship between soil organic carbon and the KL divergence, where the KL divergence increased sharply between 0 and 2% soil organic carbon content and reached a plateau at around 3% (Figure 13c). This suggests that a critical soil organic carbon content (Loveland and Webb, 2003) of around 3% may exist in this dataset, below which soil structure starts to deteriorate.

5.2.2   Climate

Mean annual air temperature was the third most important covariate in both scenarios (all samples and subsoil samples). In the scenario including all samples, the partial dependence analysis revealed a decrease in KL divergence with an increase in mean annual air temperature (Figure 13d), suggesting that soil structure in warmer regions is less well developed. On the one hand, this trend might be due to indirect effects on soil structure, because more intensive agricultural activities in warmer regions are associated with the use of heavier machinery and, consequently, a higher risk of soil structure deterioration (Björklund et al., 1999; Keller et al., 2019; Keller and Or, 2022). On the other hand, direct effects might have contributed to this trend. For example, more intense and frequent freeze-thaw cycles in colder regions have shown to periodically recover the structure of soils in colder regions (Gregory et al., 2009; Hirmas et al., 2018; Jabro et al., 2014; Ma et al., 2019).

Annual precipitation was less important than mean annual air temperature in both scenarios, and it was more important in the scenario including only subsoil samples compared to the scenario including all samples. The partial dependence analysis revealed a decrease in KL divergence with increasing precipitation, indicating a less well developed soil structure in wetter regions, in particular in the subsoil (Figure 13e). This is in line with previous studies (e.g., Caplan et al., 2019; Jorda et al., 2015; Wu et al., 2023) and, similar to mean annual air temperature, may be the result of both indirect and direct effects on soil structure. Specifically, wetter soils are generally at higher risk

of experiencing harmful soil compaction by vehicle trafficking (Jarvis et al., 2013), while shrinking and swelling is usually more pronounced in drier regions, leading to a better developed macropore structure (Bodner et al., 2013a; Hirmas et al., 2018).

5.2.3   Time

Sampling year was the second most important covariate for the scenario including only subsoil samples, while it was less important for the scenario including all samples. The partial dependence analysis revealed a decrease in KL divergence between the 1950's and 1970's, with relatively constant values thereafter (Figure 13f). This suggests a gradual degradation of soil structure in the recent past, especially in the subsoil, probably due to an overall increase in production intensity in Sweden between the 1950's and 1990's, which was associated with the use of heavier machinery and more repeated trafficking of the soil, leading to subsoil compaction (Björklund et al., 1999; Keller et al., 2019; Parvin et al., 2022).

Sampling season was the least important covariate in both scenarios, which may seem to contrast with studies highlighting the within-season variability of different soil structure metrics in agricultural soils (e.g., Alletto et al., 2015; Schwen et al., 2011). However, these dynamics have only been reported for topsoils and are mainly the result of the consolidation of soil material after tillage (*cf.* Subsection 2.4.1). The dataset used here was dominated by subsoil samples. Furthermore, most of the samples were taken in summer (44%) when some degree of consolidation has already occurred. This may explain, at least partly, why sampling season was least important in explaining the variability in KL divergence.

6. Conclusions and Future Perspectives

6.1 The new index of soil structure

Relative entropy (the KL divergence) proved to be highly useful as a quantitative index of soil structure (Section 5.1; **Paper II** and **III**). In contrast to previous soil structure indices that are derived from the soil water retention curve, the new index of soil structure is able to account for the effects of soil texture and is now applicable to large databases that include data on water retention, soil texture and total porosity. It was demonstrated that the index follows expected trends in soil structure due to changes in soil management, land use and different soil properties (e.g., soil depth and soil organic carbon content). It was shown that the KL divergence increases as pore-space heterogeneity, median pore size and soil porosity increase. This suggests that the index may also be a useful indicator for soil physical health and provide information about different soil water functions. In particular, for soils with the same texture, a larger KL divergence is expected to show faster drainage rates, but potentially also an increased capacity to retain water. This needs to be tested in future studies. Furthermore, it would be interesting to compare the new index with other soil structure indices, for example those that can be derived from X-ray CT measurements.

Despite the encouraging results, the approach to derive the KL divergence as suggested here does leave room for improvement. More experimental effort on the characterisation of the textural pore space is required to confirm (or disprove) the assumptions made with respect to the reference soil without structural pores. This particularly applies to the scaling factor for converting particle size into pore size and the textural porosity across different soil types. Such an experimental approach could be complemented by particle

packing models that are able to account for different particle sizes and shapes beyond regular spheres.

6.2 Drivers of soil structure evolution and the role of climate

Section 5.2 (**Paper IV**) demonstrated the leading role of properties of the mineral soil phase for the evolution of soil structure in arable soils of Sweden and Norway, in particular the nature of the parent material and clay content. In contrast, soil organic carbon was relatively less important and did not affect the KL divergence at contents larger than around 3%. This may raise the question to what degree soil structure is pre-determined by soil or site properties that are difficult to manage. However, it should be noted that the dataset used here was dominated by subsoil samples and that the variation in soil structure (the KL divergence) could not be reliably explained for topsoils. A follow-up study including information on soil management and other important drivers of structure development in agricultural topsoils (e.g., root morphology, soil biota activity) would be necessary to test the extent to which soil structure is actually manageable.

The gradual decrease in KL divergence in the upper subsoil over the past decades indicates that the intensification of agricultural production has had detrimental effects on soil structure. Being most sensitive to the wet range of the soil water retention curve (because this is where the reference soil and structured soil can diverge most), the decrease in KL divergence over time probably has its biggest negative consequences for soil water functions with respect to soil drainage. This highlights the need for an extensive soil structure monitoring scheme, which is able detect such gradual changes in time and allows for timely mitigation measures. The KL divergence as an index of soil structure would be useful in this context as it provides a comparatively simple way of quantifying soil structure.

The climate variables (i.e., mean annual air temperature and annual precipitation) had relatively large effects on soil structure, especially in the subsoil. However, it was not possible to resolve the question whether the effects of climate were direct or indirectly expressed, for example through soil management. In any case, the results suggest that arable soils in the temperate-boreal zone are more prone to soil structure deterioration in warmer and wetter as compared with cooler and drier regions. By

highlighting areas that are particularly vulnerable, this finding may help raise awareness and support the development of more climate-specific advisory schemes to help farmers manage their soils better. However, it should be noted that the relationship between the two climate variables and soil structure may be different in other climate regions. This also applies to the importance of climate variables relative to other driving factors. Similar studies in other climate regions, or studies covering a larger variability of climatic conditions should be conducted.

6.3 Effects of freezing and thawing on the soil pore space and soil hydraulic properties

The meta-analysis on the effects of freezing and thawing on the soil pore space (Section 4.1) explained some of the contradictory findings that have been reported in previous freeze-thaw studies. It can be concluded that the initial bulk density constitutes one important factor that determines whether freezing and thawing has a loosening (high bulk density) or consolidating effect (low bulk density) on soils. The relationship between total porosity and bulk density, which was established here, suggests a shift from consolidation to loosening at a bulk density of around 1.1 g cm^{-3}. This relationship can be useful, for example, when accounting for the effects of freezing and thawing on the soil pore space in soil-crop models.

Both the meta-analysis and the laboratory experiment (Section 4.1 and 4.2; **Paper I**) demonstrated that freezing and thawing changes the pore-size distribution of soils. There is strong evidence that pores with diameters smaller than around 200 μm are affected most by freezing and thawing, which is the pore region affecting both soil drainage and water storage (Figure 3). However, it is difficult to draw firm conclusions about the exact direction of these effects. I suggest that a critical factor in this context is the water-filled pore space, as it determines which pores are affected by the expansion of water upon freezing. As also found in the laboratory experiment, I hypothesize that pores slightly larger than the largest water-filled pores will become more abundant after freezing, probably at the expense of smaller or even larger pores. Furthermore, the redistribution of water within soils during freezing may lead to the movement of water towards specific pore sizes, which will also have effects on the pore-size distribution. Both aspects should be investigated in future experiments.

The laboratory experiment (Section 4.2; **Paper I**) demonstrated that changes in different pore-space characteristics of compacted soil layers have strong implications for their hydraulic properties. In particular, it can be concluded that freezing and thawing increases near-saturated hydraulic conductivity due to changes in X-ray visible porosity, pore-size distribution, pore connectivity and critical pore diameter. This will lead to faster soil drainage and should thus be beneficial for the often relatively wet soils of the temperate-boreal zone. Specifically, freezing and thawing may help in preventing waterlogging in late winter/early spring and thereby allow soils to be negotiable earlier without the risk of causing harmful soil compaction. Besides this, improved pore-space connectivity and the loosening of compacted soil layers may benefit root development at the onset of the growing season and facilitate water transport to roots, leading to an improved water supply to crops in spring/early summer.

Whether the observed changes in pore-space structure and soil hydraulic properties due to freezing and thawing are of a relevant magnitude for the annual soil water balance and for crop growth at the field scale is still unknown. I recommend the use of soil-crop models as a tool to explore this in future studies. Modelling could also help to investigate whether the relatively large changes in pore-size distribution of smaller pores have implications for water storage and the availability of water to crops. Furthermore, it is still unknown for how long changes in both pore-space characteristics and soil hydraulic properties in response to freezing and thawing persist. I expect that the effects in the uppermost soil layers are of relatively short duration and reversible (i.e., within season), while effects on deeper soil layers may persist for a longer time. Finally, it remains unknown how important freeze-thaw effects are in comparison to other factors, for example, soil management and the activity of soil biota.

6.4   What can be expected with climate change?

The findings from the laboratory experiment (Section 4.2; **Paper I**) suggest that climate change, if it entails an increase in the number and intensity of freeze-thaw cycles, has the potential to enhance the benefits for compacted soil layers induced by freezing and thawing (*cf.* Section 6.3). In particular, soil drainage rates under near-saturated conditions could further increase in these soil layers. Furthermore, an increase in pore connectivity, which was

observed for the finer-textured silty clay loam, might improve water supply to crops. The results from the meta-analysis (Section 4.1) also suggest that the size distribution of smaller pores is modified continuously with each freeze-thaw cycle and, thus, an increase in the number of freeze-thaw cycles may also affect water storage and plant-availability. All these effects are potentially important in a future climate, which is expected to have wetter winters and an increased likelihood of spring/early summer droughts, at least in some parts of the temperate-boreal zone. Yet again, whether the differences in soil hydraulic properties resulting from a change in freeze-thaw patterns really matter for the water balance and crop production at the field scale needs to be investigated in future studies. As suggested above, modelling could be a useful tool for this. I recommend simulating different climate scenarios to investigate in which climatic contexts freeze-thaw effects on soil structure might be beneficial or not.

The results in Section 5.2 (**Paper IV**) suggest that soil structure in warmer and wetter regions of the temperate-boreal zone is more susceptible to deterioration, although the exact mechanisms remain unclear. Nevertheless, these results are important in the context of the northward expansion of intensive agricultural practices in the temperate-boreal zone with climate change. I expect that such an expansion will accelerate in the future, both because of more favourable growing conditions due to a warmer climate and because these areas may need to compensate for the loss of agricultural productivity in other parts of the world. The results presented here suggest that an expansion of intensive agricultural practices could be accompanied by a loss of soil water functions due to soil structure degradation. The risk of soil degradation is further increased by an overall increase in precipitation during late summer and autumn in the future, as for example expected in Sweden, which may amplify processes such as soil erosion, compaction and soil sealing. How agricultural intensification in the temperate-boreal zone can be achieved without its negative consequences for soil structure and soil water functions is an important question, which can only be answered through interdisciplinary research.

References

Alletto, L., Coquet, Y. (2009). Temporal and spatial variability of soil bulk density and near-saturated hydraulic conductivity under two contrasted tillage management systems. *Geoderma*. 152, 85–94. https://doi.org/10.1016/j.geoderma.2009.05.023

Alletto, L., Pot, V., Giuliano, S., Costes, M., Perdrieux, F., Justes, E. (2015). Temporal variation in soil physical properties improves the water dynamics modeling in a conventionally-tilled soil. *Geoderma* 243–244, 18–28. https://doi.org/10.1016/j.geoderma.2014.12.006

Amundson, R., Berhe, A.A., Hopmans, J.W., Olson, C., Sztein, A.E., Sparks, D.L. (2015). Soil and human security in the 21st century. *Science*. 348, 1261071. https://doi.org/10.1126/science.1261071

Anderson, S.H., Gantzer, C.J., Brown, J.R. (1990). Soil physical properties after 100 years of continuous cultivation. *Journal of Soil and Water Conservation*. 45, 117–121.

Arthur, E., Moldrup, P., Schjønning, P., De Jonge, L.W. (2013). Water Retention, Gas Transport, and Pore Network Complexity during Short-Term Regeneration of Soil Structure. *Soil Science Society of America Journal*. 77, 1965–1976. https://doi.org/10.2136/sssaj2013.07.0270

Arya, L.M., Heitman, J.L. (2015). A Non-Empirical Method for Computing Pore Radii and Soil Water Characteristics from Particle-Size Distribution. *Soil Science Society of America Journal*. 79, 1537–1544. https://doi.org/10.2136/sssaj2015.04.0145

Arya, L.M., Paris, J.F. (1981). A Physicoempirical Model to Predict the Soil Moisture Characteristic from Particle-Size Distribution and Bulk Density Data. *Soil Science Society of America Journal*. 45, 1023–1030. https://doi.org/10.2136/sssaj1981.03615995004500060004x

Asare, S.N., Rudra, R.P., Dickinson, W.T., Wall, G.J. (1999). Effect of Freeze–thaw Cycle on the Parameters of the Green and Ampt Infiltration Equation. Journal of Agricultural Engineering Research 73, 265–274. https://doi.org/10.1006/jaer.1999.0415

Assouline, S. (2021). What Can We Learn From the Water Retention Characteristic of a Soil Regarding Its Hydrological and Agricultural Functions? Review and Analysis of Actual Knowledge. *Water Resources Research*. 57, e2021WR031026. https://doi.org/10.1029/2021WR031026

Assouline, S. (2004). Rainfall-Induced Soil Surface Sealing: A Critical Review of Observations, Conceptual Models, and Solutions. *Vadose Zone Journal*. 3, 570–591. https://doi.org/10.2136/vzj2004.0570

Assouline, S., Or, D. (2014). The concept of field capacity revisited: Defining intrinsic static and dynamic criteria for soil internal drainage dynamics. *Water Resources Research*. 50, 4787–4802. https://doi.org/10.1002/2014WR015475

Assouline, S., Or, D. (2013). Conceptual and Parametric Representation of Soil Hydraulic Properties: A Review. *Vadose Zone Journal*. 12, 1-20. https://doi.org/10.2136/vzj2013.07.0121

Assouline, S., Rouault, Y. (1997). Modeling the relationships between particle and pore size distributions in multicomponent sphere packs: application to the water retention curve. *Colloids and Surfaces A: Physicochemical and Engineering Aspects*. 127, 201–210. https://doi.org/10.1016/S0927-7757(97)00144-1

Batey, T. (2009). Soil compaction and soil management – a review. *Soil Use and Management*. 25, 335–345. https://doi.org/10.1111/j.1475-2743.2009.00236.x

Benoit, G.R., Bornstein, J. (1970). Freezing and thawing effects on drainage. *Soil Science Society of America Journal*. 34, 551–557.

Berglund, K. (1996). Properties of cultivated gyttja soils. *International Peat Journal*. 6, 5–23.

Berglund, Ö., Berglund, K. (2010). Distribution and cultivation intensity of agricultural peat and gyttja soils in Sweden and estimation of greenhouse gas emissions from cultivated peat soils. *Geoderma*. 154, 173–180. https://doi.org/10.1016/j.geoderma.2008.11.035

Bishop, C. (2006). Pattern Recognition and Machine Learning, Information Science and Statistics. Springer, New York.

Björklund, J., Limburg, K.E., Rydberg, T. (1999). Impact of production intensity on the ability of the agricultural landscape to generate ecosystem services: an example from Sweden. *Ecological Economics*. 29, 269–291. https://doi.org/10.1016/S0921-8009(99)00014-2

Bodner, G., Loiskandl, W., Buchan, G., Kaul, H.-P. (2008). Natural and management-induced dynamics of hydraulic conductivity along a cover-cropped field slope. *Geoderma*. 146, 317–325. https://doi.org/10.1016/j.geoderma.2008.06.012

Bodner, G., Scholl, P., Kaul, H.-P. (2013a). Field quantification of wetting–drying cycles to predict temporal changes of soil pore size distribution. *Soil and Tillage Research*. 133, 1–9. https://doi.org/10.1016/j.still.2013.05.006

Bodner, G., Scholl, P., Loiskandl, W., Kaul, H.-P. (2013b). Environmental and management influences on temporal variability of near saturated soil

hydraulic properties. *Geoderma*. 204–205, 120–129. https://doi.org/10.1016/j.geoderma.2013.04.015

Bodner, G., Zeiser, A., Keiblinger, K., Rosinger, C., Winkler, S.K., Stumpp, C., Weninger, T. (2023). Managing the pore system: Regenerating the functional pore spaces of natural soils by soil-health oriented farming systems. *Soil and Tillage Research*. 234, 105862. https://doi.org/10.1016/j.still.2023.105862

Bölscher, T., Koestel, J., Etana, A., Ulén, B., Berglund, K., Larsbo, M. (2021). Changes in pore networks and readily dispersible soil following structure liming of clay soils. *Geoderma*. 390, 114948. https://doi.org/10.1016/j.geoderma.2021.114948

Bonetti, S., Wei, Z., Or, D. (2021). A framework for quantifying hydrologic effects of soil structure across scales. *Communications Earth & Environment*. 2, 107. https://doi.org/10.1038/s43247-021-00180-0

Boyer, J.S. (1982). Plant Productivity and Environment. *Science*. 218, 443–448. https://doi.org/10.1126/science.218.4571.443

Bronick, C.J., Lal, R. (2005). Soil structure and management: a review. *Geoderma*. 124, 3–22. https://doi.org/10.1016/j.geoderma.2004.03.005

Bruand, A., Prost, R. (1987). Effect of water content on the fabric of a soil material: an experimental approach. *Journal of Soil Science*. 38, 461–472. https://doi.org/10.1111/j.1365-2389.1987.tb02281.x

Bryan, R.B. (1971). The influence of frost action on soil-aggregate stability. *Transactions of the Institute of British Geographers*. 54, 71–88.

Bullock, M.S., Nelson, S.D., Kemper, W.D. (1988). Soil Cohesion as Affected by Freezing, Water Content, Time and Tillage. *Soil Science Society of America Journal*. 52, 770–776. https://doi.org/10.2136/sssaj1988.03615995005200030031x

Caplan, J.S., Giménez, D., Hirmas, D.R., Brunsell, N.A., Blair, J.M., Knapp, A.K. (2019). Decadal-scale shifts in soil hydraulic properties as induced by altered precipitation. *Science Advances*. 5, eaau6635. https://doi.org/10.1126/sciadv.aau6635

Carminati, A., Javaux, M. (2020). Soil Rather Than Xylem Vulnerability Controls Stomatal Response to Drought. *Trends in Plant Science*. 25, 868–880. https://doi.org/10.1016/j.tplants.2020.04.003

Carter, M.R. (1988). Temporal variability of soil macroporosity in a fine sandy loam under mouldboard ploughing and direct drilling. *Soil and Tillage Research*. 12, 37–51. https://doi.org/10.1016/0167-1987(88)90054-2

Cassel, D.K., Nielsen, D.R. (1986). Field Capacity and Available Water Capacity. In A. Klute (ed.), *SSSA Book Series* (pp. 901–926). American Society of Agronomy, Madison, WI, USA. https://doi.org/10.2136/sssabookser5.1.2ed.c36

Chandrasekhar, P., Kreiselmeier, J., Schwen, A., Weninger, T., Julich, S., Feger, K.-H., Schwärzel, K. (2018). Why We Should Include Soil Structural Dynamics of Agricultural Soils in Hydrological Models. *Water*. 10, 1862. https://doi.org/10.3390/w10121862

Chang, C., Cheng, D., Qiao, X. (2019). Improving estimation of pore size distribution to predict the soil water retention curve from its particle size distribution. *Geoderma*. 340, 206–212. https://doi.org/10.1016/j.geoderma.2019.01.011

Chatterjee, A., Lal, R., Wielopolski, L., Martin, M.Z., Ebinger, M.H. (2009). Evaluation of Different Soil Carbon Determination Methods. *Critical Reviews in Plant Sciences*. 28, 164–178. https://doi.org/10.1080/07352680902776556

Coquet, Y., Vachier, P., Labat, C. (2005). Vertical variation of near-saturated hydraulic conductivity in three soil profiles. *Geoderma*. 126, 181–191. https://doi.org/10.1016/j.geoderma.2004.09.014

Cornelis, W.M., Corluy, J., Medina, H., Díaz, J., Hartmann, R., Van Meirvenne, M., Ruiz, M.E. (2006). Measuring and modelling the soil shrinkage characteristic curve. *Geoderma*. 137, 179–191. https://doi.org/10.1016/j.geoderma.2006.08.022

Crawford, J.W., Matsui, N., Young, I.M. (1995). The relation between the moisture-release curve and the structure of soil. *European Journal of Soil Science*. 46, 369–375. https://doi.org/10.1111/j.1365-2389.1995.tb01333.x

Czyż, E.A., Dexter, A.R. (2013). Influence of soil type on the wilting of plants. *International Agrophysics*. 27, 385–390. https://doi.org/10.2478/intag-2013-0008

Dagesse, D.F. (2013). Freezing cycle effects on water stability of soil aggregates. *Canadian Journal of Soil Science*. 93, 473–483. https://doi.org/10.4141/cjss2012-046

De Swaef, T., Pieters, O., Appeltans, S., Borra-Serrano, I., Coudron, W., Couvreur, V., Garré, S., Lootens, P., Nicolaï, B., Pols, L., Saint Cast, C., Šalagovič, J., Van Haeverbeke, M., Stock, M., Wyffels, F. (2022). On the pivotal role of water potential to model plant physiological processes. *in silico Plants*. 4, diab038. https://doi.org/10.1093/insilicoplants/diab038

DeBoot, M. (1957). Bijdrage tot de kennis van de bodemstruktuur [Contribution to the knowledge of soil structure]. Rijkslandbouwhogeschool, Gent, Belgium.

Decker, K.L.M., Wang, D., Waite, C., Scherbatskoy, T. (2003). Snow Removal and Ambient Air Temperature Effects on Forest Soil Temperatures in Northern Vermont. *Soil Science Society of America Journal*. 67, 1234–1242. https://doi.org/10.2136/sssaj2003.1234

Demand, D., Selker, J.S., Weiler, M. (2019). Influences of Macropores on Infiltration into Seasonally Frozen Soil. *Vadose Zone Journal*. 18, 1–14. https://doi.org/10.2136/vzj2018.08.0147

Dexter, A.R. (2004a). Soil physical quality: Part I. Theory, effects of soil texture, density, and organic matter, and effects on root growth. *Geoderma*. 120, 201–214. https://doi.org/10.1016/j.geoderma.2003.09.004

Dexter, A.R. (2004b). Soil physical quality: Part III: Unsaturated hydraulic conductivity and general conclusions about S-theory. *Geoderma*. 120, 227–239. https://doi.org/10.1016/j.geoderma.2003.09.006

Dexter, A.R. (2004c). Soil physical quality: Part II. Friability, tillage, tilth and hard-setting. *Geoderma*. 120, 215–225. https://doi.org/10.1016/j.geoderma.2003.09.005

Dexter, A.R. (1988). Advances in characterization of soil structure. *Soil and Tillage Research*. 11, 199–238. https://doi.org/10.1016/0167-1987(88)90002-5

Dexter, A.R., Czyż, E.A., Richard, G. (2012). Equilibrium, non-equilibrium and residual water: Consequences for soil water retention. *Geoderma*. 177–178, 63–71. https://doi.org/10.1016/j.geoderma.2012.01.029

Dexter, A.R., Czyż, E.A., Richard, G., Reszkowska, A. (2008). A user-friendly water retention function that takes account of the textural and structural pore spaces in soil. *Geoderma*. 143, 243–253. https://doi.org/10.1016/j.geoderma.2007.11.010

Diel, J., Vogel, H.-J., Schlüter, S. (2019). Impact of wetting and drying cycles on soil structure dynamics. *Geoderma*. 345, 63–71. https://doi.org/10.1016/j.geoderma.2019.03.018

Dignac, M.-F., Derrien, D., Barré, P., Barot, S., Cécillon, L., Chenu, C., Chevallier, T., Freschet, G.T., Garnier, P., Guenet, B., Hedde, M., Klumpp, K., Lashermes, G., Maron, P.-A., Nunan, N., Roumet, C., Basile-Doelsch, I. (2017). Increasing soil carbon storage: mechanisms, effects of agricultural practices and proxies. A review. *Agronomy for Sustainable Development*. 37, 14. https://doi.org/10.1007/s13593-017-0421-2

Dominati, E., Patterson, M., Mackay, A. (2010). A framework for classifying and quantifying the natural capital and ecosystem services of soils. *Ecological Economics*. 69, 1858–1868. https://doi.org/10.1016/j.ecolecon.2010.05.002

Donnelly, C., Greuell, W., Andersson, J., Gerten, D., Pisacane, G., Roudier, P., Ludwig, F. (2017). Impacts of climate change on European hydrology at 1.5, 2 and 3 degrees mean global warming above preindustrial level. *Climatic Change*. 143, 13–26. https://doi.org/10.1007/s10584-017-1971-7

Du, C. (2020). Comparison of the performance of 22 models describing soil water retention curves from saturation to oven dryness. *Vadose Zone Journal*. 19, e20072. https://doi.org/10.1002/vzj2.20072

Durner, W. (1994). Hydraulic conductivity estimation for soils with heterogeneous pore structure. *Water Resources Research*. 30, 211–223. https://doi.org/10.1029/93WR02676

Eck, D.V., Qin, M., Hirmas, D.R., Giménez, D., Brunsell, N.A. (2016). Relating Quantitative Soil Structure Metrics to Saturated Hydraulic Conductivity. *Vadose Zone Journal*. 15, 1–11. https://doi.org/10.2136/vzj2015.05.0083

Edwards, L.M. (2013). The effects of soil freeze–thaw on soil aggregate breakdown and concomitant sediment flow in Prince Edward Island: A review. *Canadian Journal of Soil Science*. 93, 459–472. https://doi.org/10.4141/cjss2012-059

European Commission. (2013). *European HYdropedological Data Inventory (EU-HYDI)* (JRC Technical Reports). Institute for Environment and Sustainability, Ispra, Italy.

Fang, J., Su, Y. (2019). Effects of Soils and Irrigation Volume on Maize Yield, Irrigation Water Productivity, and Nitrogen Uptake. *Scientific Reports*. 9, 7740. https://doi.org/10.1038/s41598-019-41447-z

Fatichi, S., Or, D., Walko, R., Vereecken, H., Young, M.H., Ghezzehei, T.A., Hengl, T., Kollet, S., Agam, N., Avissar, R. (2020). Soil structure is an important omission in Earth System Models. *Nature Communications*. 11, 522. https://doi.org/10.1038/s41467-020-14411-z

Fernández-Gálvez, J., Pollacco, J.A.P., Lilburne, L., McNeill, S., Carrick, S., Lassabatere, L., Angulo-Jaramillo, R. (2021). Deriving physical and unique bimodal soil Kosugi hydraulic parameters from inverse modelling. *Advances in Water Resources*. 153, 103933. https://doi.org/10.1016/j.advwatres.2021.103933

Fiès, J.C., Bruand, A. (1998). Particle packing and organization of the textural porosity in clay-silt-sand mixtures. *European Journal of Soil Science*. 49, 557–567. https://doi.org/10.1046/j.1365-2389.1998.4940557.x

Fiès, J.C., Bruand, A. (1990). Textural porosity analysis of a silty clay soil using pore volume balance estimation, mercury porosimetry and quantified backscattered electron scanning image (BESI). *Geoderma*. 47, 209–219. https://doi.org/10.1016/0016-7061(90)90029-9

Fiès, J.C., Stengel, P., Bourlet, M., Horoyan, J., Jeandet, C. (1981). Densité texturale de sols naturels II. - Eléments d'interprétation [Textural density of natural soils II. - Elements of interpretation]. *Agronomie*. 1, 659–666.

Frank, T., Zimmermann, I., Horn, R. (2020). Lime application in marshlands of Northern Germany—Influence of liming on the physicochemical and hydraulic properties of clayey soils. *Soil and Tillage Research*. 204, 104730. https://doi.org/10.1016/j.still.2020.104730

Fredlund, M.D., Fredlund, D.G., Wilson, G.W. (2000). An equation to represent grain-size distribution. *Canadian Geotechnical Journal*. 37, 817-827. https://doi.org/10.1139/t00-015

Fu, Q., Zhao, H., Li, T., Hou, R., Liu, D., Ji, Y., Zhou, Z., Yang, L., 2019. Effects of biochar addition on soil hydraulic properties before and after freezing-

thawing. CATENA 176, 112–124. https://doi.org/10.1016/j.catena.2019.01.008

Fukumasu, J., Jarvis, N., Koestel, J., Kätterer, T., Larsbo, M. (2022). Relations between soil organic carbon content and the pore size distribution for an arable topsoil with large variations in soil properties. *European Journal of Soil Science*. 73. https://doi.org/10.1111/ejss.13212

Gardner, W.R. (1965). Dynamic Aspects of Soil-Water Availability to Plants. *Annual Review of Plant Physiology*. 16, 323–342. https://doi.org/10.1146/annurev.pp.16.060165.001543

Gebhardt, S., Fleige, H., Horn, R. (2009). Effect of compaction on pore functions of soils in a Saalean moraine landscape in North Germany. *Journal of Plant Nutrition and Soil Science*. 172, 688–695. https://doi.org/10.1002/jpln.200800073

Ghezzehei, T.A., Or, D. (2003). Pore-Space Dynamics in a Soil Aggregate Bed under a Static External Load. *Soil Science Society of America Journal*. 67, 12–19. https://doi.org/10.2136/sssaj2003.1200

Ghezzehei, T.A., Or, D. (2000). Dynamics of soil aggregate coalescence governed by capillary and rheological processes. *Water Resources Research*. 36, 367–379. https://doi.org/10.1029/1999WR900316

Greenland, D.J. (1977). Soil damage by intensive arable cultivation: temporary or permanent? *Philosophical Transactions of the Royal Society of London. B, Biological Sciences*. 281, 193–208. https://doi.org/10.1098/rstb.1977.0133

Gregory, A.S., Ritz, K., McGrath, S.P., Quinton, J.N., Goulding, K.W.T., Jones, R.J.A., Harris, J.A., Bol, R., Wallace, P., Pilgrim, E.S., Whitmore, A.P. (2015). A review of the impacts of degradation threats on soil properties in the UK. *Soil Use and Management*. 31, 1–15. https://doi.org/10.1111/sum.12212

Gregory, A.S., Watts, C.W., Griffiths, B.S., Hallett, P.D., Kuan, H.L., Whitmore, A.P. (2009). The effect of long-term soil management on the physical and biological resilience of a range of arable and grassland soils in England. *Geoderma*. 153, 172–185. https://doi.org/10.1016/j.geoderma.2009.08.002

Grusson, Y., Wesström, I., Joel, A. (2021). Impact of climate change on Swedish agriculture: Growing season rain deficit and irrigation need. *Agricultural Water Management*. 251, 106858. https://doi.org/10.1016/j.agwat.2021.106858

Gupta, S., Bonetti, S., Lehmann, P., Or, D. (2022a). Limited role of soil texture in mediating natural vegetation response to rainfall anomalies. *Environmental Research Letters*. 17, 034012. https://doi.org/10.1088/1748-9326/ac5206

Gupta, S., Lehmann, P., Bonetti, S., Papritz, A., Or, D. (2021). Global Prediction of Soil Saturated Hydraulic Conductivity Using Random Forest in a Covariate-Based GeoTransfer Function (CoGTF) Framework. Journal of Advances in

Modeling Earth Systems. 13, e2020MS002242. https://doi.org/10.1029/2020MS002242

Gupta, S., Papritz, A., Lehmann, P., Hengl, T., Bonetti, S., Or, D. (2022b). Global Soil Hydraulic Properties dataset based on legacy site observations and robust parameterization. *Scientific Data*. 9, 444. https://doi.org/10.1038/s41597-022-01481-5

Håkansson, I., Medvedev, V.W. (1995). Protection of soils from mechanical overloading by establishing limits for stresses caused by heavy vehicles. *Soil and Tillage Research*. 35, 85–97. https://doi.org/10.1016/0167-1987(95)00476-9

Håkansson, I., Myrbeck, Å., Etana, A. (2002). A review of research on seedbed preparation for small grains in Sweden. *Soil and Tillage Research*. 64, 23–40. https://doi.org/10.1016/S0167-1987(01)00255-0

Halim, M.A., Thomas, S.C. (2018). A proxy-year analysis shows reduced soil temperatures with climate warming in boreal forest. *Scientific Reports*. 8, 16859. https://doi.org/10.1038/s41598-018-35213-w

Hayashi, Y., Ken'ichirou, K., Mizuyama, T. (2006). Changes in pore size distribution and hydraulic properties of forest soil resulting from structural development. *Journal of Hydrology*. 331, 85–102. https://doi.org/10.1016/j.jhydrol.2006.05.003

Haynes, R.J., Naidu, R. (1998). Influence of lime, fertilizer and manure applications on soil organic matter content and soil physical conditions: a review. *Nutrient Cycling in Agroecosystems*. 51, 123–137. https://doi.org/10.1023/A:1009738307837

Hirmas, D.R., Giménez, D., Nemes, A., Kerry, R., Brunsell, N.A., Wilson, C.J. (2018). Climate-induced changes in continental-scale soil macroporosity may intensify water cycle. *Nature*. 561, 100–103. https://doi.org/10.1038/s41586-018-0463-x

Hohenbrink, T.L., Jackisch, C., Durner, W., Germer, K., Iden, S.C., Kreiselmeier, J., Leuther, F., Metzger, J.C., Naseri, M., Peters, A. (2023). Soil water retention and hydraulic conductivity measured in a wide saturation range. *Earth System Science Data*. 15, 4417–4432. https://doi.org/10.5194/essd-15-4417-2023

Hoogsteen, M.J.J., Lantinga, E.A., Bakker, E.J., Groot, J.C.J., Tittonell, P.A. (2015). Estimating soil organic carbon through loss on ignition: effects of ignition conditions and structural water loss: Refining the loss on ignition method. *European Journal of Soil Science*. 66, 320–328. https://doi.org/10.1111/ejss.12224

Hu, W., Shao, M.A., Si, B.C. (2012). Seasonal changes in surface bulk density and saturated hydraulic conductivity of natural landscapes. *European Journal of Soil Science*. 63, 820–830. https://doi.org/10.1111/j.1365-2389.2012.01479.x

Hwang, S.I., Powers, S.E. (2003). Lognormal distribution model for estimating soil water retention curves for sandy soils. *Soil Science*. 168, 156–166. https://doi.org/10.1097/01.ss.0000058888.60072.e3

Hwang, S.Il., Choi, S.Il. (2006). Use of a lognormal distribution model for estimating soil water retention curves from particle-size distribution data. *Journal of Hydrology*. 323, 325–334. https://doi.org/10.1016/j.jhydrol.2005.09.005

Jabro, J.D., Iversen, W.M., Evans, R.G., Allen, B.L., Stevens, W.B. (2014). Repeated Freeze-Thaw Cycle Effects on Soil Compaction in a Clay Loam in Northeastern Montana. *Soil Science Society of America Journal*. 78, 737–744. https://doi.org/10.2136/sssaj2013.07.0280

Jarvis, N., Forkman, J., Koestel, J., Kätterer, T., Larsbo, M., Taylor, A. (2017a). Long-term effects of grass-clover leys on the structure of a silt loam soil in a cold climate. *Agriculture, Ecosystems & Environment*. 247, 319–328. https://doi.org/10.1016/j.agee.2017.06.042

Jarvis, N., Koestel, J., Messing, I., Moeys, J., Lindahl, A. (2013). Influence of soil, land use and climatic factors on the hydraulic conductivity of soil. *Hydrology and Earth System Sciences*. 17, 5185–5195. https://doi.org/10.5194/hess-17-5185-2013

Jarvis, N., Larsbo, M., Koestel, J. (2017b). Connectivity and percolation of structural pore networks in a cultivated silt loam soil quantified by X-ray tomography. *Geoderma*. 287, 71–79. https://doi.org/10.1016/j.geoderma.2016.06.026

Jarvis, N.J. (2007). A review of non-equilibrium water flow and solute transport in soil macropores: principles, controlling factors and consequences for water quality. *European Journal of Soil Science*. 58, 523–546. https://doi.org/10.1111/j.1365-2389.2007.00915.x

Jarvis, N.J., Messing, I. (1995). Near-Saturated Hydraulic Conductivity in Soils of Contrasting Texture Measured by Tension Infiltrometers. *Soil Science Society of America Journal*. 59, 27–34. https://doi.org/10.2136/sssaj1995.03615995005900010004x

Jenny, H. (1941). Factors of Soil Formation: A System of Quantitative Pedology. McGraw-Hill, USA.

Jensen, J.L., Schjønning, P., Watts, C.W., Christensen, B.T., Munkholm, L.J. (2019). Soil Water Retention: Uni-Modal Models of Pore-Size Distribution Neglect Impacts of Soil Management. *Soil Science Society of America Journal*. 83, 18–26. https://doi.org/10.2136/sssaj2018.06.0238

Jorda, H., Bechtold, M., Jarvis, N., Koestel, J. (2015). Using boosted regression trees to explore key factors controlling saturated and near-saturated hydraulic conductivity: Effects of soil properties on hydraulic conductivity. *European Journal of Soil Science*. 66, 744–756. https://doi.org/10.1111/ejss.12249

Jungqvist, G., Oni, S.K., Teutschbein, C., Futter, M.N. (2014). Effect of Climate Change on Soil Temperature in Swedish Boreal Forests. *PLoS ONE*. 9, e93957. https://doi.org/10.1371/journal.pone.0093957

Keller, T., Or, D. (2022). Farm vehicles approaching weights of sauropods exceed safe mechanical limits for soil functioning. *Proceedings of the National Academy of Sciences*. 119, e2117699119. https://doi.org/10.1073/pnas.2117699119

Keller, T., Sandin, M., Colombi, T., Horn, R., Or, D. (2019). Historical increase in agricultural machinery weights enhanced soil stress levels and adversely affected soil functioning. *Soil and Tillage Research*. 194, 104293. https://doi.org/10.1016/j.still.2019.104293

Kirchmann, H., Persson, J., Carlgren, K. (1994). *The Ultuna long-term soil organic matter experiment, 1956-1991* (Reports and Dissertations No. 17). Department of Soil Sciences, Swedish University of Agricultural Sciences, Uppsala, Sweden.

Klöffel, T., Young, E.H., Borchard, N., Vallotton, J.D., Nurmi, E., Shurpali, N.J., Urbano Tenorio, F., Liu, X., Young, G.H.F., Unc, A. (2022). The challenges fraught opportunity of agriculture expansion into boreal and Arctic regions. *Agricultural Systems*. 203, 103507. https://doi.org/10.1016/j.agsy.2022.103507

Koestel, J., Dathe, A., Skaggs, T.H., Klakegg, O., Ahmad, M.A., Babko, M., Giménez, D., Farkas, C., Nemes, A., Jarvis, N. (2018). Estimating the Permeability of Naturally Structured Soil From Percolation Theory and Pore Space Characteristics Imaged by X-Ray. *Water Resources Research*. 54, 9255–9263. https://doi.org/10.1029/2018WR023609

Koestel, J., Larsbo, M., Jarvis, N. (2020). Scale and REV analyses for porosity and pore connectivity measures in undisturbed soil. *Geoderma*. 366, 114206. https://doi.org/10.1016/j.geoderma.2020.114206

Koopmans, R.W.R., Miller, R.D. (1966). Soil Freezing and Soil Water Characteristic Curves. *Soil Science Society of America Journal*. 30, 680–685. https://doi.org/10.2136/sssaj1966.03615995003000060011x

Kosugi, K. (1996). Lognormal Distribution Model for Unsaturated Soil Hydraulic Properties. *Water Resources Research*. 32, 2697–2703. https://doi.org/10.1029/96WR01776

Kosugi, K. (1994). Three-parameter lognormal distribution model for soil water retention. *Water Resources Research*. 30, 891–901. https://doi.org/10.1029/93WR02931

Kreiselmeier, J., Chandrasekhar, P., Weninger, T., Schwen, A., Julich, S., Feger, K.-H., Schwärzel, K. (2019). Quantification of soil pore dynamics during a winter wheat cropping cycle under different tillage regimes. *Soil and Tillage Research*. 192, 222–232. https://doi.org/10.1016/j.still.2019.05.014

Kukal, M.S., Irmak, S., Dobos, R., Gupta, S. (2023). Atmospheric dryness impacts on crop yields are buffered in soils with higher available water capacity. *Geoderma*. 429, 116270. https://doi.org/10.1016/j.geoderma.2022.116270

Kullback, S., Leibler, R.A. (1951). On Information and Sufficiency. *The Annals of Mathematical Statistics*. 22, 79–86.

Leuther, F., Mikutta, R., Wolff, M., Kaiser, K., Schlüter, S. (2023). Structure turnover times of grassland soils under different moisture regimes. *Geoderma*. 433, 116464. https://doi.org/10.1016/j.geoderma.2023.116464

Leuther, F., Schlüter, S. (2021). Impact of freeze–thaw cycles on soil structure and soil hydraulic properties. *SOIL*. 7, 179–191. https://doi.org/10.5194/soil-7-179-2021

Liu, B., Fan, H., Han, W., Zhu, L., Zhao, X., Zhang, Y., Ma, R. (2021). Linking soil water retention capacity to pore structure characteristics based on X-ray computed tomography: Chinese Mollisol under freeze-thaw effect. *Geoderma*. 401, 115170. https://doi.org/10.1016/j.geoderma.2021.115170

Loveland, P., Webb, J. (2003). Is there a critical level of organic matter in the agricultural soils of temperate regions: a review. *Soil and Tillage Research*. 70, 1–18. https://doi.org/10.1016/S0167-1987(02)00139-3

Lu, J., Zhang, Q., Werner, A.D., Li, Y., Jiang, S., Tan, Z. (2020). Root-induced changes of soil hydraulic properties – A review. *Journal of Hydrology*. 589, 125203. https://doi.org/10.1016/j.jhydrol.2020.125203

Lu, N. (2020). Unsaturated Soil Mechanics: Fundamental Challenges, Breakthroughs, and Opportunities. *Journal of Geotechnical and Geoenvironmental Engineering*. 146, 02520001. https://doi.org/10.1061/(ASCE)GT.1943-5606.0002233

Lu, N. (2016). Generalized Soil Water Retention Equation for Adsorption and Capillarity. *Journal of Geotechnical and Geoenvironmental Engineering*. 142, 04016051. https://doi.org/10.1061/(ASCE)GT.1943-5606.0001524

Lucas, M., Nguyen, L.T.T., Guber, A., Kravchenko, A.N. (2022). Cover crop influence on pore size distribution and biopore dynamics: Enumerating root and soil faunal effects. *Frontiers in Plant Science*. 13, 928569. https://doi.org/10.3389/fpls.2022.928569

Lucas, M., Vetterlein, D., Vogel, H., Schlüter, S. (2020). Revealing pore connectivity across scales and resolutions with X-ray CT. *European Journal of Soil Science*. 72, 546–560. https://doi.org/10.1111/ejss.12961

Luo, L., Lin, H., Schmidt, J. (2010). Quantitative Relationships between Soil Macropore Characteristics and Preferential Flow and Transport. *Soil Science Society of America Journal*. 74, 1929–1937. https://doi.org/10.2136/sssaj2010.0062

Luo, S., Lu, N., Zhang, C., Likos, W. (2022). Soil water potential: A historical perspective and recent breakthroughs. *Vadose Zone Journal*. 21. https://doi.org/10.1002/vzj2.20203

Luomaranta, A., Aalto, J., Jylhä, K. (2019). Snow cover trends in Finland over 1961–2014 based on gridded snow depth observations. *International Journal of Climatology*. 39, 3147–3159. https://doi.org/10.1002/joc.6007

Luxmoore, R.J. (1981). Micro-, Meso-, and Macroporosity of Soil. *Soil Science Society of America Journal*. 45, 671–672. https://doi.org/10.2136/sssaj1981.03615995004500030051x

Ma, Q., Zhang, K., Jabro, J.D., Ren, L., Liu, H. (2019). Freeze–thaw cycles effects on soil physical properties under different degraded conditions in Northeast China. *Environmental Earth Sciences*. 78, 321. https://doi.org/10.1007/s12665-019-8323-z

Ma, R., Jiang, Y., Liu, B., Fan, H. (2021). Effects of pore structure characterized by synchrotron-based micro-computed tomography on aggregate stability of black soil under freeze-thaw cycles. *Soil and Tillage Research*. 207, 104855. https://doi.org/10.1016/j.still.2020.104855

Mapa, R.B., Green, R.E., Santo, L. (1986). Temporal Variability of Soil Hydraulic Properties with Wetting and Drying Subsequent to Tillage. *Soil Science Society of America Journal*. 50, 1133–1138. https://doi.org/10.2136/sssaj1986.03615995005000050008x

Messing, I., Alriksson, A., Johansson, W. (1997). Soil physical properties of afforested and arable land. *Soil Use and Management*. 13, 209–217. https://doi.org/10.1111/j.1475-2743.1997.tb00588.x

Messing, I., Jarvis, N.J. (1993). Temporal variation in the hydraulic conductivity of a tilled clay soil as measured by tension infiltrometers. *Journal of Soil Science*. 44, 11–24. https://doi.org/10.1111/j.1365-2389.1993.tb00430.x

Meurer, K., Barron, J., Chenu, C., Coucheney, E., Fielding, M., Hallett, P., Herrmann, A.M., Keller, T., Koestel, J., Larsbo, M., Lewan, E., Or, D., Parsons, D., Parvin, N., Taylor, A., Vereecken, H., Jarvis, N. (2020). A framework for modelling soil structure dynamics induced by biological activity. *Global Change Biology*. 26, 5382–5403. https://doi.org/10.1111/gcb.15289

Miranda-Vélez, J.F., Leuther, F., Köhne, J.M., Munkholm, L.J., Vogeler, I. (2023). Effects of freeze-thaw cycles on soil structure under different tillage and plant cover management practices. *Soil and Tillage Research*. 225, 105540. https://doi.org/10.1016/j.still.2022.105540

Mohammadi, M.H., Vanclooster, M. (2011). Predicting the Soil Moisture Characteristic Curve from Particle Size Distribution with a Simple Conceptual Model. *Vadose Zone Journal*. 10, 594–602. https://doi.org/10.2136/vzj2010.0080

Mohammed, A.A., Kurylyk, B.L., Cey, E.E., Hayashi, M. (2018). Snowmelt Infiltration and Macropore Flow in Frozen Soils: Overview, Knowledge Gaps, and a Conceptual Framework. *Vadose Zone Journal*. 17, 1–15. https://doi.org/10.2136/vzj2018.04.0084

Mubarak, I., Mailhol, J.C., Angulo-Jaramillo, R., Ruelle, P., Boivin, P., Khaledian, M. (2009). Temporal variability in soil hydraulic properties under drip irrigation. *Geoderma*. 150, 158–165. https://doi.org/10.1016/j.geoderma.2009.01.022

Nasta, P., Franz, T.E., Gibson, J.P., Romano, N. (2023). Revisiting the definition of field capacity as a functional parameter in a layered agronomic soil profile beneath irrigated maize. *Agricultural Water Management*. 284, 108368. https://doi.org/10.1016/j.agwat.2023.108368

Naveed, M., Moldrup, P., Vogel, H.-Jö., Lamandé, M., Wildenschild, D., Tuller, M., de Jonge, L.W. (2014). Impact of long-term fertilization practice on soil structure evolution. *Geoderma*. 217–218, 181–189. https://doi.org/10.1016/j.geoderma.2013.12.001

Nemes, A., Schaap, M.G., Leij, F.J., Wösten, J.H.M. (2001). Description of the unsaturated soil hydraulic database UNSODA version 2.0. *Journal of Hydrology*. 251, 151–162. https://doi.org/10.1016/S0022-1694(01)00465-6

Nimmo, J.R. (2013). Porosity and Pore Size Distribution. In *Reference Module in Earth Systems and Environmental Sciences*. Elsevier. https://doi.org/10.1016/B978-0-12-409548-9.05265-9

Nimmo, J.R. (1997). Modeling Structural Influences on Soil Water Retention. *Soil Science Society of America Journal*. 61, 712–719. https://doi.org/10.2136/sssaj1997.03615995006100030002x

Nimmo, J.R., Herkelrath, W.N., Laguna Luna, A.M. (2007). Physically Based Estimation of Soil Water Retention from Textural Data: General Framework, New Models, and Streamlined Existing Models. *Vadose Zone Journal*. 6, 766–773. https://doi.org/10.2136/vzj2007.0019

Or, D., Ghezzehei, T.A. (2002). Modeling post-tillage soil structural dynamics: a review. *Soil and Tillage Research*. 64, 41–59. https://doi.org/10.1016/S0167-1987(01)00256-2

Or, D., Keller, T., Schlesinger, W.H. (2021). Natural and managed soil structure: On the fragile scaffolding for soil functioning. *Soil and Tillage Research*. 208, 104912. https://doi.org/10.1016/j.still.2020.104912

Parvin, N., Coucheney, E., Gren, I.-M., Andersson, H., Elofsson, K., Jarvis, N., Keller, T. (2022). On the relationships between the size of agricultural machinery, soil quality and net revenues for farmers and society. *Soil Security*. 6, 100044. https://doi.org/10.1016/j.soisec.2022.100044

Peng, X., Horn, R., Smucker, A. (2007). Pore Shrinkage Dependency of Inorganic and Organic Soils on Wetting and Drying Cycles. *Soil Science Society of America Journal*. 71, 1095–1104. https://doi.org/10.2136/sssaj2006.0156

Peters, A., Durner, W. (2008). Simplified evaporation method for determining soil hydraulic properties. *Journal of Hydrology*. 356, 147–162. https://doi.org/10.1016/j.jhydrol.2008.04.016

Poeplau, C., Don, A., Six, J., Kaiser, M., Benbi, D., Chenu, C., Cotrufo, M.F., Derrien, D., Gioacchini, P., Grand, S., Gregorich, E., Griepentrog, M., Gunina, A., Haddix, M., Kuzyakov, Y., Kühnel, A., Macdonald, L.M., Soong, J., Trigalet, S., Vermeire, M.-L., Rovira, P., van Wesemael, B., Wiesmeier, M., Yeasmin, S., Yevdokimov, I., Nieder, R. (2018). Isolating organic carbon fractions with varying turnover rates in temperate agricultural soils – A comprehensive method comparison. *Soil Biology and Biochemistry*. 125, 10–26. https://doi.org/10.1016/j.soilbio.2018.06.025

Pollacco, J.A.P., Fernández-Gálvez, J., Carrick, S. (2020). Improved prediction of water retention curves for fine texture soils using an intergranular mixing particle size distribution model. *Journal of Hydrology*. 584, 124597. https://doi.org/10.1016/j.jhydrol.2020.124597

Pollacco, J.A.P., Webb, T., McNeill, S., Hu, W., Carrick, S., Hewitt, A., Lilburne, L. (2017). Saturated hydraulic conductivity model computed from bimodal water retention curves for a range of New Zealand soils. *Hydrology and Earth System Sciences*. 21, 2725–2737. https://doi.org/10.5194/hess-21-2725-2017

Pulliainen, J., Luojus, K., Derksen, C., Mudryk, L., Lemmetyinen, J., Salminen, M., Ikonen, J., Takala, M., Cohen, J., Smolander, T., Norberg, J. (2020). Patterns and trends of Northern Hemisphere snow mass from 1980 to 2018. *Nature*. 581, 294–298. https://doi.org/10.1038/s41586-020-2258-0

Rabot, E., Wiesmeier, M., Schlüter, S., Vogel, H.-J. (2018). Soil structure as an indicator of soil functions: A review. *Geoderma*. 314, 122–137. https://doi.org/10.1016/j.geoderma.2017.11.009

Renard, P., Allard, D. (2013). Connectivity metrics for subsurface flow and transport. *Advances in Water Resources*. 51, 168–196. https://doi.org/10.1016/j.advwatres.2011.12.001

Reynolds, W.D. (2017). Use of bimodal hydraulic property relationships to characterize soil physical quality. *Geoderma*. 294, 38–49. https://doi.org/10.1016/j.geoderma.2017.01.035

Reynolds, W.D., Drury, C.F., Tan, C.S., Fox, C.A., Yang, X.M. (2009). Use of indicators and pore volume-function characteristics to quantify soil physical quality. *Geoderma*. 152, 252–263. https://doi.org/10.1016/j.geoderma.2009.06.009

Richard, G., Cousin, I., Sillon, J.F., Bruand, A., Guérif, J. (2001). Effect of compaction on the porosity of a silty soil: influence on unsaturated hydraulic properties. *European Journal of Soil Science*. 52, 49–58. https://doi.org/10.1046/j.1365-2389.2001.00357.x

Robinson, D.A., Hopmans, J.W., Filipovic, V., Van Der Ploeg, M., Lebron, I., Jones, S.B., Reinsch, S., Jarvis, N., Tuller, M. (2019). Global environmental changes impact soil hydraulic functions through biophysical feedbacks. *Global Change Biology*. 25, 1895–1904. https://doi.org/10.1111/gcb.14626

Robinson, David.A., Jones, S.B., Lebron, I., Reinsch, S., Domínguez, M.T., Smith, A.R., Jones, D.L., Marshall, M.R., Emmett, B.A. (2016). Experimental evidence for drought induced alternative stable states of soil moisture. *Scientific Reports*. 6, 20018. https://doi.org/10.1038/srep20018

Romano, N., Nasta, P., Severino, G., Hopmans, J.W. (2011). Using Bimodal Lognormal Functions to Describe Soil Hydraulic Properties. *Soil Science Society of America Journal*. 75, 468–480. https://doi.org/10.2136/sssaj2010.0084

Ross, P.J., Smettem, K.R.J. (1993). Describing Soil Hydraulic Properties with Sums of Simple Functions. *Soil Science Society of America Journal*. 57, 26–29. https://doi.org/10.2136/sssaj1993.03615995005700010006x

Rouault, Y., Assouline, S. (1998). A probabilistic approach towards modeling the relationships between particle and pore size distributions: the multicomponent packed sphere case. *Powder Technology*. 96, 33–41. https://doi.org/10.1016/S0032-5910(97)03355-X

Roudier, P., Andersson, J.C.M., Donnelly, C., Feyen, L., Greuell, W., Ludwig, F. (2016). Projections of future floods and hydrological droughts in Europe under a +2°C global warming. *Climatic Change*. 135, 341–355. https://doi.org/10.1007/s10584-015-1570-4

Rousi, E., Fink, A.H., Andersen, L.S., Becker, F.N., Beobide-Arsuaga, G., Breil, M., Cozzi, G., Heinke, J., Jach, L., Niermann, D., Petrovic, D., Richling, A., Riebold, J., Steidl, S., Suarez-Gutierrez, L., Tradowsky, J.S., Coumou, D., Düsterhus, A., Ellsäßer, F., Fragkoulidis, G., Gliksman, D., Handorf, D., Haustein, K., Kornhuber, K., Kunstmann, H., Pinto, J.G., Warrach-Sagi, K., Xoplaki, E. (2023). The extremely hot and dry 2018 summer in central and northern Europe from a multi-faceted weather and climate perspective. *Natural Hazards and Earth System Sciences*. 23, 1699–1718. https://doi.org/10.5194/nhess-23-1699-2023

Sandin, M., Koestel, J., Jarvis, N., Larsbo, M. (2017). Post-tillage evolution of structural pore space and saturated and near-saturated hydraulic conductivity in a clay loam soil. *Soil and Tillage Research*. 165, 161–168. https://doi.org/10.1016/j.still.2016.08.004

Scarlett, B., Van Der Kraan, M., Janssen, R.J.M. (1998). Porosity: a parameter with no direction. *Philosophical Transactions of the Royal Society of London. Series A: Mathematical, Physical and Engineering Sciences*. 356, 2623–2648. https://doi.org/10.1098/rsta.1998.0290

Schindler, U., Durner, W., Von Unold, G., Müller, L. (2010). Evaporation Method for Measuring Unsaturated Hydraulic Properties of Soils: Extending the Measurement Range. *Soil Science Society of America Journal*. 74, 1071–1083. https://doi.org/10.2136/sssaj2008.0358

Schlüter, S., Albrecht, L., Schwärzel, K., Kreiselmeier, J. (2020). Long-term effects of conventional tillage and no-tillage on saturated and near-saturated

hydraulic conductivity – Can their prediction be improved by pore metrics obtained with X-ray CT? *Geoderma*. 361, 114082. https://doi.org/10.1016/j.geoderma.2019.114082

Schultz, J. (2005). *The Ecozones of the World*. Springer, Berlin, Germany.

Schwen, A., Bodner, G., Scholl, P., Buchan, G.D., Loiskandl, W. (2011). Temporal dynamics of soil hydraulic properties and the water-conducting porosity under different tillage. *Soil and Tillage Research*. 113, 89–98. https://doi.org/10.1016/j.still.2011.02.005

Sekera, F. (1951). Gesunder und kranker Boden: ein praktischer Wegweiser zur Gesunderhaltung des Ackers [Healthy and sick soil: a practical guide to keeping the field healthy]. Paul Parey, Berlin, Germany.

Shiklomanov, N.I. (2012). Non-climatic factors and long-term, continental-scale changes in seasonally frozen ground. *Environmental Research Letters*. 7, 011003. https://doi.org/10.1088/1748-9326/7/1/011003

Sillers, W.S., Fredlund, D.G., Zakerzaheh, N. (2001). Mathematical attributes of some soil–water characteristic curve models. *Geotechnical and Geological Engineering*. 19, 243–283. https://doi.org/10.1023/A:1013109728218

Skaalsveen, K., Ingram, J., Clarke, L.E. (2019). The effect of no-till farming on the soil functions of water purification and retention in north-western Europe: A literature review. *Soil and Tillage Research*. 189, 98–109. https://doi.org/10.1016/j.still.2019.01.004

Smith, C.W., Johnston, M.A., Lorentz, S. (1997). Assessing the compaction susceptibility of South African forestry soils. I. The effect of soil type, water content and applied pressure on uni-axial compaction. *Soil and Tillage Research*. 41, 53–73. https://doi.org/10.1016/S0167-1987(96)01084-7

Spinoni, J., Vogt, J.V., Naumann, G., Barbosa, P., Dosio, A. (2018). Will drought events become more frequent and severe in Europe?. *International Journal of Climatology*. 38, 1718–1736. https://doi.org/10.1002/joc.5291

Stähli, M., Jansson, P.-E., Lundin, L.-C. (1999). Soil moisture redistribution and infiltration in frozen sandy soils. *Water Resources Research*. 35, 95–103. https://doi.org/10.1029/1998WR900045

Starkloff, T., Larsbo, M., Stolte, J., Hessel, R., Ritsema, C. (2017). Quantifying the impact of a succession of freezing-thawing cycles on the pore network of a silty clay loam and a loamy sand topsoil using X-ray tomography. *CATENA*. 156, 365–374. https://doi.org/10.1016/j.catena.2017.04.026

Strandberg, G., Bärring, L., Hansson, U., Jansson, C., Jones, C., Kjellström, E., Kolax, M., Kupiainen, M., Nikulin, G., Samuelsson, P., Ullerstig, A., Wang, S. (2014). *CORDEX scenarios for Europe from the Rossby Centre regional climate model RCA4* (Report Meteorology and Climatology No. 116). SMHI, Norrköping, Sweden.

Strudley, M., Green, T., Ascoughii, J. (2008). Tillage effects on soil hydraulic properties in space and time: State of the science. *Soil and Tillage Research*. 99, 4–48. https://doi.org/10.1016/j.still.2008.01.007

Sullivan, P.L., Billings, S.A., Hirmas, D., Li, L., Zhang, X., Ziegler, S., Murenbeeld, K., Ajami, H., Guthrie, A., Singha, K., Giménez, D., Duro, A., Moreno, V., Flores, A., Cueva, A., Koop, Aronson, E.L., Barnard, H.R., Banwart, S.A., Keen, R.M., Nemes, A., Nikolaidis, N.P., Nippert, J.B., Richter, D., Robinson, D.A., Sadayappan, K., De Souza, L.F.T., Unruh, M., Wen, H. (2022). Embracing the dynamic nature of soil structure: A paradigm illuminating the role of life in critical zones of the Anthropocene. *Earth-Science Reviews*. 225, 103873. https://doi.org/10.1016/j.earscirev.2021.103873

Svensson, D.N. (2020). *Influence of cropping and fertilization on soil pore characteristics in a long-term field study* (Master's Thesis). Swedish University of Agricultural Sciences, Uppsala, Sweden.

Taina, I.A., Heck, R.J., Deen, W., Ma, E.Y.T. (2013). Quantification of freeze–thaw related structure in cultivated topsoils using X-ray computer tomography. *Canadian Journal of Soil Science*. 93, 533–553. https://doi.org/10.4141/cjss2012-044

Torres, L.C., Keller, T., Paiva De Lima, R., Antônio Tormena, C., Veras De Lima, H., Fabíola Balazero Giarola, N. (2021). Impacts of soil type and crop species on permanent wilting of plants. *Geoderma*. 384, 114798. https://doi.org/10.1016/j.geoderma.2020.114798

Totsche, K.U., Amelung, W., Gerzabek, M.H., Guggenberger, G., Klumpp, E., Knief, C., Lehndorff, E., Mikutta, R., Peth, S., Prechtel, A., Ray, N., Kögel-Knabner, I. (2018). Microaggregates in soils. *Journal of Plant Nutrition and Soil Science*. 181, 104–136. https://doi.org/10.1002/jpln.201600451

Tuller, M., Or, D., Dudley, L.M. (1999). Adsorption and capillary condensation in porous media: Liquid retention and interfacial configurations in angular pores. *Water Resources Research*. 35, 1949–1964. https://doi.org/10.1029/1999WR900098

Unger, P.W. (1991). Overwinter Changes in Physical Properties of No-Tillage Soil. *Soil Science Society of America Journal*. 55, 778–782. https://doi.org/10.2136/sssaj1991.03615995005500030024x

van Genuchten, M.T. (1980). A Closed-form Equation for Predicting the Hydraulic Conductivity of Unsaturated Soils. *Soil Science Society of America Journal*. 44, 892–898. https://doi.org/10.2136/sssaj1980.03615995004400050002x

Vaz, C.M.P., de Freitas Iossi, M., de Mendonça Naime, J., Macedo, Á., Reichert, J.M., Reinert, D.J., Cooper, M. (2005). Validation of the Arya and Paris Water Retention Model for Brazilian Soils. *Soil Science Society of America Journal*. 69, 577–583. https://doi.org/10.2136/sssaj2004.0104

Veihmeyer, F.J., Hendrickson, A.H. (1931). The moisture equivalent as a measure of the field capacity of soils. *Soil Science*. 32, 181–194.

Veihmeyer, F.J., Hendrickson, A.H. (1928). Soil moisture at permanent wilting of plants. *Plant Physiology*. 3, 355–357.

Vidal, A., Klöffel, T., Guigue, J., Angst, G., Steffens, M., Hoeschen, C., Mueller, C.W. (2021). Visualizing the transfer of organic matter from decaying plant residues to soil mineral surfaces controlled by microorganisms. *Soil Biology and Biochemistry*. 160, 108347. https://doi.org/10.1016/j.soilbio.2021.108347

Vogel, H., Balseiro-Romero, M., Kravchenko, A., Otten, W., Pot, V., Schlüter, S., Weller, U., Baveye, P.C. (2022). A holistic perspective on soil architecture is needed as a key to soil functions. *European Journal of Soil Science*. 73. https://doi.org/10.1111/ejss.13152

Vogel, H.-J., Weller, U., Schlüter, S. (2010). Quantification of soil structure based on Minkowski functions. *Computers & Geosciences*. 36, 1236–1245. https://doi.org/10.1016/j.cageo.2010.03.007

Wiecheteck, L.H., Giarola, N.F.B., De Lima, R.P., Tormena, C.A., Torres, L.C., De Paula, A.L. (2020). Comparing the classical permanent wilting point concept of soil (−15,000 hPa) to biological wilting of wheat and barley plants under contrasting soil textures. *Agricultural Water Management*. 230, 105965. https://doi.org/10.1016/j.agwat.2019.105965

Wolf, M.K., Wiesmeier, M., Macholdt, J. (2023). Importance of soil fertility for climate-resilient cropping systems: The farmer's perspective. *Soil Security*. 13, 100119. https://doi.org/10.1016/j.soisec.2023.100119

Wu, X., Yuan, Z., Li, D., Zhou, J., Liu, T. (2023). Geographic variations of pore structure of clayey soils along a climatic gradient. *CATENA*. 222, 106861. https://doi.org/10.1016/j.catena.2022.106861

Yoon, S.W. (2009). *A measure of soil structure derived from water retention properties: a Kullback-Leibler Distance approach* (Dissertation). Rutgers University, New Brunswick, USA.

Yoon, S.W., Giménez, D. (2012). Entropy Characterization of Soil Pore Systems Derived From Soil-Water Retention Curves. *Soil Science*. 177, 361–368. https://doi.org/10.1097/SS.0b013e318256ba1c

You, T., Li, S., Guo, Y., Wang, C., Liu, X., Zhao, J., Wang, D. (2022). A superior soil–water characteristic curve for correcting the Arya-Paris model based on particle size distribution. *Journal of Hydrology*. 613, 128393. https://doi.org/10.1016/j.jhydrol.2022.128393

Young, I.M., Crawford, J.W., Rappoldt, C. (2001). New methods and models for characterising structural heterogeneity of soil. *Soil and Tillage Research*. 61, 33–45. https://doi.org/10.1016/S0167-1987(01)00188-X

Zech, W., Schad, P., Hintermaier-Erhard, G. (2022). Soils of the World. Springer, Berlin, Germany. https://doi.org/10.1007/978-3-540-30461-6

Zhang, M., Lu, Y., Heitman, J., Horton, R., Ren, T. (2017). Temporal Changes of Soil Water Retention Behavior as Affected by Wetting and Drying Following Tillage. *Soil Science Society of America Journal*. 81, 1288–1295. https://doi.org/10.2136/sssaj2017.01.0038

Zhang, R. (1997). Determination of Soil Sorptivity and Hydraulic Conductivity from the Disk Infiltrometer. *Soil Science Society of America Journal*. 61, 1024–1030. https://doi.org/10.2136/sssaj1997.03615995006100040005x

Zhang, X., Neal, A.L., Crawford, J.W., Bacq-Labreuil, A., Akkari, E., Rickard, W. (2021). The effects of long-term fertilizations on soil hydraulic properties vary with scales. *Journal of Hydrology*. 593, 125890. https://doi.org/10.1016/j.jhydrol.2020.125890

Zhang, Y., Weihermüller, L., Toth, B., Noman, M., Vereecken, H. (2022). Analyzing dual porosity in soil hydraulic properties using soil databases for pedotransfer function development. *Vadose Zone Journal*. 21. https://doi.org/10.1002/vzj2.20227

Popular science summary

News about record-breaking dry and wet spells are becoming more and more frequent in our daily lives and there is no doubt that this is the result of climate change. These periods of "too much" and "too little" water often have negative consequences for food production all over the world, including Scandinavia. Agricultural soils – the basis of food production on which we all depend – have the capacity to buffer such water deficits or surpluses. However, soils are highly variable from place to place, which means that not all of them are equally fit for this important task. This variability can easily be noted in the landscape, where soils vary, for example, in colour (some soils are redder or darker than others) or with respect to their grain sizes: some soils are composed of sand particles, and these soils drain quickly but hold little water, while others are clay-rich, which means they can hold more water, but they drain very slowly. Another important aspect of variability is how the particles of a soil are arranged, which is also referred to as soil structure.

   Soil structure is very important when it comes to the capacity of soils to buffer dry and wet spells. The reason for this is its strong link to water storage in and transport through soils. For example, soil grains may be packed very closely to each other such that water hardly infiltrates a soil and only a small volume is available for water storage. In contrast, if the grains of a soil are loosely packed, the soil volume and also the capacity to store water will be larger. The structure of a soil, and with this also its water storage and transport capacity, is affected by many different factors, with human factors including soil tillage being prominent examples. Perhaps less obvious, soil structure is also affected by processes that are related to climate. The main objective of this thesis was therefore to better understand the link between climate and soil structure, its effects on different soil water functions (e.g.,

water storage, drainage), and potential consequences in the context of climate change.

First, a new method to describe soil structure in a quantitative way was developed and successfully tested. In a subsequent study, this method was applied to agricultural soils across Sweden and Norway to investigate the importance of climate for the evolution of soil structure relative to other factors (e.g., particle-size distribution, time, soil organic matter content). A major finding of this study was that climate is an important driver of soil structure in Scandinavia: in general, the soils in warmer and wetter regions had a poorer structure than soils in cooler and drier regions. This was especially evident at greater soil depths. Although the exact reasons for this trend remain unclear, it is likely that the effects of climate are partly indirect. For example, the warmer regions of Sweden and Norway are more suitable for crop production and therefore are more frequently trafficked by heavy machinery, compacting the soil. This leads to a reduced capacity to store and transport water and the soil becomes less capable of buffering dry and wet spells.

The effects of one climate-driven process, namely freezing and thawing, were studied in more detail. In a laboratory experiment, it was investigated how freezing and thawing during winter might affect the structure of compacted soil layers and whether this process could restore their water storage and transport capacity. Besides this, the question was asked whether a shift in the amount and intensity of freeze-thaw cycles has any important consequences for soil structure and soil water functions. It was found that freezing and thawing can increase the pore-space volume and the connectivity of the pore space in compacted soil layers, which has potential benefits for drainage, water storage and plant water supply. Furthermore, it was found that a shift in freeze-thaw patterns has the potential to increase drainage rates of compacted soil layers under wet conditions, if this entails an increase in the number and intensity of freeze-thaw cycles. The potential benefits in this context are expected to be largest for soils composed of clay-sized particles. All these findings are important under future climate conditions in Scandinavia, when soils are likely to become wetter during autumn and winter, while early summer droughts are expected to become more frequent.

Populärvetenskaplig sammanfattning

Nyheter om rekordlånga torr- och regnperioder blir allt vanligare i vår vardag och det råder ingen tvekan om att detta är ett resultat av klimatförändringar. Perioder med "för mycket" och "för lite" vatten får ofta negativa konsekvenser för livsmedelsproduktion över hela världen, inklusive den tempererade boreala zonen som Sverige är en del av. Jordbruksmarken ligger till grund för den livsmedelsproduktion som vi alla är beroende av och har förmågan att dämpa stora skillnader i vattentillgång. Alla jordar är dock inte lika lämpade för denna uppgift, en av de främsta orsakerna till detta är att det finns en stor variation mellan olika jordar. Denna variation kan lätt noteras i landskapet, där jordar varierar i färg (från ljusare till mörkare) eller har olika partikelstorlek (från sand till ler). En annan viktig faktor för variabilitet är hur partiklarna i en jord är fördelade, vilket också kallas jordstruktur.

Markstrukturen är mycket viktig när det gäller markens förmåga att dämpa torra och våta perioder, eftersom strukturen styr vattenlagring och transport. Till exempel kan jordpartiklar packas mycket tätt intill varandra så att vatten knappast infiltrerar jorden och endast en liten volym är tillgänglig för vattenlagring. Om jordpartiklarna däremot är löst packade blir jordvolymen större och därmed också förmågan att lagra vatten. En jords struktur, och därmed också dess förmåga att lagra och transportera vatten, påverkas av många olika faktorer varav jordbearbetning är en särskilt viktig aspekt. Något som kan vara mindre uppenbart är att markstrukturen också påverkas av processer som är relaterade till klimatet. Huvudsyftet med denna avhandling var därför att bättre förstå kopplingen mellan klimat och markstruktur, dess effekter på olika markvattenfunktioner (till exempel vattenlagring och dränering) och potentiella konsekvenser i samband med klimatförändringar.

Först utvecklades och testades en ny metod för att beskriva markstrukturen på ett kvantitativt sätt. I en efterföljande studie tillämpades denna metod på jordbruksjordar i Sverige och Norge för att undersöka klimatets betydelse för utvecklingen av markstrukturen i förhållande till andra faktorer såsom partikelstorleksfördelning, tid och mängden humus. Ett viktigt resultat av denna studie var att klimatet är en viktig drivkraft för markstrukturen, där jordar i varmare och våtare regioner hade mindre porsystem än jordar i svalare och torrare regioner. Detta var särskilt tydligt vid större jorddjup. Även om de exakta orsakerna till denna trend fortfarande är delvis okända, är effekterna från klimatet troligen indirekta. Till exempel är de varmare regionerna i Sverige och Norge mer lämpade för växtproduktion och trafikeras därför oftare av tunga maskiner som kompakterar jorden och förstör markens porsystem. Detta leder till en minskad förmåga att lagra och transportera vatten och marken blir mindre kapabel att balansera vattentillgången under torra och våta perioder.

I en annan studie undersöktes en klimatdriven process mer i detalj, nämligen frysning och upptining av jordar. Man testade hur frysning och upptining under vintern påverkar strukturen hos kompakterade jordlager och om denna process kan återställa vattenlagrings- och transportkapaciteten. Dessutom undersöktes det om en förändring i antalet och intensiteten av frysning- och tiningscykler har några viktiga konsekvenser för markstruktur och markvattenfunktioner. Det visade sig att frysning och upptining kan öka porvolymen och vattnets förbindelse i kompakta jordlager, vilket har potentiella fördelar för dränering, vattenlagring och växtvattenförsörjning. Vidare konstaterades att fler och intensivare frys- och tiningscykler har potential att öka dräneringshastigheten för kompakterade jordlager under mycket våta förhållanden. De potentiella fördelarna i detta sammanhang förväntas dock vara störst för jordar som består av mindre jordpartiklar. Alla dessa resultat är viktiga i samband med fuktigare markförhållanden under höst och vinter och en ökad sannolikhet för försommartorka som förväntas för vissa delar av den tempererade boreala zonen i framtiden.

Acknowledgements

This work would not have been possible without the technical, mental and loving support by many people. These people accompanied me during different stages of this PhD and I am deeply grateful to all of them. I would like to mention at least some of them here.

To my mentors and friends outside SLU, *Carsten Müller* and *Peter Schad*: Both of you have been truly inspiring for me during my studies in Munich and you were instrumental in developing my passion for soil science. I consider myself (and countless other students) very lucky having had you as teachers. Without your immense support from the very beginning, I would never have been able to take up this position. You are wonderful scientists and personalities and I hope we continue to keep in touch.

To my main supervisor *Jennie Barron*: Thank you for accepting me for this position and allowing me to start this PhD. I appreciate the confidence you had in my abilities and that you supported basically every idea I came up with. You gave me a lot of freedom, which was also challenging at times, but in the end I have grown a lot from it so I thank you for that. Thank you for all the understanding, for constantly reminding me about the practical implications of research and thereby preventing me from drifting off into the "academic bubble" – I am definitely going to take this with me.

To my, what I would consider, second main supervisor *Nick Jarvis*: You have been such a great mentor to me during this PhD and I cannot tell how much I learned from you (not only about soil physics). Your continued support, kindness, humility, curiosity and wealth of knowledge have been truly inspiring. I hope we keep in touch so that I can continue to learn from you.

To *Mats Larsbo*: You have been extremely supportive and patient with me over these four years, especially when it came to the X-ray machine. I could always count on your help and I thank you a lot for that.

To the members of the team "Barefoot Germany" *Peter Schad*, *Andreas Wild*, *Vincent Buness* and *Lena Reifschneider*: Thank you for all the unforgettable field trips we have had over the last four years in different parts of Europe. It is always a great learning experience for me standing in the soil pit with you … barefoot of course!

To *Jesús Fernández-Gálvez*: Thank you for welcoming me to Granada and making my stay there a wonderful one. Thank you for all your support and for sharing your knowledge with me. I hope we keep in touch and meet again … preferably in Granada.

To *Louis Dufour*: I am really grateful having had you as an office mate. Thank you for supporting me throughout this PhD and for our at times very philosophical conversations. It was a pleasure seeing you and your family grow over the last years – you and Anna deserve the greatest respect for what you have achieved. Thank you also for the nice picnics and dinners we have had together. I wish you all the best for the future!

To *Ana Maria Mingot*: Thank you for having been so supportive and patient with my soil samples and for doing your best in the soil physics lab.

To *Jumpei Fukumasu*, *David Nimblad Svensson*, *Elsa Arrazola Vasquez*, *Eduardo Vázquez Garcia*, *Viktoria Wiklicky*, *Erica Packard*, *Frederic Leuther*, *Evelin Pihlap*, *Lukas Hallberg*, *Johannes Koestel*, *Jelena Rakovic*, *Miyanda Chilipamushi*, *Getachew Gemtesa Tiruneh*, *Tamlyn Gangiah*, *Thomas Keller*, *Tino Colombi*, *Geert Cornelis*, *Olive Tuyishime*, *Haichao Li*, *Marius Tuyishime*, *Judith Schubert*, *Francesco Bergese*, and *Wiebke Mareile Heinze*: Thank you very much for having supported me and my PhD work over these years through sampling, moving samples, moving me, answering questions, reviewing manuscripts, encouraging words, nice field and weekend trips, countless fika and lunch breaks, paragliding adventures, dinners, musical experiences, sauna evenings and lake dips, inspiring conversations, or by just being otherwise inspiring.

To *my parents* and *brother (German)*: Ihr habt mich mein ganzes Leben lang bei allem unterstützt, was ich gemacht habe und machen wollte, und dafür bin ich euch für immer dankbar. Ihr habt mich am meisten zu dem gemacht, der ich heute bin. Deshalb ist das nicht mein, sondern euer Erfolg!

To *Miriam*: Thank you for staying with me over these years, despite us being separated by seven hours of train ride. We have mastered and experienced so much during this time, and I am looking forward to everything that is coming!

II

ORIGINAL ARTICLE

European Journal of **Soil Science** **WILEY**

Relative entropy as an index of soil structure

Tobias Klöffel[1] | **Nicholas Jarvis[1]** | **Sung Won Yoon[2]** | **Jennie Barron[1]** | **Daniel Giménez[3]**

[1]Department of Soil and Environment, Swedish University of Agricultural Sciences, Uppsala, Sweden

[2]Department of Nano, Chemical & Biological Engineering, Seokyeong University, Seoul, South Korea

[3]Department of Environmental Sciences, Rutgers University, New Brunswick, New Jersey, USA

Correspondence
Tobias Klöffel, Department of Soil and Environment, Swedish University of Agricultural Sciences, Uppsala, Sweden.
Email: tobias.kloffel@slu.se

Abstract

Soil structure controls key soil functions in both natural and agro-ecosystems. Thus, numerous attempts have been made to develop methods aiming at its characterization. Here we propose an index of soil structure that uses relative entropy to quantify differences in the porosity and pore(void)-size distribution (VSD) between a structured soil derived from soil water retention data and the same soil without structure (a so-called reference soil) estimated from its particle-size distribution (PSD). The difference between these VSDs, which is the result of soil structure, is quantified using the Kullback–Leibler Divergence (KL divergence). We applied the method to soil data from two Swedish field experiments that investigate the long-term effects of soil management (fallow vs. inorganic fertilizer vs. manure) and land use (afforested land vs. agricultural land dominated by grass/clover ley) on soil properties. The KL divergence was larger for the soil receiving regular addition of manure compared with the soils receiving no organic amendments. Furthermore, soils under afforested land showed significantly larger KL divergences compared to agricultural soils near the soil surface, but smaller KL divergences in deeper soil layers, which closely mirrored the distribution of organic matter in the soil profile. Indeed, a significant positive correlation ($r = 0.374$, $p < 0.001$) was found between soil organic carbon concentrations and KL divergences across all sites and treatments. Despite challenges related to modelling the VSD of the reference soil without structure, the proposed index proved useful for evaluating differences in soil structure in response to soil management and land-use change and reflected the expected effects of soil organic matter on soil structure. We conclude that relative entropy shows great potential to serve as an easy-to-use index of soil structure, as it only requires widely available data on soil physical and hydraulic properties.

Highlights

- A new index of soil structure is proposed based on relative entropy
- A method is developed that separates the effects of soil texture and structure on the pore space

- The index identified soil structural differences in response to land use and soil organic carbon concentrations (SOC)
- The index shows the potential to serve as an easy-to-use metric of soil structure

1 | INTRODUCTION

Soil structure, defined as the spatial arrangement of soil solid constituents and the pore space (Rabot et al., 2018), is a key determining factor for a multitude of soil processes supporting the functioning of natural and agricultural ecosystems (Dominati et al., 2010; Or et al., 2021; Robinson et al., 2009). Examples are the regulation of biochemical cycling by controlling trophic interactions of soil biota (Erktan et al., 2020), the support of crop vigour (Or et al., 2021) and the control of fundamental hydrological processes such as surface runoff, infiltration and drainage (Fatichi et al., 2020; Mueller et al., 2013). Soil structure can also serve as an indicator of soil development (Bucka et al., 2021). The quantification and assessment of soil structure as well as the development of related indices are therefore of critical importance and have been the subject of extensive research in the past (e.g., Crawford et al., 1995; Dexter, 2004; Reynolds et al., 2009; Vogel et al., 2010; Yoon & Giménez, 2012). Although the use of advanced imaging technologies (e.g., X-ray computed tomography) to investigate soil structure is gaining increasing popularity (e.g., Jarvis, Forkman, et al., 2017; Jarvis, Larsbo, & Koestel, 2017; Lucas et al., 2020; Luo et al., 2008), their availability remains limited and their application expensive, while the processing of large datasets is time-consuming (Young et al., 2001). To avoid these limitations, it is desirable to develop a quantitative index of soil structure that only requires data from routine soil physical analyses.

The Minkowski functions represent a concise way to describe the geometry and topology of a multi-scale binary medium like soil (Vogel et al., 2010). These are defined as the volume and connectivity of the pore phase and the surface area and curvature of its interface with the solids, all expressed as a function of pore diameter. Many endeavours to quantify soil structure have focused directly or indirectly on the use of the soil water retention curve (SWRC) as a proxy for the pore(void)-size distribution (VSD), that is, one of the Minkowski functions, and its integral, the total soil porosity (ϕ). The SWRC describes the functional relationship between the water content (volumetric or gravimetric, θ) and matric potential (ψ_m) and allows the estimation of ϕ and the VSD, both of which are strongly affected by the physical, chemical and biological processes underlying the dynamic evolution of soil structure (Meurer, Barron, et al., 2020; Regelink et al., 2015). However, the direct quantification of soil structure from the SWRC is difficult since it is also influenced by the pore space created by the random packing of soil particles, also referred to as textural pore space (Nimmo, 1997). Thus, as noted by Yoon and Giménez (2012), robust quantification of soil structure from the SWRC and VSD requires a method that is insensitive to the particle-size distribution (PSD).

Entropy, being a measure of complexity, information and "order", has been recognized as a potential indicator for soil change such as the formation or degradation of soil structure (Dexter, 1977; Lin, 2011; Meurer, Barron, et al., 2020; Yoon, 2009; Yoon & Giménez, 2012). Structure-forming processes including the activity of soil biota, the influence of roots, wet-dry and freeze–thaw cycles, and soil tillage can be regarded as actions that "add information" to a given soil volume, thereby increasing the entropy of properties and functions related to soil structure, such as the VSD. For example, the multi-scale nature of structure-forming processes can result in a bimodal or multimodal VSD (e.g., Dexter et al., 2008; Durner, 1994; Reynolds, 2017) and, in this way, increase its heterogeneity. This implies that the entropy of a VSD is minimized for a hypothetical soil devoid of any structural features (Meurer, Barron, et al., 2020) and that the difference in entropy between such a hypothetical soil and a natural soil will increase with the degree of structural development in the latter. Therefore, relative entropy, being a measure of entropy *difference* between two distributions, may be a suitable indicator for the degree of soil structure. Indeed, the concept of relative entropy is not new to soil science and has been applied in various contexts (e.g., Hou & Rubin, 2005; Kim et al., 2016; Tarquis et al., 2008).

In this study, we propose the use of relative entropy as an index of soil structure. With this approach, we aim to eliminate the effects of soil texture on the VSD by exploiting the relationship between the PSD and the

VSD. Furthermore, we only use data from routine soil physical analyses. In the following, we first explain relative entropy and show how it can be used as an index of soil structure. We then apply it to soil data from two Swedish field experiments investigating the long-term effects of (i) soil management practices (bare fallow vs. mineral fertilizer addition vs. farmyard manure addition) and (ii) land use (tree plantations vs. crop rotations dominated by grass/clover ley) on soil properties. Finally, we discuss the result of these preliminary tests and the suitability of relative entropy as an index of soil structure.

2 | MATERIALS AND METHODS

2.1 | Relative entropy as an index of soil structure

Relative entropy, also known as the Kullback–Leibler Divergence (KL divergence), originates from information theory and is a dimensionless measure of the difference between two probability distributions of the same random variable (Goodfellow et al., 2016; Kullback & Leibler, 1951). One of the probability distributions acts as a reference distribution to which the second distribution is compared. The choice of the reference probability distribution is important since the KL divergence is asymmetric, that is, it differs with respect to this choice. Another property of the KL divergence is that it is always non-negative, such that a value of zero is obtained for two identical distributions (Bishop, 2006; Goodfellow et al., 2016).

In the case of two discrete probability distributions of the same random variable X, the KL divergence is defined as follows (MacKay, 2002):

$$D_{KL}\left(P\middle\|Q\right) = \sum_{x \in X} P(x)\log\left(\frac{P(x)}{Q(x)}\right) \quad (1)$$

where $Q(x)$ is the value of the reference probability distribution Q at x and $P(x)$ is the value of the probability distribution P at x. If X is continuous, the KL divergence reads as follows (Bishop, 2006):

$$D_{KL}\left(P\middle\|Q\right) = \int_{-\infty}^{\infty} p(x)\log\left(\frac{p(x)}{q(x)}\right) \quad (2)$$

where q is the probability density function (PDF) of the reference distribution and p is the PDF of the second distribution. Figure 1 illustrates how the KL divergence is determined and how it increases as the difference between two probability density curves increases.

Soil structure is manifested through its direct impact on the soil pore space characteristics by enhancing ϕ and changing the median pore radius (e.g., Bodner et al., 2013; Kreiselmeier et al., 2019) as well as the heterogeneity (i.e., variance) of the VSD (e.g., Crawford et al., 1995; Hwang & Choi, 2006). The latter has been suggested to be the result of processes such as aggregation of primary particles and the influence of soil biota, roots and microcracking (Hwang & Choi, 2006). Broader VSDs show larger standard deviations and, thus, lead to a larger entropy (Yoon & Giménez, 2012). This motivates the use of the KL divergence as a measure to quantify changes in VSD in response to the formation and degradation of soil structure. For this, a suitable reference distribution is required.

The most suitable reference to quantify changes in VSD due to soil structure is a hypothetical soil devoid of any structural features, which we adopt and define here as the "reference soil". The porosity and VSD of a soil without structure are a function of the size distribution, shape and packing of its particles (e.g., Arya & Heitman, 2015; Arya & Paris, 1981; Crisp & Williams, 1971; Fiès & Bruand, 1998; Fiès & Stengel, 1981; Haverkamp & Parlange, 1986; Nimmo et al., 2007). Strictly speaking, this implies that the reference soil is unique for any natural soil given a specific PSD. This definition makes the reference soil conceptually equivalent to the textural component of a natural soil (Childs, 1969; Meurer, Barron, et al., 2020).

The KL divergence can be applied as an index of soil structure by following the individual steps 1–4 described below. We focus on the lognormal distribution to describe the PSD and VSD of soil (e.g., Brutsaert, 1966; Hwang & Choi, 2006; Kosugi, 1996), since it is uniquely defined by parameters with a clear physical meaning. These are the median (or geometric mean) particle or pore radius and the standard deviation (σ), which characterizes the broadness of a PSD or VSD (Kosugi, 1996).

2.1.1 | Step 1: Modelling the PSD of the reference soil

The Kosugi (1996) model is adopted to model the PSD in the following way (Hwang & Powers, 2003):

$$g(r_P) = \frac{1}{r_P \sigma_P \sqrt{2\pi}} \exp\left\{-\frac{(\ln r_P - \ln r_{m,P})}{2\sigma_P^2}\right\} \quad (3)$$

where r_P is the particle radius [cm], $r_{m,P}$ is the median particle radius [cm] and σ_P is the standard deviation of the PSD.
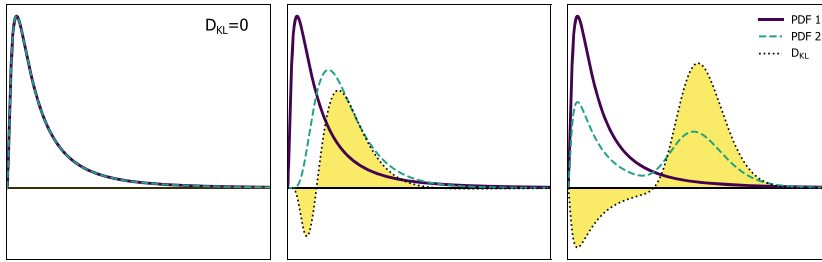
FIGURE 1 Illustration of how the KL divergence (D_{KL}) is determined. Each subplot shows two probability density curves that differ from one another increasingly from left to right. The purple solid curve represents the reference distribution to which the green dashed curve is compared. The black dotted curve is obtained by solving the expression in Equation (1) for each point along the horizontal axis. Integrating the yellow area above/below the dotted curve yields the KL divergence, which equals zero ($D_{KL} = 0$) when the two curves are identical (left subplot)

2.1.2 | Step 2: Modelling the VSD of the structured soil

The VSD of the structured soil is estimated from soil water retention measurements, that is, θ-ψ_m measurement pairs. First, ψ_m is mapped to an equivalent pore radius (r) through the Young–Laplace relationship:

$$r = -\frac{2\gamma\cos\delta}{\rho_w g \psi_m} \qquad (4)$$

where ψ_m and r are in [cm], γ is the surface tension at the air-water interface [g s^{-2}], δ is the contact angle between the water and solid phase [°], ρ_w is the density of water [g cm^{-3}], and g is the acceleration due to gravity [cm s^{-2}]. In this study, we assume full contact between water and solid phase and the physical properties of water at 20°C (Brutsaert, 1966). This simplifies Equation (4) to $r = -0.149 \div \psi_m$.

Many mathematical expressions have been proposed to model the relationship between ψ_m/r and θ (Assouline & Or, 2013; Sillers et al., 2001), some of which are derived from the lognormal distribution (Brutsaert, 1966; Kosugi, 1994, 1996). We adopt the model by Kosugi (1996), which, for the unimodal case, is given as follows:

$$f_S(r) = \frac{(\theta_s - \theta_r)}{r\sigma_S\sqrt{2\pi}}\exp\left\{-\frac{(\ln r - \ln r_{m,S})}{2\sigma_S^2}\right\} \qquad (5)$$

where θ_s and θ_r are the saturated and residual water contents [m^3 m^{-3}], respectively, σ_S is the standard deviation of the lognormal VSD [−] and $r_{m,S}$ is the median pore-radius [cm]. The subscript "S" indicates that the parameters refer to the VSD of the structured soil.

Water retention measurements suggesting a bimodal or multimodal VSD can be modelled by superimposing two or more unimodal distributions (Dexter et al., 2008; Durner, 1994; Pollacco et al., 2017; e.g., Ross & Smettem, 1993). Generally, this procedure leads to an improved description of the SWRC in structured soils (Reynolds, 2017). Using the Kosugi (1996) model, this gives:

$$f_S(r) = \sum_{i=1}^{n}\frac{(\theta_{s,i} - \theta_{r,i})}{r\sigma_{S,i}\sqrt{2\pi}}\exp\left\{-\frac{(\ln r - \ln r_{m,S,i})}{2\sigma_{S,i}^2}\right\} \qquad (6)$$

where n indicates the number of superimposed pore classes/domains (i.e., lognormal distributions) and the subscript i defines the affinity of a parameter to the respective lognormal distribution. Note that for $i \geq 2$, θ_r no longer represents the residual water content, but the saturated water content of the $i − 1$th pore class/domain (Pollacco et al., 2017).

2.1.3 | Step 3: Modelling the VSD of the reference soil

The PSD is translated into the VSD of the reference soil without structure using the model by Arya and Paris (1981). This model has been noted to perform particularly well for soils with little structural development (Nimmo et al., 2007). It assumes that the VSD and PSD are linearly related, which implies shape similarity between both distributions. The few attempts that have been undertaken to experimentally investigate the textural pore space showed that particles of different sizes result in pores of specific sizes and characteristics (Fiès et al., 1981; Fiès & Bruand, 1990, 1998; Fiès & Stengel, 1981). This suggests

that the VSD of the textural pore space closely follows the PSD. In particular, we assume that the PSD defines the main properties of the textural VSD such as σ and the median pore radius. Moreover, the assumption of shape similarity should be valid for a soil without structure as has been shown for poly-disperse sphere packs with dense random packing (Assouline & Rouault, 1997).

Arya and Paris (1981) assume that a natural soil can be represented by several uniform sphere packs, which are packed in "discrete domains" and subsequently assembled to give the same bulk density (ρ_b) as the natural soil. First, the PSD curve is subdivided into a number of size fractions (usually 20 or more) and the relative abundance of each fraction is multiplied with the sample weight yielding weight fractions. Given the soil particle density (ρ_s) and ρ_b, these weight fractions provide information on the number of uniform spheres in each domain, which are then assembled into a hypothetical closed-packed cube with the void ratio of the bulk soil (e). Finally, r is calculated for the ith size fraction with the following relationship:

$$r_i = 0.816 r_{P,i} \sqrt{en_i^{(1-\alpha_i)}} \tag{7}$$

where $r_{P,i}$ is the mean particle radius of the ith size fraction [cm] and α_i is a scaling parameter that links the ideal sphere pack to the natural soil (Arya et al., 1999). In a later study, Arya et al. (1999) present and discuss different ways to determine this parameter. Note that α_i becomes 1 when the ideal sphere pack and the natural soil are equivalent.

To determine the VSD of the reference soil using Equation (7), e is calculated by

$$e = \frac{\phi_{tex}}{1 - \phi_{tex}} \tag{8}$$

where ϕ_{tex} denotes the porosity of the textural pore space. As noted before, detailed empirical studies on the textural pore space remain scarce. This might be due to challenges related to this task such as controlling the packing of soil particles, which exacerbates comparability between individual experiments. Furthermore, theoretical studies based on multicomponent sphere packs (e.g., Farr & Groot, 2009; Gupta & Larson, 1979; Shen et al., 2019) are not especially applicable to estimate ϕ_{tex} of real soils because soil particles in these models are represented as spheres that are packed in the densest way possible. This can yield unrealistically small values of porosity. In fact, ϕ in these models can approach zero when the PSD becomes increasingly right-skewed, that is, when a large number of small spheres can be fitted

into the gaps between larger ones (Farr & Groot, 2009; Gupta & Larson, 1979). Here we assume a random closed packing of soil particles in the reference soil and follow Nimmo (2013), who suggested that a value of 0.30 should be an appropriate estimate for ϕ_{tex}. We acknowledge that this value may not be a reasonable estimate for all soils. However, as we demonstrate below, the KL divergence is relatively insensitive to ϕ_{tex}, so that its precise estimation is not of critical importance.

The shape similarity between PSD and VSD allows $r_{P,i}$ in Equation (7) to be replaced with $r_{m,P}$ to obtain the median pore radius of the reference soil ($r_{m,R}$). This we do setting α to 1, which gives:

$$r_{m,R} = 0.816 r_{m,P} \sqrt{e} \tag{9}$$

Furthermore, the assumption that the VSD of a soil without structure closely follows its PSD justifies that:

$$\sigma_R = \sigma_P \tag{10}$$

where σ_R is the standard deviation of the VSD of the reference soil. Finally, it is reasonable to assume that θ_r is the same for both structured and reference soil and that θ_s can be approximated by ϕ_{tex} so that the VSD of the reference soil can be described by the following:

$$f_R(r) = \frac{(\phi_{tex} - \theta_r)}{r \sigma_R \sqrt{2\pi}} \exp\left\{ -\frac{(\ln r - \ln r_{m,R})}{2\sigma_R^2} \right\} \tag{11}$$

2.1.4 | Step 4: Calculating the KL-divergence between reference and structured soil

Substituting the VSDs for the structured (Equation (5)) and reference soils (Equation (11)) into Equation (2), where $q(x)$ represents the VSD of the reference soil (f_R) and $p(x)$ the VSD of the structured soil (f_S), gives the analytical expression for the KL divergence as (see Appendix A for derivation):

$$D_{KL}\left(f_S \middle\| f_R\right) = (\theta_s - \theta_r)\left(\log \frac{(\theta_s - \theta_r)\sigma_R}{(\phi_{tex} - \theta_r)\sigma_s} - \frac{1}{2} \right. \tag{12}$$

$$\left. + \left[\frac{\sigma_s^2 + (\log r_{m,S} - \log r_{m,R})^2}{2\sigma_R^2} \right] \right)$$

It is clear from Equation (12) that the KL divergence increases as θ_s, σ_S and the difference between $r_{m,S}$ and $r_{m,R}$ increase, whereas it decreases as ϕ_{tex} and σ_R
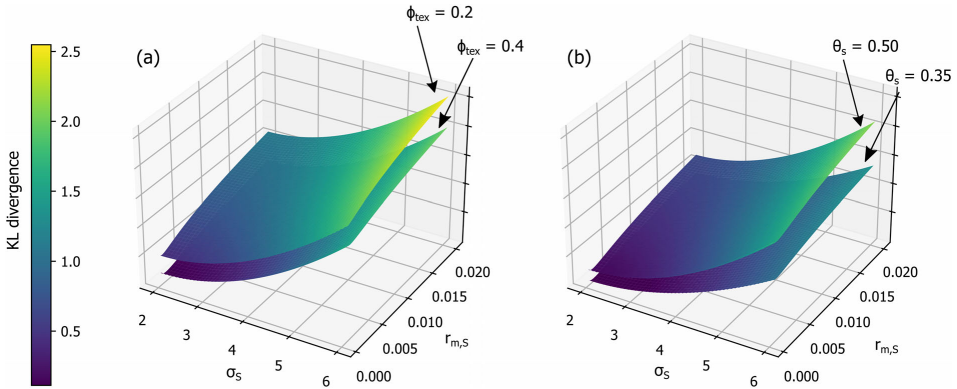
FIGURE 2 3D plots illustrating the sensitivity of parameters for calculating the KL divergence related to the structured soil (i.e., with subscript "S" in Equation (12)) with varying textural porosity (ϕ_{tex}, (a)) and saturated water content (θ_s, (b)). The parameters related to the reference soil were fixed at values that fall into the range of natural soils (see Tables S1 and S2), where the median pore radius ($r_{m,R}$) and the standard deviation (σ_R) were set to 0.002 cm and 2, respectively. The residual water content was set to zero. In subplot (a) θ_s was fixed at 0.50 m^3 m^{-3} and in subplot (b) ϕ_{tex} was fixed at 0.35 m^3 m^{-3}

increase. However, the KL divergence is not equally sensitive to each of these parameters. The standard deviations σ_S and σ_R appear as squared terms, which means that they should have a stronger impact on the KL divergence than the other parameters. The 3D plots shown in Figure 2 illustrate the sensitivity of the parameters in Equation (12) that are related to the structured soil, whilst the parameters of the reference (non-structured) soil remain fixed. This is shown for different values of ϕ_{tex} (Figure 2a) and θ_s (Figure 2b). It can be seen that $r_{m,S}$ and ϕ_{tex} show relatively minor effects on the KL divergence, while θ_s becomes more relevant with increasing KL divergence by acting as a scalar (Equation (12)). The largest effect on the KL divergence, however, is exerted by σ_S.

An analytical expression for the KL divergence cannot be obtained when the soil water retention curve is best described by a bimodal VSD, which is often the case for structured soils (Dexter et al., 2008; Jensen et al., 2019; Reynolds, 2017). This proved to be the case for nearly all of the samples in the applications of the method to the two field experiments described below. We therefore determined the KL divergence numerically by inserting Equation (6) (instead of Equation (5)) for $p(x)$ in Equation (2) and applying discrete integration similar to Riemann's integral (e.g., Axler, 2020). For this, a pore-size range with lower and upper limits at 0 and 10 cm was defined and subdivided into four sub-intervals (0–10^{-5} cm, 10^{-5}–10^{-3} cm, 10^{-3}–0.1 cm, 0.1–10 cm). Each sub-interval was partitioned into 5×10^8 rectangles of equal width and the height of each rectangle was

determined by solving the expression in Equation (1) at the mid-point of each rectangle. The number of rectangles was considered a good compromise between computation time and accuracy. Finally, the area of each rectangle was calculated and all areas were summed to obtain the KL divergence. The procedure can be summarized with the following equation:

$$
\begin{aligned}
D_{KL}\left(P\middle\|Q\right) = \sum_{j=1}^{4} \sum_{i=1}^{5\times10^8} &\left(x_{j,i+1} - x_{j,i}\right) \\
&\left[P\left(\frac{x_{j,i} + x_{j,i+1}}{2}\right) \log\left(\frac{P\left(\frac{x_{j,i}+x_{j,i+1}}{2}\right)}{Q\left(\frac{x_{j,i}+x_{j,i+1}}{2}\right)}\right)\right]
\end{aligned}
\tag{13}
$$

where j refers to the subinterval and i ($i + 1$) to the left (right) position of the border of each rectangle. The other variables are the same as in Equation (1). The procedure was successfully validated for a unimodal case by comparing results obtained with the analytical solution (Equation (12)) with those obtained by the discrete integration method.

2.2 | Site descriptions and measurements

In the following, we demonstrate the use of the KL divergence as an index of soil structure for two case studies from Swedish field experiments. The first dataset is from a field experiment initiated in 1956 to monitor the long-term

effects of mineral nitrogen fertilizers and organic matter amendments on soil organic matter contents, crop yields and physical soil properties (Kirchmann et al., 1994). The experimental site is located near the Swedish University of Agricultural Sciences at Ultuna, close to Uppsala (59.92°N, 17.65°E). The topsoil has a clay loam texture and the soil was classified as a *Eutric Cambisol* (FAO, 1989). The soil PSD at Ultuna was measured for seven classes using sedimentation and wet sieving (Kirchmann et al., 1994). Note that the soil texture was assumed to be the same for all treatments due to the small size (4 m^2) and close proximity of the plots. All plots in this experiment are managed by hand with digging in autumn and spring and have been planted with fodder maize since the year 2000. Further details about the experiment and site conditions are described in Kirchmann et al. (1994). Details on sampling for soil water retention are given in Svensson (2020) and shortly summarized here. Undisturbed soil cores (65.5 mm inner diameter and 74.8 mm height) were collected during early autumn in 2019 before harvest from plots with three different treatments: a bare fallow treatment with no additions (hereafter "fallow" treatment) and two cropped treatments. One of these is fertilized with calcium nitrate (Ca[NO$_3$]$_2$) at a rate of 80 kg N ha^{-1} (hereafter "Ca[NO$_3$]$_2$" treatment), while the other receives biennial additions of solid cow manure at a rate of 9.5 t ha^{-1} (hereafter "manure" treatment). Two replicate cores per treatment were sampled from four blocks (eight replicates per treatment in total) in between rows of maize just below the soil surface. Of these, one replicate core from the fallow treatment had to be discarded. Water retention was measured for each core on a suction plate at ψ_m of −10, −30, −100, −300 and −600 hPa. Furthermore, dry ρ_b and ρ_s were determined for each replicate and ϕ was calculated. Particle density was calculated from the volume displacement of a sample of fine earth (<2 mm) with ethanol. Tables 1 and 2 show selected soil properties for the three treatments at Ultuna.

The second dataset was taken from Messing et al. (1997), who measured soil hydraulic properties at several sites in southern Sweden on adjacent fields with similar site conditions but under different land uses. One field represented agricultural land that had been afforested with aspen (*Populus deltoides*) or silver birch (*Betula pendula*) 30 years before the study was conducted (hereafter termed the "FOR" treatment), while the other field represented current agricultural land use dominated by grass/clover leys in rotation with cereals (hereafter termed the "AGR" treatment). For this application, three of the five sites studied by Messing et al. (1997) were selected (Almnäs, Siggebohyttan, Vik) due to their relatively coarse-textured soils (Table 1), as fine-textured soils are covered by the Ultuna case study. Undisturbed soil

samples were collected with cylindrical soil cores (inner diameter 72 mm, height 50 mm) from 0–35 cm depth at four (Almnäs and Siggebohyttan) and from 0–30 cm depth at six (Vik) depth intervals. Three to four replicates per depth interval were sampled at each site and for each treatment. Water retention was measured at six values of ψ_m, namely −5, −30, −50, −100, −300 and −600 hPa using porous sand blocks for −5 hPa and ceramic plates for the other pressure heads. The PSD in seven classes was measured on disturbed soil samples taken at 10 to 15 cm depth with wet sieving and sedimentation using the pipette method. We assume that the soil texture at this depth is representative of the full depth ranges due to past (FOR treatment) and ongoing (AGR treatment) tillage. Bulk density and ρ_s, which were used to calculate ϕ, were determined from the undisturbed and disturbed samples, respectively. Selected properties of the soils from the three sites are summarised in Tables 1 and 2.

2.3 | Fitting distributions and statistical analysis

All fitting was done with the least-squares method (Levenberg–Marquardt algorithm) available in the Python module *SciPy* (Virtanen et al., 2020). The parameters $r_{m,P}$ and σ_P in Equation (3) were obtained by integration and subsequent fitting to the cumulative PSD. Note that only unimodal PSDs can be modelled with Equation (3) although multimodal PSDs do exist (Fredlund et al., 2000). This issue is addressed in the discussion below.

The modelling of the VSD on the water retention measurements of the structured soils was mostly done assuming a bimodal VSD (Equation (6) with $i = 2$). This improved the goodness-of-fit as compared with using Equation (5) assuming a unimodal VSD. The bimodality of the pore system from the Ultuna data clearly resulted from a well-developed macropore system in this fine-textured soil. In contrast, many of the samples from the dataset collected by Messing et al. (1997) show bimodality in the size range of matrix pores. In addition, some of the samples in this dataset suggest a third pore domain reflecting the presence of macropores. Clearly, a bimodal model cannot be made to fit satisfactorily to data that indicates three pore regions. Preliminary testing showed that the estimated KL divergence is very sensitive to the quality of the fit to the water retention measurements across a wide range of soil water tensions. This third (macropore) region was therefore effectively neglected in the fitting of the bimodal model to the data for the coarse-textured soils at Almnäs, Siggebohyttan and Vik, by excluding the measured ϕ in the fitting. The measured ϕ was only included in the curve fitting for the samples at Ultuna, with its value fixed at a pore radius of 3 mm ($\psi_m \approx$

Site	Treatment	Sand[a] [g g^{-1}]	Silt[b] [g g^{-1}]	Clay[c] [g g^{-1}]
Ultuna[d]	-	0.22	0.41	0.37
Almnäs[e]	AGR	0.69	0.20	0.11
	FOR	0.66	0.23	0.11
Siggebohyttan[e]	AGR	0.44	0.48	0.08
	FOR	0.61	0.31	0.08
Vik[e]	AGR	0.53	0.38	0.09
	FOR	0.59	0.33	0.08

TABLE 1 Soil properties of sites selected to demonstrate the KL divergence

Abbreviations: AGR, agricultural land; FOR, afforested land.
[a]2–0.06 mm particle diameter.
[b]0.06–0.002 mm particle diameter.
[c]<0.002 mm particle diameter.
[d]Data from Kirchmann et al. (1994) (assumed to be representative for all treatments at Ultuna).
[e]Data from Messing et al. (1997) (assumed to be representative for the entire investigated depth range).

−0.5 hPa), which is equivalent to assuming that there were no pores larger than this.

Adopting the Kosugi (1996) model to describe a bimodal VSD requires the optimization of seven parameters (see Equation (6)). Determining seven fitting parameters by inverse modelling against datasets comprising six data points clearly raises the issue of non-uniqueness, that is, the likelihood that different parameter sets will fit the measurements equally well as judged by some goodness-of-fit measure (Beven, 1993; Fernández-Gálvez et al., 2021). We therefore investigated ways to constrain the fitting to ensure unique solutions. First, we set θ_r to zero, which reduced the number of parameters to six. This is also justifiable in principle because θ was not measured at ψ_m-values less than −600 hPa and, consequently, the residual water content would anyway not be identifiable. We then tested constraining θ_s (the sum of $\theta_{s,1}$ and $\theta_{s,2}$) to equal the measured ϕ to further reduce the number of fitting parameters. However, this notably reduced the quality of the model fit to the data across a wide range of ψ_m-values, especially in cases where a third macropore domain was present. Thus, both $\theta_{s,1}$ and $\theta_{s,2}$ were included as fitting parameters. Besides this, we tested the hypothesis that the small pore region only comprises textural pores by setting $\sigma_{S,1}$ equal to σ_R ($= \sigma_P$) and $r_{m,S,1}$ equal to a fraction of $r_{m,P}$, which reduced the number of fitting parameters to four. However, this procedure also reduced the quality of the model fit to the water retention data, demonstrating that the small pore region also comprises structural pores. Hence, both $\sigma_{S,1}$ and $r_{m,S,1}$ were retained as fitting parameters. The final model for describing the VSD of the structured soil, therefore, requires six parameters to be optimized as follows:

$$f_S(r) = \frac{\theta_{s,1}}{r\sigma_{S,1}\sqrt{2\pi}} \exp\left\{ -\frac{(\ln r - \ln r_{m,S,1})}{2\sigma_{S,1}^2} \right\} + \frac{\theta_{s,2}}{r\sigma_{S,2}\sqrt{2\pi}} \exp\left\{ -\frac{(\ln r - \ln r_{m,S,2})}{2\sigma_{S,2}^2} \right\} \quad (14)$$

We adopted a procedure for fitting Equation (14) to our data which acknowledges the likelihood of non-unique solutions (Fernández-Gálvez et al., 2021; Pollacco et al., 2017) and therefore uncertainty in the derived KL divergences. Firstly, we found that choosing appropriate initial parameter value guesses for the fitting algorithm was crucial to improve convergence towards physically realistic parameter values. Hence, we derived the set of initial parameter value guesses following physically-based considerations: $\theta_{s,1}$ was assumed to be close to but larger than ϕ_{tex}, so that its initial estimate was set to 0.35 m^3 m^{-3}. Initial testing revealed a physically plausible correlation between σ_P and $\sigma_{S,1}$ (the standard deviation of the smaller pore domain), such that $2\sigma_P$ was found to be a good initial guess for $\sigma_{S,1}$. Similarly, a correlation was detected between $r_{m,S,1}$ (the median pore radius of the smaller pore domain) and $r_{m,P}$, such that $0.04 r_{m,P}$ was considered an appropriate initial guess for $r_{m,S,1}$. Finally, an initial guess for $\theta_{s,2}$ was derived from the difference between the measured porosity ϕ and the initial guess for $\theta_{s,1}$ ($= 0.35$ m^3 m^{-3}). Selecting appropriate initial parameter guesses for $\sigma_{S,2}$ and $r_{m,S,2}$ was more difficult since the larger pore domain could either reflect macropore (Ultuna) or matrix pore regions (Almnäs, Siggebohyttan, Vik). To address this issue, we produced 100 initial parameter sets for each VSD to be fitted, where $\sigma_{S,2}$ ranged from 0.2 to 2 and $r_{m,S,2}$ from 0.001 to 0.008 cm, which were considered to be physically realistic ranges for these parameters (Fernández-Gálvez et al., 2021).

TABLE 2 Soil organic carbon concentrations (SOC) and total porosities (ϕ) for all sites and treatments

		Treatment									
		AGR		FOR		Fallow		Ca(NO$_3$)$_2$		Manure	
Site	Depth [cm]	SOC [%]	ϕ [cm^3 cm^{-3}]	SOC [%]	ϕ [cm^3 cm^{-3}]	SOC[a] [%]	ϕ [cm^3 cm^{-3}]	SOC[a] [%]	ϕ [cm^3 cm^{-3}]	SOC[a] [%]	ϕ [cm^3 cm^{-3}]
Ultuna	0–5	-	-	-	-	0.9	0.47	1.2	0.53	2.1	0.58
Almnäs	0–5	4.5	0.49	3.8	0.62	-	-	-	-	-	-
	5–15	4.3	0.47	2.2	0.53	-	-	-	-	-	-
	15–25	4.0	0.49	1.5	0.50	-	-	-	-	-	-
	25–35	2.1	0.49	0.4	0.47	-	-	-	-	-	-
Siggebohyttan	0–5	2.5	0.49	5.3	0.59	-	-	-	-	-	-
	5–15	1.9	0.46	3.0	0.52	-	-	-	-	-	-
	15–25	1.8	0.47	2.2	0.51	-	-	-	-	-	-
	25–35	0.5	0.44	0.6	0.43	-	-	-	-	-	-
Vik	0–5	3.1	0.52	5.3	0.63	-	-	-	-	-	-
	5–10	2.9	0.54	3.6	0.58	-	-	-	-	-	-
	10–15	2.9	0.51	2.8	0.56	-	-	-	-	-	-
	15–20	2.9	0.49	2.8	0.52	-	-	-	-	-	-
	20–25	2.5	0.51	2.2	0.54	-	-	-	-	-	-
	25–30	2.0	0.50	1.8	0.54	-	-	-	-	-	-

Note: The values represent averages over replicates.

Abbreviations: AGR, agricultural land; FOR, afforested land.

[a]Values extracted from Figure 6 in Svensson (2020).

Finally, similar to fitting the cumulative PSD, Equation (14) was integrated and optimized against the water retention data for these 100 combinations of initial parameter guesses. Any physically implausible optimized parameter sets were then discarded. This was considered to be the case if (i) any of the six final parameter values were negative, (ii) $\sigma_{S,1}$ was smaller than σ_R ($= \sigma_P$), or (iii) the sum of $\theta_{s,1}$ and $\theta_{s,2}$ was more than 10% larger than the measured ϕ. The root mean squared error (RMSE) was used to evaluate the goodness-of-fit of these physically plausible parameter sets, in order to define a number of "acceptable" parameter sets with which to calculate the KL divergence. This was achieved by retaining all parameter sets with RMSE values less than 10% larger than the best-fit parameter set (i.e., smallest RMSE). The KL divergences of these acceptable parameter sets were then calculated numerically (Equation (13)) and the median KL divergence was used as an index of soil structure for each sample/replicate for subsequent statistical analyses.

The unimodal model (Equation (5)) proved sufficient for modelling the VSD of only a small number of samples from the soils at Vik. In these cases, the initial parameter guesses for σ_S and $r_{m,S}$ were derived in the same way as for $\sigma_{S,1}$ and $r_{m,S,1}$ in the bimodal case. The initial guess for θ_s was set equal to the measured ϕ. The same physical constraints as for the bimodal model were applied in the optimization of the unimodal model, that is, σ_S was only allowed to be larger than σ_R ($=\sigma_P$) and θ_s was not allowed to be 10% larger than the measured ϕ. For the curve fitting, Equation (5) was integrated and the three parameters were optimized against the water retention data. The analytical solution of Equation (12) was used to calculate the KL divergences.

The KL divergences determined for the three treatments at Ultuna and the two land uses at the three sites in Messing et al. (1997) were tested for significant differences using R (R Core Team, 2019). Each group of replicates was tested for normality using the Shapiro–Wilk test. The Tukey method available from the *emmeans* package (Lenth, 2020) was used for pairwise comparison between treatments for the Ultuna data and, within each location, between treatments and depth intervals for data from Almnäs and Siggebohyttan. The KL divergences of one replicate from Vik did not pass the normality test. Hence, pairwise comparison between treatments and depth intervals for this site were done with Dunn's method using the *PMCMR* package (Pohlert, 2014) with automatic Holm p-value correction. Differences were considered significant if $p < 0.05$. Correlations were investigated with the Pearson correlation coefficient (Pearson's r).
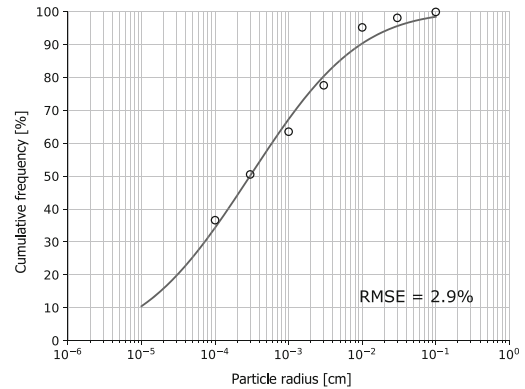

FIGURE 3 Cumulative particle-size distribution for the soil at Ultuna (circles indicate measured data and the line was fitted using Equation (3)). The root-mean-square error (RMSE) is indicated on the plot

3 | RESULTS

The PSD of the fine-textured soil at Ultuna was modelled well with Equation (3) (Figure 3; RMSE = 2.9%). Furthermore, the double lognormal model of Equation (14) gave excellent fits to the water retention data for all treatments at Ultuna (Figures 4, S1 and S2) with a largest RMSE of $0.0076 \, \text{m}^3 \, \text{m}^{-3}$. Figure 4 shows fits and KL divergences for the example of the $\text{Ca(NO}_3)_2$ treatment at Ultuna. Most of the time, the best fits according to RMSE (indicated by the red triangles) are close to the median KL divergences (indicated by the orange horizontal lines), which were used for statistical analysis. Some variation is evident in the larger pore region, which also affects the KL divergence as indicated by the boxplots. The number of acceptable fits for the replicates ranged between one and 29. Figure 5 shows that the means of the KL divergences increase in the order fallow $< \text{Ca(NO}_3)_2 <$ manure treatment. Although the mean values are larger for the manure treatment compared to the fallow and $\text{Ca(NO}_3)_2$ treatment, these differences were not significant ($p = 0.076$ for fallow vs. manure, and $p = 0.091$ for $\text{Ca(NO}_3)_2$ vs. manure). The difference in KL divergence between the $\text{Ca(NO}_3)_2$ and fallow treatment was also not significant ($p = 0.99$). The pattern shown in Figure 5 is supported by the values of the fitted parameters, which indicate no large differences in VSD between the $\text{Ca(NO}_3)_2$ and fallow treatments, except that the modelled total pore space ($\theta_{s,1} + \theta_{s,2}$) is on average larger in the former compared to the latter (Table S1).
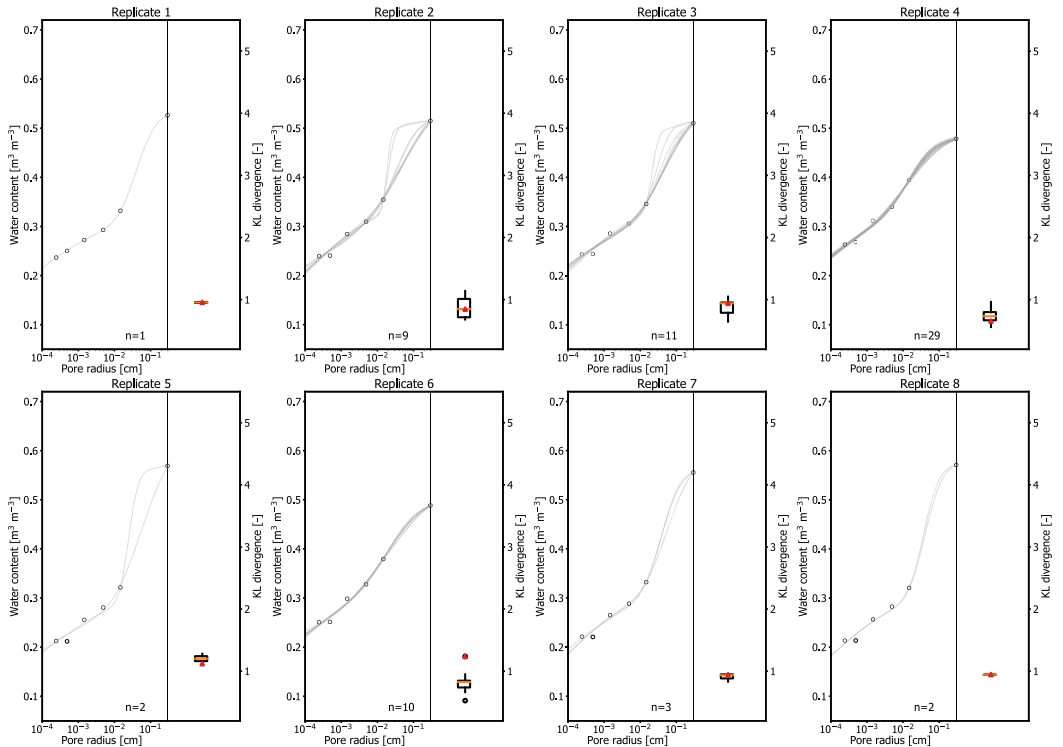
FIGURE 4 Acceptable model fits of cumulative pore-size distributions for each sample replicate (left side of each subplot) with corresponding KL divergences shown as boxplots (right side of each subplot) for the ca(NO$_3$)$_2$ treatment at Ultuna. On the left side of each subplot, open circles indicate measured values, where the right-most value represents the total measured porosity, which was fixed at a pore radius of 3 mm. The grey lines indicate acceptable model fits and n the number of acceptable model fits for the individual sample. Bars in boxplots on the right side of each subplot indicate 1.5 times the interquartile range and open circles indicate values outside this range. The orange horizontal line shows the median KL divergence. This value was used for statistical analysis. The red triangles show the KL divergence of the best fit according to the root mean square error

The fits of Equation (3) to the measured PSDs of the coarse-textured soils at Almnäs, Siggebohyttan and Vik showed larger RMSE's (2.9%–7.3%; Figures S3–S5) as compared to the fine-textured soil at Ultuna. This is because the relative abundance of the fine silt and clay fractions was underestimated, especially at Almnäs and Siggebohyttan (Figures S3–S5). The double lognormal model of Equation (14) and the single lognormal model of Equation (4) yielded excellent fits to the water retention data of these soils with RMSE's below 0.012 m^3 m^{-3} across all sites, treatments and depths (Figures 6, S6–S10). The example of the FOR treatment at Siggebohyttan is shown in Figure 6. Similar to the Ultuna site, the best fits according to the RMSE are close to the median KL divergences (Figures 6, S6–S10). The fitting parameters obtained for each site and treatment are given

in Table S2. Figure 7 shows the KL divergence for the AGR and FOR treatments at Almnäs, Siggebohyttan and Vik for each depth interval. At all three sites, the KL divergence of the FOR treatments decreases significantly with soil depth. At Vik, the KL divergence showed a slight increase for the AGR treatment in the deepest soil layer (Figure 7c), while at Almnäs and Siggebohyttan the KL divergence increased in the soil layer at 15–25 cm depth followed by a decrease in the deepest soil layer (Figure 7a,b). However, there were no significant differences in soil depth in the AGR treatment. Furthermore, the FOR treatments showed larger KL divergences in the upper soil layers and smaller KL divergences in the deeper soil layers compared to the AGR treatments at all three sites (Figure 7). These differences were significant for the uppermost soil layer at Almnäs.
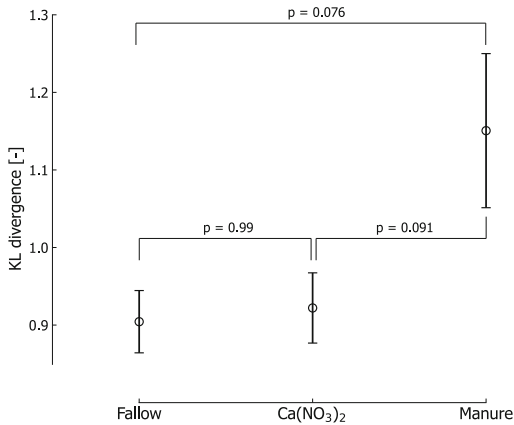
FIGURE 5 KL divergences for the different treatments at Ultuna. Error bars indicate standard errors

It is evident from the optimized model parameters that, at all four sites, larger KL divergences are associated with wider pore-size distributions (i.e., larger $\sigma_{S,1}$ and/or $\sigma_{S,2}$) and/or a larger modelled total pore space (i.e., large $\theta_{s,1} + \theta_{s,2}$) (Tables S1 and S2). A significant relationship was detected between the optimized standard deviations of the PSD (σ_P) and the small pore region ($\sigma_{S,1}$) (Pearson's $r = 0.783$, $p < 0.001$; Figure 8a). Furthermore, although the trend is less strong, the median pore radius of the small pore region ($r_{m,S,1}$) is also significantly correlated with the median particle radius across all sites and treatments ($r_{m,P}$) (Pearson's $r = 0.250$, $p = 0.004$; Figure 8b).

4 | DISCUSSION

Soil PSDs are sometimes more complex than can be described with simple unimodal distributions due to complicated breakdown processes or because soil particles originate from different parent materials (Gardner, 1956). The soils at Almnäs and Siggebohyttan are rather poorly graded, being dominated by the sand fraction, but with a small "hump" in the clay fraction. The lognormal distribution of Equation (3) is not suited to describing bimodal or gap-graded PSDs, and therefore does not match this data very well (Figures S3–S5). As a result, the modelled PSD appears to be narrower than is indicated by the measured values at these sites. This suggests that the KL divergence would have been smaller if the PSD had been modelled more accurately. Nevertheless, the relative difference in KL divergence between the FOR and AGR treatments would not have been affected in this case. More flexible

PSD models have been proposed such as the ones by Fredlund et al. (2000) or Assouline et al. (1998), which have been shown to perform better than the lognormal distribution for a broad range of soil textures (Hwang, 2004). These models could be used to determine the VSD of the reference soil given that a linear relationship with the PSD is assumed. The lognormal distribution was chosen here mainly because it allows an explicit analytical solution (Equation (12)) and because its parameters have inherent physical meaning.

One debatable aspect of the method presented here is the linearity that we assumed between the PSD and VSD for the reference soil. It is clear that such an assumption would most likely not be valid for structured soils (Crisp & Williams, 1971; Haverkamp & Parlange, 1986; Hwang & Choi, 2006; Hwang & Powers, 2003). It does not even hold for simulations of tetrahedral (i.e., closest possible) packing of multicomponent sphere packs (Assouline et al., 1998; Assouline & Rouault, 1997). Nevertheless, previous studies of textural porosity do suggest a strong link between the PSD and the VSD (Fiès & Bruand, 1990, 1998). Whether this link is strictly linear remains to be investigated. We chose the model by Arya and Paris (1981) for the linear transformation from PSD to VSD of the reference soil, setting the scaling parameter α to 1, which implies no difference between an ideal sphere pack and the reference soil (Arya et al., 1999). The nature of the scaling parameter α has been strongly debated in the literature and its value seems to vary from soil to soil (Arya et al., 1999, 2008; Basile & D'Urso, 1997; Vaz et al., 2005). It is not clear, however, whether this variation is the result of soil structure, soil texture or both because the Arya and Paris (1981) model has mostly been tested on structured soils. Nevertheless, α commonly shows values close to 1 for a variety of soil textures (Vaz et al., 2005), which is why we adopted it here. Several other models for translating particle radii into pore radii have been proposed (Arya & Heitman, 2015; Chan & Govindaraju, 2004; e.g., Haverkamp & Parlange, 1986; Mohammadi & Vanclooster, 2011; Pollacco et al., 2020), which would lead to different results, since the KL divergence automatically depends on the model selected for this purpose. We tested the more recent model by Arya and Heitman (2015) on the same dataset and obtained smaller equivalent pore radii for the reference soil than for the Arya and Paris (1981) model. This increased the KL divergences but had only negligible effects on the relative differences between treatments and sites.

All treatments at Ultuna including the bare fallow treatment showed a bimodal VSD, which is probably the result of the high clay content at this site (37%). Nevertheless, differences in measured ϕ are clearly visible between the treatments with the manure treatment
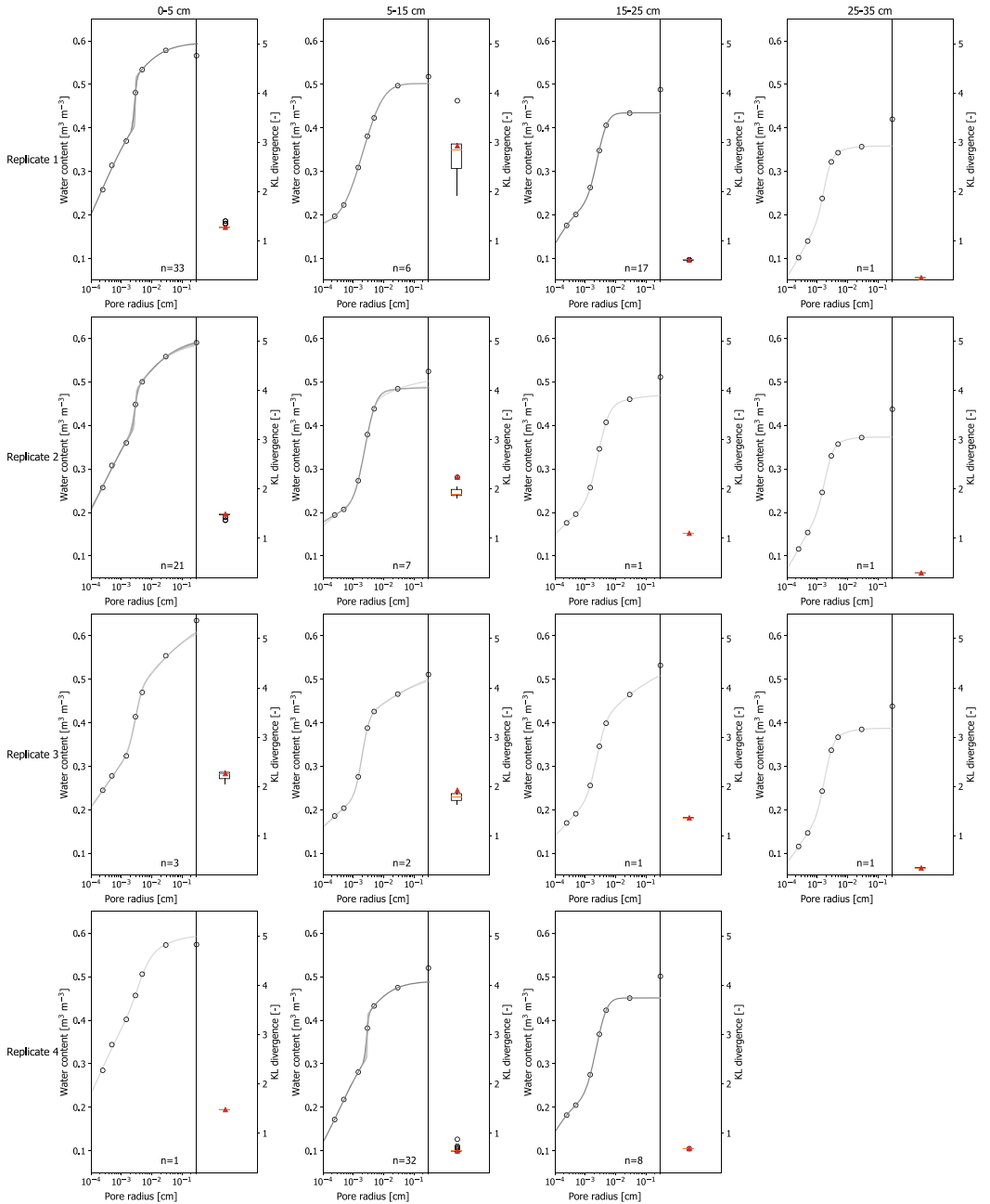
FIGURE 6 Acceptable model fits for each sample (left side of each subplot) with corresponding KL divergences shown as boxplots (right side of each subplot) for the afforested land at Siggebohyttan. For explanation of the individual figure features, see the caption for Figure 4
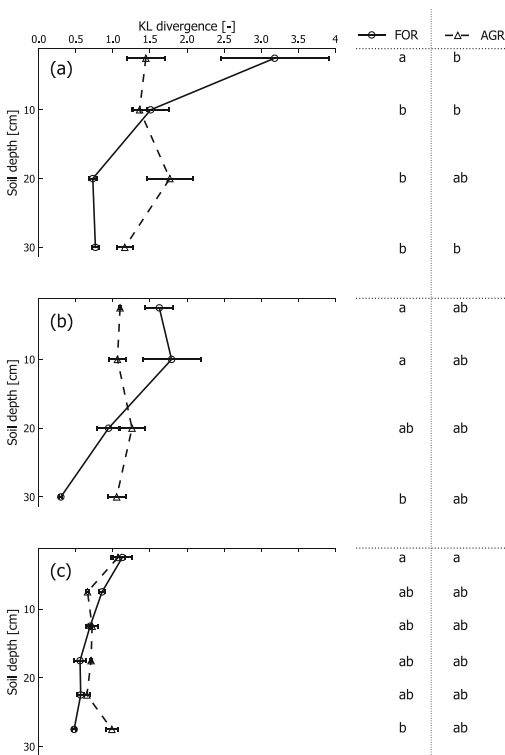
FIGURE 7 The variation of the median KL divergence of the acceptable parameter sets with soil depth in the agricultural (AGR) and afforested land (FOR) at (a) Almnäs, (b) Siggebohyttan, and (c) Vik. Symbols indicate arithmetic means and error bars indicate standard errors for each treatment and depth. Letters on the right side of the figure indicate significant differences ($p < 0.05$) in KL divergence between treatments and depth intervals for each site. Statistical comparisons between sites were not conducted

showing the largest and the bare fallow treatment the smallest value (Table 2). Water retention measurements and X-ray computed tomography analyses of other studies corroborate that the long-term addition of animal manure increases ϕ and changes the relative abundance of pore-size classes with main effects on macroporosity (e.g., Anderson et al., 1990; Naveed et al., 2014; Pagliai & Vignozzi, 1998; Zhang et al., 2021). This increases the heterogeneity as well as the broadness of the VSD (see values of $\sigma_{S,1}$ in Table S2), which explains the larger KL divergence in the manure treatment compared to the other two treatments. Apart from a larger ϕ, it seems that the regular addition of $Ca(NO_3)_2$ fertilizer and the presence of crops did not lead to noticeable differences in the VSD of this treatment compared to the bare fallow as

indicated by the similar KL divergences in these two treatments. We found no studies that directly investigated the influence of $Ca(NO_3)_2$ addition on soil structure. While calcium is considered an important driver for micro-aggregation (Pihlap et al., 2021; Totsche et al., 2018), its overall effect on the VSD has been found to be limited even with the addition of far larger amounts than practiced in the long-term field site at Ultuna (Frank et al., 2020; Mamedov et al., 2021). Frank et al. (2020) noted that regular tillage can undermine the effects of liming on the pore space and that fine-textured soils require considerable amounts of lime for effects to be visible. We assume that the amount of calcium added as $Ca(NO_3)_2$ was not sufficient to induce detectable changes in the VSD of the fine-textured soil at Ultuna. Instead, the observed increase in macroporosity compared with the fallow treatment (Table 2) should be the result of crop growth, which creates root biopores and enhances soil faunal activity due to the input of carbon (Meurer, Barron, et al., 2020).

For the dataset reported by Messing et al. (1997), our results show a clear positive correlation (Pearson's $r = 0.374$, $p < 0.001$) between soil organic carbon concentrations and KL divergences across all three sites and both FOR and AGR treatments (Figure 9). The different trends in KL divergence with soil depth between the FOR and AGR treatments can therefore be largely explained by the depth distribution of soil organic matter, which is much more homogeneous in the AGR treatment (Table 2). Regular soil tillage probably contributed to the homogenization of both soil organic matter and KL divergence in the AGR treatments. Soil organic matter is known to be an important driver for soil structural development in the form of aggregation at the micro-scale (Chenu & Cosentino, 2011; Dignac et al., 2017; Vidal et al., 2021; Witzgall et al., 2021). Many studies have shown that soil organic matter has a significant positive effect on total porosity (Jarvis, Forkman, et al., 2017; Johannes et al., 2017; Meurer et al., 2020,b), whereas only a few studies have investigated the effects of SOM on the VSD. However, experiments have found impacts on a wide range of pore diameters, including both smaller matrix pores and larger mesopores (Fukumasu et al., 2022; Kirchmann & Gerzabek, 1999; Meurer, Chenu, et al., 2020; Sekucia et al., 2020; Zhang et al., 2021), which implies an increase in the heterogeneity of the VSD and, therefore, the KL divergence. The strong relationships observed between the model parameters of the PSD and the small pore region of the bimodal model (Figure 8a,b) do suggest that the latter is dominated by textural pore space. However, it seems clear that the small pore region does not consist exclusively of textural pores, since a simpler four-parameter model that we tested based on this assumption did not give good fits to
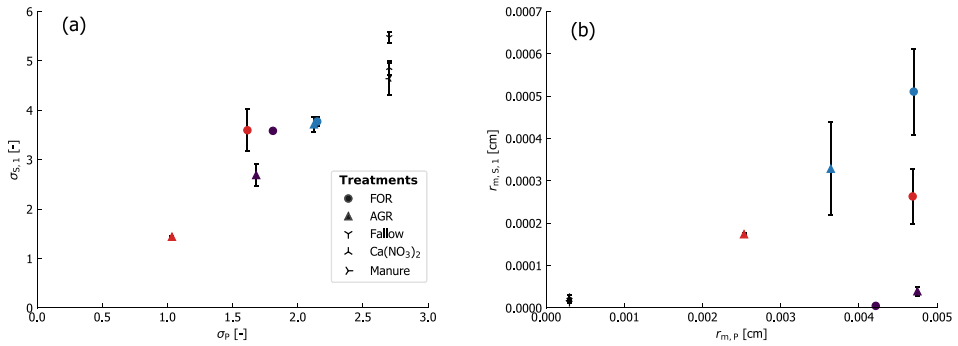
FIGURE 8 Illustration of the physical link between particle-size distribution and pore-size distribution of the small pore region (subscript 1 in Equation (14)) across sites and treatments (FOR = afforested land, AGR = agricultural land). (a) Shows the standard deviation parameter of the PSD (σ_P) against the standard deviation parameter of the small pore region ($\sigma_{S,1}$), and (b) shows the median particle radius ($r_{m,P}$) against the median pore radius of the small pore region ($r_{m,S,1}$). Error bars indicate standard errors and sites are represented by different colours (Almnäs: Dark purple, Siggebohyttan: Red, Vik: Blue, Ultuna: Black symbols)

the data. Thus, our results demonstrate that the small pore region also includes structural pore space, presumably related to aggregation by soil organic matter. Finally, Figure 9 shows that the KL divergences at Ultuna follow a similar trend with soil organic carbon concentrations (both increase in the order fallow < Ca(NO$_3$)$_2$ < manure), although in this case soil organic carbon is probably mostly acting as a proxy for the impacts of biological activity on macroporosity.
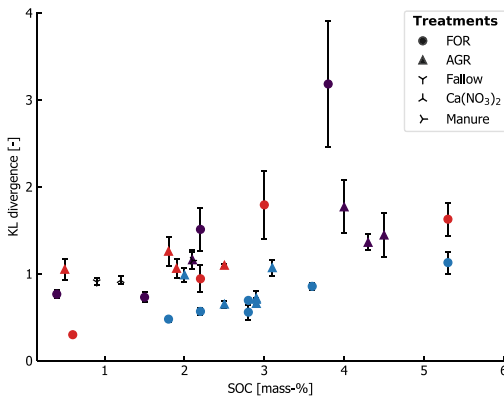

FIGURE 9 Illustration of the relationship between KL divergences and soil organic carbon concentrations (SOC) across sites and treatments (FOR = afforested land, AGR = agricultural land). Error bars indicate standard errors and sites are represented by different colours (Almnäs: Dark purple, Siggebohyttan: Red, Vik: Blue, and Ultuna: Black symbols)

5 | CONCLUSIONS

In this study, we described and demonstrated the applicability of relative entropy, the Kullback–Leibler (KL) divergence, as an index of soil structure. A large KL divergence, which may arise from combinations of a large structural porosity, large median pore size and a wide distribution of pore sizes (i.e., a large standard deviation) is indicative of a well-developed soil structure. We showed that the KL divergence follows expected trends in soil structural development between different treatments and management systems (tree plantations vs. agricultural land; bare fallow vs. Ca(NO$_3$)$_2$ addition vs. manure addition). The significant correlation found between soil organic carbon concentrations and KL divergences across the tested range of soil textures and management systems underlines this finding. We conclude therefore that the KL divergence may also have the potential to serve as an indicator of soil physical quality in agricultural soils under different management systems. Finally, because only routine soil data are required for this method, we expect it to be particularly useful for assessing the degree of soil structure for existing larger datasets of soil physical and hydraulic properties.

Some uncertainties of the presented method remain regarding the derivation of the VSD of the reference soil, which requires additional experimental efforts that focus on the study of textural porosity. Careful application of the curve fitting procedures is also necessary in order to ensure that the results are not unduly affected by problems related to non-uniqueness and parameter identification. In this respect, the calculated KL divergence values

are also very sensitive to the quality of the fit. Further testing is necessary to confirm the general applicability of the method in contrasting soil types. However, from the results presented here, we conclude that relative entropy shows potential as an index of soil structure.

AUTHOR CONTRIBUTIONS

Tobias Klöffel: Formal analysis (equal); methodology (equal); writing – original draft (equal). **Nicholas Jarvis:** Methodology (equal); supervision (equal); writing – review and editing (equal). **Sung Won Yoon:** Methodology (equal). **Jennie Barron:** Project administration (equal); supervision (equal); writing – review and editing (equal). **Daniel Giménez:** Methodology (equal); writing – review and editing (equal).

ACKNOWLEDGEMENTS

FUNDING INFORMATION

CONFLICT OF INTEREST

The authors declare that they have no known competing financial interests or personal relationships that could have influenced the work of this paper.

DATA AVAILABILITY STATEMENT

Data available on request due to privacy/ethical restrictions. The Python scripts to calculate the KL divergence from two lognormal distributions or using discrete integration is publicly available in the GitHub repository: https://github.com/tobikloeff.

ORCID

Tobias Klöffel https://orcid.org/0000-0002-5518-376X
Jennie Barron https://orcid.org/0000-0002-3292-3438

REFERENCES

Anderson, S. H., Gantzer, C. J., & Brown, J. R. (1990). Soil physical properties after 100 years of continuous cultivation. *Journal of Soil and Water Conservation*, *45*(1), 117–121.

Arya, L. M., Bowman, D. C., Thapa, B. B., & Cassel, D. K. (2008). Scaling soil water characteristics of golf course and athletic Field Sands from particle-size distribution. *Soil Science Society of America Journal*, *72*(1), 25–32. https://doi.org/10.2136/sssaj2006.0232

Arya, L. M., & Heitman, J. L. (2015). A non-empirical method for computing pore radii and soil water characteristics from particle-size distribution. *Soil Science Society of America Journal*, *79*(6), 1537–1544. https://doi.org/10.2136/sssaj2015.04.0145

Arya, L. M., Leij, F. J., van Genuchten, M. T., & Shouse, P. J. (1999). Scaling parameter to predict the soil water characteristic from particle-size distribution data. *Soil Science Society of America Journal*, *63*(3), 510–519. https://doi.org/10.2136/sssaj1999.03615995006300030013x

Arya, L. M., & Paris, J. F. (1981). A Physicoempirical model to predict the soil moisture characteristic from particle-size distribution and bulk density data. *Soil Science Society of America Journal*, *45*(6), 1023–1030. https://doi.org/10.2136/sssaj1981.03615995004500060004x

Assouline, S., & Or, D. (2013). Conceptual and parametric representation of soil hydraulic properties: A review. *Vadose Zone Journal*, *12*(4), 1–20. https://doi.org/10.2136/vzj2013.07.0121

Assouline, S., & Rouault, Y. (1997). Modeling the relationships between particle and pore size distributions in multicomponent sphere packs: Application to the water retention curve. *Colloids and Surfaces A: Physicochemical and Engineering Aspects*, *127*(1–3), 201–210. https://doi.org/10.1016/S0927-7757(97)00144-1

Assouline, S., Tessier, D., & Bruand, A. (1998). A conceptual model of the soil water retention curve. *Water Resources Research*, *34*(2), 223–231. https://doi.org/10.1029/97WR03039

Axler, S. (2020). Riemann Integration. In S. Axler (Ed.), *Measure, integration & real analysis* (Vol. 282, pp. 1–12). Springer International Publishing. https://doi.org/10.1007/978-3-030-33143-6_1

Basile, A., & D'Urso, G. (1997). Experimental corrections of simplified methods for predicting water retention curves in clay-loamy soils from particle-size determination. *Soil Technology*, *10*(3), 261–272. https://doi.org/10.1016/S0933-3630(96)00020-7

Beven, K. (1993). Prophecy, reality and uncertainty in distributed hydrological modelling. *Advances in Water Resources*, *16*(1), 41–51. https://doi.org/10.1016/0309-1708(93)90028-E

Bishop, C. (2006). *Pattern recognition and machine learning*. Springer-Verlag. https://www.springer.com/gp/book/9780387310732

Bodner, G., Scholl, P., & Kaul, H.-P. (2013). Field quantification of wetting–drying cycles to predict temporal changes of soil pore size distribution. *Soil and Tillage Research*, *133*, 1–9. https://doi.org/10.1016/j.still.2013.05.006

Brutsaert, W. (1966). Probability laws for pore-size distributions. *Soil Science*, *101*(2), 85–92.

Bucka, F. B., Pihlap, E., Kaiser, J., Baumgartl, T., & Kögel-Knabner, I. (2021). A small-scale test for rapid assessment of the soil development potential in post-mining soils. *Soil and Tillage Research*, *211*, 105016. https://doi.org/10.1016/j.still.2021.105016

Chan, T. P., & Govindaraju, R. S. (2004). Estimating soil water retention curve from particle-size distribution data based on Polydisperse sphere systems. *Vadose Zone Journal*, *3*(4), 1443–1454. https://doi.org/10.2113/3.4.1443

Chenu, C., & Cosentino, D. (2011). Microbial regulation of soil structural dynamics. In K. Ritz & I. Young (Eds.), *The*

architecture and biology of soils: Life in inner space (pp. 37–70). CABI. https://doi.org/10.1079/9781845935320.0037

Childs, E. C. (1969). Chapter 6: The soil pore space. In *Introduction to the Physical Basis of Soil Water Phenomena* (pp. 92-96). *John Wiley & Sons*.

Crawford, J. W., Matsui, N., & Young, I. M. (1995). The relation between the moisture-release curve and the structure of soil. *European Journal of Soil Science*, *46*(3), 369–375. https://doi.org/10.1111/j.1365-2389.1995.tb01333.x

Crisp, D. J., & Williams, R. (1971). Direct measurement of pore-size distribution on artificial and natural deposits and prediction of pore space accessible to interstitial organisms. *Marine Biology*, *10*(3), 214–226. https://doi.org/10.1007/BF00352810

Dexter, A. R. (1977). A statistical measure of the structure of tilled soil. *Journal of Agricultural Engineering Research*, *22*(1), 101–104. https://doi.org/10.1016/0021-8634(77)90099-3

Dexter, A. R. (2004). Soil physical quality. *Geoderma*, *120*(3–4), 201–214. https://doi.org/10.1016/j.geoderma.2003.09.004

Dexter, A. R., Czyż, E. A., Richard, G., & Reszkowska, A. (2008). A user-friendly water retention function that takes account of the textural and structural pore spaces in soil. *Geoderma*, *143*(3–4), 243–253. https://doi.org/10.1016/j.geoderma.2007.11.010

Dignac, M.-F., Derrien, D., Barré, P., Barot, S., Cécillon, L., Chenu, C., Chevallier, T., Freschet, G. T., Garnier, P., Guenet, B., Hedde, M., Klumpp, K., Lashermes, G., Maron, P.-A., Nunan, N., Roumet, C., & Basile-Doelsch, I. (2017). Increasing soil carbon storage: Mechanisms, effects of agricultural practices and proxies. A review. *Agronomy for Sustainable Development*, *37*(2), 14. https://doi.org/10.1007/s13593-017-0421-2

Dominati, E., Patterson, M., & Mackay, A. (2010). A framework for classifying and quantifying the natural capital and ecosystem services of soils. *Ecological Economics*, *69*(9), 1858–1868. https://doi.org/10.1016/j.ecolecon.2010.05.002

Durner, W. (1994). Hydraulic conductivity estimation for soils with heterogeneous pore structure. *Water Resources Research*, *30*(2), 211–223. https://doi.org/10.1029/93WR02676

El-Baz, A., Nayak, T.K. (2004). Efficiency of composite sampling for estimating a lognormal distribution. *Environmental and Ecological Statistics*, *11*(3), 283–294. https://doi.org/10.1023/B:EEST.0000038016.20656.21

Erktan, A., Or, D., & Scheu, S. (2020). The physical structure of soil: Determinant and consequence of trophic interactions. *Soil Biology and Biochemistry*, *148*, 107876. https://doi.org/10.1016/j.soilbio.2020.107876

FAO. (1989). *Soil map of the world* (Technical Paper No. 20). ISRIC.

Farr, R. S., & Groot, R. D. (2009). Close packing density of polydisperse hard spheres. *The Journal of Chemical Physics*, *131*(24), 244104. https://doi.org/10.1063/1.3276799

Fatichi, S., Or, D., Walko, R., Vereecken, H., Young, M. H., Ghezzehei, T. A., Hengl, T., Kollet, S., Agam, N., & Avissar, R. (2020). Soil structure is an important omission in earth system models. *Nature Communications*, *11*(1), 522. https://doi.org/10.1038/s41467-020-14411-z

Fernández-Gálvez, J., Pollacco, J. A. P., Lilburne, L., McNeill, S., Carrick, S., Lassabatere, L., & Angulo-Jaramillo, R. (2021). Deriving physical and unique bimodal soil Kosugi hydraulic parameters from inverse modelling. *Advances in Water Resources*, *153*, 103933. https://doi.org/10.1016/j.advwatres.2021.103933

Fiès, J. C., & Bruand, A. (1990). Textural porosity analysis of a silty clay soil using pore volume balance estimation, mercury porosimetry and quantified backscattered electron scanning image (BESI). *Geoderma*, *47*(3–4), 209–219. https://doi.org/10.1016/0016-7061(90)90029-9

Fiès, J. C., & Bruand, A. (1998). Particle packing and organization of the textural porosity in clay-silt-sand mixtures. *European Journal of Soil Science*, *49*(4), 557–567. https://doi.org/10.1046/j.1365-2389.1998.4940557.x

Fiès, J. C., & Stengel, P. (1981). Densite texturale de sols naturels. I. - Methode de mesure. *Agronomie*, *1*(8), 651–658.

Fiès, J. C., Stengel, P., Bourlet, M., Horoyan, J., & Jeandet, C. (1981). Densité texturale de sols naturels II. - Eléments d'interprétation. *Agronomie*, *1*(8), 659–666.

Frank, T., Zimmermann, I., & Horn, R. (2020). Lime application in marshlands of northern Germany—Influence of liming on the physicochemical and hydraulic properties of clayey soils. *Soil and Tillage Research*, *204*, 104730. https://doi.org/10.1016/j.still.2020.104730

Fredlund, M. D., Fredlund, D. G., & Wilson, G. W. (2000). An equation to represent grain-size distribution. *Canadian Geotechnical Journal*, *37*, 817–827. https://doi.org/10.1139/t00-015

Fukumasu, J., Jarvis, N., Koestel, J., Kätterer, T., & Larsbo, M. (2022). Relations between soil organic carbon content and the pore size distribution for an arable topsoil with large variations in soil properties. *European Journal of Soil Science*, *73*(1), e13212. https://doi.org/10.1111/ejss.13212

Gardner, W. R. (1956). Representation of soil aggregate-size distribution by a logarithmic-Normal distribution. *Soil Science Society of America Journal*, *20*(2), 151–153. https://doi.org/10.2136/sssaj1956.03615995002000020003x

Gil, M. (2011). *On Renyi divergence measures for continuous alphabet sources* [thesis]. https://qspace.library.queensu.ca/handle/1974/6680

Goodfellow, I., Bengio, Y., & Courville, A. (2016). *Deep learning* (illustrated edition). The MIT Press.

Gupta, S., & Larson, W. (1979). A model for predicting packing density of soils using particle-size Distribution1. *Soil Science Society of America Journal - SSSAJ*, *43*, 758–764. https://doi.org/10.2136/sssaj1979.03615995004300040028x

Haverkamp, R., & Parlange, J.-Y. (1986). Predicting the water-retention curve from particle-size distribution: 1. Sandy soils without organic matter. *Soil Science*, *142*(6), 325–339.

Hou, Z., & Rubin, Y. (2005). On minimum relative entropy concepts and prior compatibility issues in vadose zone inverse and forward modeling. *Water Resources Research*, *41*, W1245. https://doi.org/10.1029/2005WR004082

Hwang, S. I. (2004). Effect of texture on the performance of soil particle-size distribution models. *Geoderma*, *123*(3), 363–371. https://doi.org/10.1016/j.geoderma.2004.03.003

Hwang, S. I., & Powers, S. E. (2003). Lognormal distribution model for estimating soil water retention curves for sandy soils. *Soil Science*, *168*(3), 156–166. https://doi.org/10.1097/01.ss.0000058888.60072.e3

Hwang, S. I., & Choi, S. I. (2006). Use of a lognormal distribution model for estimating soil water retention curves from particle-size distribution data. *Journal of Hydrology*, *323*(1–4), 325–334. https://doi.org/10.1016/j.jhydrol.2005.09.005

Jarvis, N., Forkman, J., Koestel, J., Kätterer, T., Larsbo, M., & Taylor, A. (2017). Long-term effects of grass-clover leys on the structure of a silt loam soil in a cold climate. *Agriculture, Ecosystems & Environment*, *247*, 319–328. https://doi.org/10.1016/j.agee.2017.06.042

Jarvis, N., Larsbo, M., & Koestel, J. (2017). Connectivity and percolation of structural pore networks in a cultivated silt loam soil quantified by X-ray tomography. *Geoderma*, *287*, 71–79. https://doi.org/10.1016/j.geoderma.2016.06.026

Jensen, J. L., Schjønning, P., Watts, C. W., Christensen, B. T., & Munkholm, L. J. (2019). Soil water retention: Uni-modal models of pore-size distribution neglect impacts of soil management. *Soil Science Society of America Journal*, *83*, 18–26. https://doi.org/10.2136/sssaj2018.06.0238

Johannes, A., Matter, A., Schulin, R., Weisskopf, P., Baveye, P. C., & Boivin, P. (2017). Optimal organic carbon values for soil structure quality of arable soils. Does clay content matter? *Geoderma*, *302*, 14–21. https://doi.org/10.1016/j.geoderma.2017.04.021

Kim, J., Ivanov, V. Y., & Fatichi, S. (2016). Environmental stochasticity controls soil erosion variability. *Scientific Reports*, *6*, 22065. https://doi.org/10.1038/srep22065

Kirchmann, H., & Gerzabek, M. H. (1999). Relationship between soil organic matter and micropores in a long-term experiment at Ultuna, Sweden. *Journal of Plant Nutrition and Soil Science*, *162*, 493–498.

Kirchmann, H., Persson, J., & Carlgren, K. (1994). *The Ultuna long-term soil organic matter experiment, 1956-1991* (Department of Soil Sciences, reports and dissertations no. 17). Swedish University of Agricultural Sciences.

Kosugi, K. (1994). Three-parameter lognormal distribution model for soil water retention. *Water Resources Research*, *30*(4), 891–901. https://doi.org/10.1029/93WR02931

Kosugi, K. (1996). Lognormal distribution model for unsaturated soil hydraulic properties. *Water Resources Research*, *32*(9), 2697–2703. https://doi.org/10.1029/96WR01776

Kreiselmeier, J., Chandrasekhar, P., Weninger, T., Schwen, A., Julich, S., Feger, K.-H., & Schwärzel, K. (2019). Quantification of soil pore dynamics during a winter wheat cropping cycle under different tillage regimes. *Soil and Tillage Research*, *192*, 222–232. https://doi.org/10.1016/j.still.2019.05.014

Kullback, S., & Leibler, R. A. (1951). On information and sufficiency. *The Annals of Mathematical Statistics*, *22*(1), 79–86.

Lenth, R. (2020). *Emmeans: Estimated marginal means, aka least-squares means* [manual]. https://CRAN.R-project.org/package=emmeans

Lin, H. (2011). Three principles of soil change and Pedogenesis in time and space. *Soil Science Society of America Journal*, *75*(6), 2049–2070. https://doi.org/10.2136/sssaj2011.0130

Lucas, M., Pihlap, E., Steffens, M., Vetterlein, D., & Kögel-Knabner, I. (2020). Combination of imaging infrared spectroscopy and X-ray computed microtomography for the investigation of bio- and physicochemical processes in structured soils. *Frontiers in Environmental Science*, *8*, 42. https://doi.org/10.3389/fenvs.2020.00042

Luo, L., Lin, H., & Halleck, P. (2008). Quantifying soil structure and preferential flow in intact soil using X-ray computed tomography. *Soil Science Society of America Journal*, *72*(4), 1058–1069. https://doi.org/10.2136/sssaj2007.0179

MacKay, D. J. C. (2002). *Information theory*. Cambridge University Press.

Mamedov, A. I., Fujimaki, H., Tsunekawa, A., Tsubo, M., & Levy, G. J. (2021). Structure stability of acidic Luvisols: Effects of tillage type and exogenous additives. *Soil and Tillage Research*, *206*, 104832. https://doi.org/10.1016/j.still.2020.104832

Messing, I., Alriksson, A., & Johansson, W. (1997). Soil physical properties of afforested and arable land. *Soil Use and Management*, *13*(4), 209–217. https://doi.org/10.1111/j.1475-2743.1997.tb00588.x

Meurer, K., Barron, J., Chenu, C., Coucheney, E., Fielding, M., Hallett, P., Herrmann, A. M., Keller, T., Koestel, J., Larsbo, M., Lewan, E., Or, D., Parsons, D., Parvin, N., Taylor, A., Vereecken, H., & Jarvis, N. (2020). A framework for modelling soil structure dynamics induced by biological activity. *Global Change Biology*, *26*(10), 5382–5403. https://doi.org/10.1111/gcb.15289

Meurer, K. H. E., Chenu, C., Coucheney, E., Herrmann, A. M., Keller, T., Kätterer, T., Nimblad Svensson, D., & Jarvis, N. (2020). Modelling dynamic interactions between soil structure and the storage and turnover of soil organic matter. *Biogeosciences*, *17*(20), 5025–5042. https://doi.org/10.5194/bg-17-5025-2020

Mohammadi, M. H., & Vanclooster, M. (2011). Predicting the soil moisture characteristic curve from particle size distribution with a simple conceptual model. *Vadose Zone Journal*, *10*(2), 594–602. https://doi.org/10.2136/vzj2010.0080

Mueller, L., Shepherd, G., Schindler, U., Ball, B. C., Munkholm, L. J., Hennings, V., Smolentseva, E., Rukhovic, O., Lukin, S., & Hu, C. (2013). Evaluation of soil structure in the framework of an overall soil quality rating. *Soil and Tillage Research*, *127*, 74–84. https://doi.org/10.1016/j.still.2012.03.002

Naveed, M., Moldrup, P., Vogel, H.-J., Lamandé, M., Wildenschild, D., Tuller, M., & de Jonge, L. W. (2014). Impact of long-term fertilization practice on soil structure evolution. *Geoderma*, *217–218*, 181–189. https://doi.org/10.1016/j.geoderma.2013.12.001

Nimmo, J. R. (1997). Modeling structural influences on soil water retention. *Soil Science Society of America Journal*, *61*(3), 712–719. https://doi.org/10.2136/sssaj1997.03615995006100030002x

Nimmo, J. R. (2013). Porosity and pore size distribution. In *Reference Module in Earth Systems and Environmental Sciences*. Elsevier. https://doi.org/10.1016/B978-0-12-409548-9.05265-9

Nimmo, J. R., Herkelrath, W. N., & Laguna Luna, A. M. (2007). Physically based estimation of soil water retention from textural data: General framework, new models, and streamlined existing models. *Vadose Zone Journal*, *6*(4), 766–773. https://doi.org/10.2136/vzj2007.0019

Or, D., Keller, T., & Schlesinger, W. H. (2021). Natural and managed soil structure: On the fragile scaffolding for soil functioning. *Soil and Tillage Research*, *208*, 104912. https://doi.org/10.1016/j.still.2020.104912

Pagliai, M., & Vignozzi, N. (1998). Use of manures for soil improvement. In *Handbook of soil conditioners: Substances that enhance the physical properties of soil: Substances that enhance the physical properties of soil* (pp. 119–139). CRC Press.

Pihlap, E., Steffens, M., & Kögel-Knabner, I. (2021). Initial soil aggregate formation and stabilisation in soils developed from calcareous loess. *Geoderma*, *385*, 114854. https://doi.org/10.1016/j.geoderma.2020.114854

Pohlert, T. (2014). *The pairwise multiple comparison of mean ranks package (PMCMR)* [manual]. https://CRAN.R-project.org/package=PMCMR

Pollacco, J. A. P., Fernández-Gálvez, J., & Carrick, S. (2020). Improved prediction of water retention curves for fine texture soils using an intergranular mixing particle size distribution model. *Journal of Hydrology*, *584*, 124597. https://doi.org/10.1016/j.jhydrol.2020.124597

Pollacco, J. A. P., Webb, T., McNeill, S., Hu, W., Carrick, S., Hewitt, A., & Lilburne, L. (2017). Saturated hydraulic conductivity model computed from bimodal water retention curves for a range of New Zealand soils. *Hydrology and Earth System Sciences*, *21*(6), 2725–2737. https://doi.org/10.5194/hess-21-2725-2017

R Core Team. (2019). *R: A language and environment for statistical computing* [manual]. https://www.R-project.org/

Rabot, E., Wiesmeier, M., Schlüter, S., & Vogel, H.-J. (2018). Soil structure as an indicator of soil functions: A review. *Geoderma*, *314*, 122–137. https://doi.org/10.1016/j.geoderma.2017.11.009

Regelink, I. C., Stoof, C. R., Rousseva, S., Weng, L., Lair, G. J., Kram, P., Nikolaidis, N. P., Kercheva, M., Banwart, S., & Comans, R. N. J. (2015). Linkages between aggregate formation, porosity and soil chemical properties. *Geoderma*, *247–248*, 24–37. https://doi.org/10.1016/j.geoderma.2015.01.022

Reynolds, W. D. (2017). Use of bimodal hydraulic property relationships to characterize soil physical quality. *Geoderma*, *294*, 38–49. https://doi.org/10.1016/j.geoderma.2017.01.035

Reynolds, W. D., Drury, C. F., Tan, C. S., Fox, C. A., & Yang, X. M. (2009). Use of indicators and pore volume-function characteristics to quantify soil physical quality. *Geoderma*, *152*(3–4), 252–263. https://doi.org/10.1016/j.geoderma.2009.06.009

Robinson, D. A., Lebron, I., & Vereecken, H. (2009). On the definition of the natural Capital of Soils: A framework for description, evaluation, and monitoring. *Soil Science Society of America Journal*, *73*(6), 1904–1911. https://doi.org/10.2136/sssaj2008.0332

Ross, P. J., & Smettem, K. R. J. (1993). Describing soil hydraulic properties with sums of simple functions. *Soil Science Society of America Journal*, *57*(1), 26–29. https://doi.org/10.2136/sssaj1993.03615995005700010006x

Sekucia, F., Dlapa, P., Kollár, J., Cerdá, A., Hrabovský, A., & Svobodová, L. (2020). Land-use impact on porosity and water retention of soils rich in rock fragments. *Catena*, *195*, 104807. https://doi.org/10.1016/j.catena.2020.104807

Shen, C., Liu, S., Xu, S., & Wang, L. (2019). Rapid estimation of maximum and minimum void ratios of granular soils. *Acta Geotechnica*, *14*(4), 991–1001. https://doi.org/10.1007/s11440-018-0714-x

Sillers, W. S., Fredlund, D. G., & Zakerzaheh, N. (2001). Mathematical attributes of some soil–water characteristic curve models. *Geotechnical and Geological Engineering*, *19*(3/4), 243–283. https://doi.org/10.1023/A:1013109728218

Svensson, D. N. (2020). *Influence of cropping and fertilization on soil pore characteristics in a long-term field study* [Master's thesis, Swedish University of Agricultural Sciences]. https://stud.epsilon.slu.se/15593/

Tarquis, A. M., Bird, N. R. A., Whitmore, A. P., Cartagena, M. C., & Pachepsky, Y. (2008). Multiscale entropy-based analysis of soil transect data. *Vadose Zone Journal*, *7*(2), 563–569. https://doi.org/10.2136/vzj2007.0039

Totsche, K. U., Amelung, W., Gerzabek, M. H., Guggenberger, G., Klumpp, E., Knief, C., Lehndorff, E., Mikutta, R., Peth, S., Prechtel, A., Ray, N., & Kögel-Knabner, I. (2018). Microaggregates in soils. *Journal of Plant Nutrition and Soil Science*, *181*(1), 104–136. https://doi.org/10.1002/jpln.201600451

Vaz, C. M. P., de Freitas Iossi, M., de Mendonça Naime, J., Macedo, Á., Reichert, J. M., Reinert, D. J., & Cooper, M. (2005). Validation of the Arya and Paris water retention model for Brazilian soils. *Soil Science Society of America Journal*, *69*(3), 577–583. https://doi.org/10.2136/sssaj2004.0104

Vidal, A., Klöffel, T., Guigue, J., Angst, G., Steffens, M., Hoeschen, C., & Mueller, C. W. (2021). Visualizing the transfer of organic matter from decaying plant residues to soil mineral surfaces controlled by microorganisms. *Soil Biology and Biochemistry*, *160*, 108347. https://doi.org/10.1016/j.soilbio.2021.108347

Virtanen, P., Gommers, R., Oliphant, T. E., Haberland, M., Reddy, T., Cournapeau, D., Burovski, E., Peterson, P., Weckesser, W., Bright, J., van der Walt, S. J., Brett, M., Wilson, J., Millman, K. J., Mayorov, N., Nelson, A. R. J., Jones, E., Kern, R., Larson, E., ... van Mulbregt, P. (2020). SciPy 1.0: Fundamental algorithms for scientific computing in python. *Nature Methods*, *17*(3), 261–272. https://doi.org/10.1038/s41592-019-0686-2

Vogel, H.-J., Weller, U., & Schlüter, S. (2010). Quantification of soil structure based on Minkowski functions. *Computers & Geosciences*, *36*(10), 1236–1245. https://doi.org/10.1016/j.cageo.2010.03.007

Witzgall, K., Vidal, A., Schubert, D. I., Höschen, C., Schweizer, S. A., Buegger, F., Pouteau, V., Chenu, C., & Mueller, C. W. (2021). Particulate organic matter as a functional soil component for persistent soil organic carbon. *Nature Communications*, *12*(1), 4115. https://doi.org/10.1038/s41467-021-24192-8

Yoon, S. W. (2009). *A measure of soil structure derived from water retention properties: A Kullback-Leibler distance approach* [dissertation]. Rutgers University.

Yoon, S. W., & Giménez, D. (2012). Entropy characterization of soil pore systems derived from soil-water retention curves. *Soil Science*, *177*(6), 361–368. https://doi.org/10.1097/SS.0b013e318256ba1c

Young, I. M., Crawford, J. W., & Rappoldt, C. (2001). New methods and models for characterising structural heterogeneity of soil. *Soil and Tillage Research*, *61*(1–2), 33–45. https://doi.org/10.1016/S0167-1987(01)00188-X

Zhang, X., Neal, A. L., Crawford, J. W., Bacq-Labreuil, A., Akkari, E., & Rickard, W. (2021). The effects of long-term fertilizations on soil hydraulic properties vary with scales. *Journal of Hydrology*, *593*, 125890. https://doi.org/10.1016/j.jhydrol.2020.125890

SUPPORTING INFORMATION

Additional supporting information may be found in the online version of the article at the publisher's website.

APPENDIX A: Derivation of the KL divergence for two lognormal distributions

The KL divergence has been derived for two lognormal distributions before (e.g., El-Baz et al., 2004; Gil, 2011). However, for the specific case of two VSDs, Equation (12) may not be trivial from these derivations (Yoon, 2009). Hence, we show step-by-step how Equation (12) is developed from Equations (5) and (11) in the following.

We start with Equation (2) and substitute $p(x)$ with Equation (5) and $q(x)$ with Equation (11). Since both are lognormal distributions, the lower integral limit is adapted to 0, giving:

$$D_{KL}\left(f_S \middle\| f_R\right) = \int_0^\infty f_S(r)\log\left(\frac{\frac{(\theta_s-\theta_r)_S}{r\sigma_S\sqrt{2\pi}}\exp\left\{-\frac{(\log r - \log r_{m,S})^2}{2\sigma_S^2}\right\}}{\frac{(\theta_s-\theta_r)_R}{r\sigma_R\sqrt{2\pi}}\exp\left\{-\frac{(\log r - \log r_{m,R})^2}{2\sigma_R^2}\right\}}\right)dr \quad (A1)$$

which can be written as follows:

$$D_{KL}\left(f_S \middle\| f_R\right) = \log\frac{(\theta_s-\theta_r)_S\,\sigma_R}{(\theta_s-\theta_r)_R\,\sigma_S}\int_0^\infty f_S(r)dr \quad (A2)$$
$$+ \int_0^\infty f_S(r)\left[-\frac{(\log r - \log r_{m,S})^2}{2\sigma_S^2}\right.$$
$$\left. + \frac{(\log r - \log r_{m,R})^2}{2\sigma_R^2}\right]dr$$

The first integral in Equation (A2) can be substituted with $(\theta_s - \theta_r)_S$ and the equation transformed to

$$D_{KL}\left(f_S \middle\| f_R\right) = (\theta_s-\theta_r)_S\log\frac{(\theta_s-\theta_r)_S\,\sigma_R}{(\theta_s-\theta_r)_R\,\sigma_S}$$
$$+ \frac{1}{2\sigma_S^2}\left(-\int_0^\infty f_S(r)(\log r - \log r_{m,S})^2 dr\right)$$
$$+ \frac{1}{2\sigma_R^2}\left(-\int_0^\infty f_S(r)(\log r - \log r_{m,R})^2 dr\right) \quad (A3)$$

The two integrals in Equation (A3) can be solved using the following relationship:

$$\mathrm{E}\left[X^2\right] = \sigma^2 - \mathrm{E}[X]^2 \quad (A4)$$

where E denotes the expected value and X is a random variable and where $E[X]$ can be expressed as follows:

$$\mathrm{E}[X] = \int_{-\infty}^\infty x f(x)\,dx \quad (A5)$$

and $E[X^2]$ as:

$$\mathrm{E}\left[X^2\right] = \int_{-\infty}^\infty x^2 f(x)\,dx \quad (A6)$$

where $f(x)$ denotes a probability density function of X.

Applying the relationships Equation (A4) through (A6) to Equation (A3) and after further simplification we obtain the following:

$$D_{KL}\left(f_S \middle\| f_R\right) = (\theta_s-\theta_r)_S\log\frac{(\theta_s-\theta_r)_S\,\sigma_R}{(\theta_s-\theta_r)_R\,\sigma_S} + \frac{(\theta_s-\theta_r)_S}{2}$$
$$+ (\theta_s-\theta_r)_S\left[\frac{\sigma_S^2 + (\log r_{m,S} - \log r_{m,R})^2}{2\sigma_R^2}\right] \quad (A7)$$

Finally, the term $(\theta_s - \theta_r)_S$ can be factorized to yield Equation (12):

$$D_{KL}\left(f_S \middle\| f_R\right) = (\theta_s-\theta_r)_S\left(\log\frac{(\theta_s-\theta_r)_S\,\sigma_R}{(\theta_s-\theta_r)_R\,\sigma_s} - \frac{1}{2}\right. \quad (A8)$$
$$\left. + \left[\frac{\sigma_s^2 + (\log r_{m,S} - \log r_{m,R})^2}{2\sigma_R^2}\right]\right)$$

III

CORRECTION

Erratum to "Relative entropy as an index of soil structure"

Equations based on the Kosugi (1996) model were erroneously reproduced by Klöffel et al. In particular, a "squared" sign is consistently missing in the numerator of the exponential terms.

Equation (3) should be:

$$g(r_P) = \frac{1}{r_P \sigma_P \sqrt{2\pi}} \exp\left\{ -\frac{(\ln r_P - \ln r_{m,P})^2}{2\sigma_P^2} \right\}$$

Equation (5) should be:

$$f_S(r) = \frac{(\theta_s - \theta_r)}{r \sigma_S \sqrt{2\pi}} \exp\left\{ -\frac{(\ln r - \ln r_{m,S})^2}{2\sigma_S^2} \right\}$$

Equation (6) should be:

$$f_S(r) = \sum_{i=1}^{n} \frac{(\theta_{s,i} - \theta_{r,i})}{r \sigma_{S,i} \sqrt{2\pi}} \exp\left\{ -\frac{(\ln r - \ln r_{m,S,i})^2}{2\sigma_{S,i}^2} \right\}$$

Equation (11) should be:

$$f_R(r) = \frac{(\phi_{tex} - \theta_r)}{r \sigma_R \sqrt{2\pi}} \exp\left\{ -\frac{(\ln r - \ln r_{m,R})^2}{2\sigma_R^2} \right\}$$

Equation (14) should be:

$$f_S(r) = \frac{\theta_{s,1}}{r \sigma_{S,1} \sqrt{2\pi}} \exp\left\{ -\frac{(\ln r - \ln r_{m,S,1})^2}{2\sigma_{S,1}^2} \right\} + \frac{\theta_{s,2}}{r \sigma_{S,2} \sqrt{2\pi}} \exp\left\{ -\frac{(\ln r - \ln r_{m,S,2})^2}{2\sigma_{S,2}^2} \right\}$$

REFERENCE

Kosugi, K. (1996). Lognormal distribution model for unsaturated soil hydraulic properties. *Water Resources Research*, *32*, 2697–2703.

We apologize for this error.

The main objective of this thesis was to improve our understanding of the effects of climate-driven processes on soil structure. This was done to assess potential implications for soil water functions in the context of climate change with a focus on the temperate-boreal zone. The presented results are relevant in the context of wetter soil conditions, early summer droughts, and an intensification of agricultural practices as expected for this part of the world in a future climate.

Tobias Klöffel received his graduate education at the Department of Soil and Environment, Swedish University of Agricultural Sciences (SLU), Sweden. He holds a M.Sc. degree in Environmental Engineering from the Technical University of Munich, Germany.

Acta Universitatis Agriculturae Sueciae presents doctoral theses from the Swedish University of Agricultural Sciences (SLU).

SLU generates knowledge for the sustainable use of biological natural resources. Research, education, extension, as well as environmental monitoring and assessment are used to achieve this goal.